Design, Characterization and Evaluation of Lipid Based Nanoparticulate Temozolomide for Enhanced Delivery to the Brain

THESIS

Submitted in partial fulfilment
of the requirements for the degree of
DOCTOR OF PHILOSOPHY

by

ARCHANA KHOSA

Under the Supervision of

PROF. RANENDRA. N. SAHA

BITS Pilani
Pilani | Dubai | Goa | Hyderabad

BIRLA INSTITUTE OF TECHNOLOGY AND SCIENCE, PILANI

2018

BIRLA INSTITUTE OF TECHNOLOGY AND SCIENCE, PILANI

CERTIFICATE

This is to certify that the thesis entitled "**Design, Characterization and Evaluation of Lipid Based Nanoparticulate Temozolomide for Enhanced Delivery to the Brain**" submitted by **Archana Khosa**, ID. No. **2012PHXF0434P** for award of Ph.D. degree of the institute, embodies original work done by her under my supervision.

Dr. Ranendra N. Saha, Senior Professor

Director

Birla Institute of Technology and Science, Pilani, Dubai Campus

Dubai, UAE

Date:

Acknowledgements

I express my sincere gratitude and deepest appreciation for my research supervisor Prof. Ranendra N. Saha, Shri B.K. Birla & Smt. Sarala Birla Chair Professor and Director, BITS, Pilani, Dubai Campus for his guidance, constant support and encouragement. I will always remain indebted to him for taking me under his wing and encouraging me to think independently and strive for higher standards in research. His passion towards research and his capability to efficiently multitask has and always will be a source of inspiration for me.

I am grateful to Prof. Souvik Bhattacharyya, Vice Chancellor. BITS, Pilani, Prof. Ashoke K. Sarkar, Director, BITS, Pilani, Pilani campus and Prof. S.K.Verma, Dean, Academic Research (PhD Program) for their support.

I express my special gratitude to Prof. Hemant R. Jadhav, Associate Dean, ARD, BITS, Pilani and Prof. R. Mahesh for their guidance and administrative support during the course of my doctoral research.

I am thankful to Dr. Anil Gaikwad, Head, Department of Pharmacy and Dr. S. Murugesan, Former Head, Department of Pharmacy for their constant support at the departmental level and facilitating resources required during my research work. I am also grateful to Dr. Shrikant Charde, former Head, Department of Pharmacy for his excellent leadership, motivation and helping me overcome apprehensions during the initial days of my doctoral research.

I would also like to express my sincere thanks to Dr. Atish Paul, Convener, Departmental Research Committee, Dr. Sunil K Dubey and Dr. Anil Jindal, Doctoral Advisory Committee members for their valuable comments and guidance while compiling this thesis.

I am heartily grateful to my former and current colleagues Dr. Gautam Singhvi, Dr. Sunil K Dubey, Dr. Murali Manohar Pandey and Dr. Mahaveer Singh for their immense support, motivation and patient listening whenever I was feeling low and demotivated. I am also thankful to my colleagues Dr. Rajeev Taliyan, Dr. Priti Jain, Dr. Aniruddha Roy, Dr. Deepak Chitkara, Dr. Anupama Mittal and Dr. Sandeep Sundriyal.

I also wish to express my thanks to Dr. Sushil Yadav for his support and cooperation especially during in vivo studies. I also heartily thank Dr. Emil Joseph, Dr. Garima Balwani, Dr. Prashant Raut, Dr. Vibhu, Dr. Yashwant Kurhe, Dr. Pankaj, Dr. Subhash and Mr. Satish Reddi for their motivation and friendly support. I also appreciate all the research scholars of Department of Pharmacy for their support and maintaining lively working environment which made the long working hours in the lab seem less tedious. I specially thank K.V. Krishna for his active participation and invaluable inputs in the research work.

I express my gratitude to Dr. Prabhat Jha and Dr. Jitendra Panwar for allowing me to use the various laboratory facilities in Biological sciences department. I am grateful to Dr. Rajdeep Chowdhury for his support in performing MTT assay.

I gratefully acknowledge Neon Laboratories Ltd, Mac-Chem Products and especially Dr. Jagadeesh B. Rangisetty CEO, Biophore India Pharmaceuticals Pvt. Ltd for providing gift samples of Temozolomide, Gattefosse for providing gift samples of glyceryl monostearate, Precirol ATO5 and Compritol 888 ATO, Lipoid GmbH for the gift samples of soy lecithin and Evonik Industries for providing samples of PLGA. I also acknowledge Department of physics for providing their DST-FIST supported X-Ray diffraction facility and The Central Analytical Facility, BITS Pilani for the SEM facility.

I express my thanks to the non-teaching staff in the Pharmacy department, Mandeep Kumar, Ram Suthar Ji, Naveen Ji, Tarachand Ji, Lakshman Ji, Puran Ji, Sajjan Ji, Mahender Ji, Vishal Ji ,Mukesh Ji, Shyam Sunder Ji and Shiv Kumar Ji for their support and many a times going out of their way to facilitating things required for my research work. I also wish to thank all my students who have been a constant source of inspiration and joy.

I express my gratitude to Mrs. Dipa Saha, who with her affection and understanding nature has been a source of strength. I express my heartfelt thanks and gratitude to all my friends Kuljeet, Sangeeta, Archana, Usha, Rajesh, Tridev, Niraj, Rohit, Vikas, Shivaji, Reena, Gowher, Suhani and Swati who have supported me directly or indirectly and been by my side throughout.

“Parents are the embodiment of God on the earth” Whatever I am today is all because of my parents, the values they have inculcated in me, the love and support they have provided

throughout my life without any consideration to their own comforts and no expectations. I am and always will be indebted to my parents Mr. Roshan Lal Khosa and Mrs. Lalita Khosa for their love and belief in me. I also express my gratitude to my brother Vikram, sister-in law, Rashmi and my nephew and niece, Agastya and Bouin, for their love, encouragement, undying confidence in me and pulling me up whenever I felt low or dejected. I also wish to thank my husband Amit as all this would not have been possible without him. The decision to move to Pilani was a hard one and it is only because of him that I managed to step forward and pursue my dream of pursuing PhD. I also express my deep affection and gratitude to the apple of my eye, Gyanvi for being extremely patient, understanding, providing comfort and immeasurable unconditional love throughout.

Last but not the least I thank "The Almighty" for showering His blessings and opening new doors whenever I thought that life was over. He is the one who has always held me when I have fallen and always guided me towards realizing my dreams and live a blessed life of dignity, integrity and perseverance.

Archana Khosa

Abstract

The delivery of therapeutics to the brain especially for the treatment of brain tumors still remains a challenge despite various strategies which have been investigated over the years. The major challenge in delivery of therapeutics to the brain is the presence of the blood-brain barrier (BBB). Nanoparticulate delivery systems with their ability to protect the therapeutics from degradation cross the barriers easily because of their small size and specifically targeting various transport systems in the brain endothelial cells have developed as an attractive strategy for delivery of therapeutics across the BBB. Temozolomide (TMZ) is an anti-cancer drug approved by the USFDA for the treatment of brain tumors. TMZ needs to be given in high doses as it undergoes degradation at physiological pH into MTIC, which due to its hydrophilicity is unable to cross the BBB. Further, due to non-specific cytotoxicity it leads to various dose dependent adverse effects. The objective of this present work was to design and evaluate nanoparticulate drug delivery systems to protect TMZ from degradation and enhance its delivery to the brain with reduced adverse effects.

As analytical methods form the backbone of successful development of drug delivery systems, in-house simple, selective, accurate and precise UV-spectrophotometric and RP-HPLC (analytical and bioanalytical) methods suitable for the current work were developed and successfully validated. The analytical methods were successfully applied for the determination of TMZ during various preformulation and formulation characterization studies. The bioanalytical method was sensitive and selective for the determination of TMZ in rat plasma and various tissues. The method was successfully applied in pharmacokinetic and biodistribution studies for the pure drug and the optimized nanoparticulate formulations in rats.

Preformulation studies demonstrated that TMZ has pH independent solubility in aqueous buffers in the pH range of 1-6. Solubility in many commonly used organic solvents such as acetone, methanol, dichloromethane, acetonitrile was comparable to the aqueous media with maximum solubility observed in DMSO and least solubility in isopropyl alcohol. Solution state and solid state stability indicated that TMZ is susceptible to moisture mediated degradation and the degradation rate increases as the pH shifts from acidic to neutral and basic. DSC and FTIR studies confirmed that TMZ was compatible with the excipients

selected for the formulation development. Various formulations were fabricated including polymeric nanoparticle, solid lipid nanoparticles (SLN) and nanostructured lipid carriers (NLC). However, polymeric nanoparticles and SLN formulations were not evaluated further because of poor drug entrapment. NLC using glyceryl monostearate, Precirol ATO 5 and Compritol 888 ATO as the solid lipids and oleic acid as the liquid lipid were fabricated successfully using hot emulsion-ultrasonication technique. The formulations were easy to prepare, resulted in particles of size < 250 nm with satisfactory entrapment efficiency and drug loading. The influence of various formulation variables such as drug-to-lipid ratio, lipid-to-oil ratio and surfactant concentration on responses such as particle size, entrapment efficiency and drug loading were studied in detail using Design of Experiments (DOE). Extended drug release for 24 h was observed during in vitro release studies of the optimized formulations.

The SEM images revealed that the particles were anisometric in shape with an irregular surface.

The particles were easily redispersible after freeze drying and no significant change was observed in particle size, entrapment efficiency and drug release for formulations stored under refrigerated condition for 6 months. In vitro cytotoxicity study by MTT assay showed that the TMZ loaded nanoparticles were more cytotoxic as compared to the pure drug.

The pharmacokinetic and biodistribution studies of TMZ and the NLC formulations by i.p route of administration showed that compared to pure TMZ solution, the NLC formulations showed higher AUC and prolonged residence time in the rat vasculature. Further, an enhanced permeation of TMZ into the brain was observed for all the three formulations compared to the TMZ solution. Studies showed low uptake of nanoparticles in the heart and kidneys, reducing the possibility of adverse effects on the organs. During the course of the study, no adverse events were observed indicating that the nanoformulations were well tolerated by the rats.

Collectively, the results indicate that the optimized NLC formulations of TMZ are promising candidates to enhance delivery of TMZ in the brain with the possibility of reducing the dose and the adverse effects.

List of Tables

List of Figures

Abbreviations and Symbols

%	Percentage
% CDR	Percentage cumulative drug release
% RSD	Percentage relative standard deviation
% RTD	Percentage remaining to be degraded
%, w/w	Percentage weight by weight
%, w/v	Percentage weight by volume
% CV	Percentage coefficient of variance
λ_{max}	Wavelength of maximum absorbance
<	Less than
>	More than
≤	Less than equal to
≥	More than Equal to
=	Equal to
≈	Approximately equal to
σ	Standard deviation of y intercept of regression equation
˚C	Degree Centigrade
3D	Three dimensional
µm	Micrometer
µL	Micro liter
µg mL^{-1}	Micro gram per milliliter
µg L^{-1}	Microgram per liter
µg h L^{-1}	Micro gram hour per liter
α	Alpha
β	Beta
β'	Beta prime
β	Shape parameter
AC	Acetone
ACN	Acetonitrile
AFM	Atomic force microscopy
AGT	O^6-alkylguanine transferase
AIC	Akaike Information Criterion
AIC	5-amino-imidazole-4-carboxamide
ALL	Acute lymphoblastic leukemia
AMT	Adsorption mediated transport
ANC	Absolute neutrophil count

ANOVA	Analysis of variance
API	Active pharmaceutical ingredient
AT	Accelerated temperature
AUC	Area under curve
AUMC	Area under the first moment curve
$AUC_{(0-\infty)}$	Area under plasma concentration-time curve
BBB	Blood brain barrier
BBD	Box-Behnken design
BCS	Biopharmaceutical classifications system
BER	Base excision repair
CAF	Central animal facility
CBTRUS	Central Brain Tumor Registry of the United States
CCT	Critical crystallization temperature
CDS	Chemical delivery system
CF	Continuous flow
CL/F	Oral clearance
CL_{cr}	Creatinine clearance
cm	Centimeter
cm^2	Centimeter square
CMC	Critical micelle concentration
CMT	Carrier mediated transport
CNLC	TMZ loaded Compritol nanostructured lipid carriers
CNS	Central nervous system
CNT	Carbon nanotubes
C_{max}	Maximum concentration
CMV	Cytomegalovirus
COM	Compritol 888 ATO
Conc.	Concentration
cps	Centipoises
CPCSEA	Committee for the Purpose of Control and Supervision of Experiments on Animals
CR	Controlled release
CRT	Controlled room temperature (25 ± 2 ºC/60 ± 5 % RH)
C_0	Initial drug loading in the matrix
C_s	Saturation solubility
CSF	Cerebrospinal fluid
CTC	Common toxicity criteria

CyP450	Cytochrome P450
D	Diffusion coefficient
Da	Daltons
DCM	Dichloromethane
DM	Dialysis membrane
DMSO	Dimethyl sulfoxide
DNA	Deoxyribonucleic acid
DL	Drug loading
DLS	Dynamic light scattering
DOE	Design of experimentation
DOPA	Dihydroxyphenylalanine
DSC	Differential scanning calorimetry
D_TR	Diphtheria toxin receptor
EA	Ethyl acetate
EE	Entrapment efficiency
EDTA	Ethylene diamine tetra acetic acid
EMA	European medicine agency (EMA)
EPR	Enhanced permeation and retention
ESR	Electron spin resonance
EtOH	Ethanol
F	Fraction (%) of drug released in time t
FESEM	Field emission scanning electron microscope
FFD	Fractional factorial design
F_r	Relative bioavailability
FT	Refrigerated temperature (5 ± 2 °C)
FTIR	Fourier transform infra-red
FUS	Focused ultrasound
g	Gram
g L^{-1}	Gram per liter
GLUT	Glucose transporter
GMS	Glyceryl monostearate
GNLC	TMZ loaded glyceryl monostearate nanostructured lipid carriers
h	Hour
HCl	Hydrochloric acid
HETP	Height equivalent to theoretical plates
HIV	Human immunodeficiency virus
HPLC	High performance liquid chromatography

HPLC-MS/MS	High performance liquid chromatography-tandem mass spectrometry
HPTLC	High performance thin layer chromatography
HPH	High pressure homogenization
HQC	Higher quality control sample
HRP	Horseradish peroxidase
5-HT	5-Hydroxytryptamine
IAEC	Institutional Animal Ethics Committee
ICH	International conference on harmonization
IPA	Isopropyl alcohol
i.p	Intraperitoneal
IS	Internal standard
i.v	Intravenous
J g^{-1}	Joule per gram
k’	Capacity factor
k_{BL}	Combined release constant in Baker-Lonsdale model
k_{HC}	Release constant in Hixson-Crowell model
k_{KP}	Release rate constant for 'Korsmeyer-Peppas’ empirical equation
k_{MB}	Release rate constant for Makoid- Banaker
K_0	Zero order release rate constant
K_1	First order release rate constant
K_{deg}	Degradation rate constant
Kg	Kilogram
kg cm^{-2}	Kilogram per square centimeter
K_H	Higuchi release constant
L	Liter
L day^{-1}	Liter per day
L kg^{-1}	Liter per kilogram
LCMS	Liquid chromatography coupled with mass spectrophotometer
L $h^{-1}kg^{-1}$	Liter per hour per kilogram
L kg^{-1}	Liter per kilogram
Lec	Soy lecithin
LLOQ	Lower limit of quantification
LOD	Limit of detection
log % RTD	Log percentage remaining to be degraded
log P	Log of oil water partition coefficient
LOQ	Limit of quantification
LQC	Lower quality control

M	Molar
MALS	Multi-angle light scattering
MCT	Medium chain triglycerides
MEKC	Micellar electrokinetic capillary chromatography
MeOH	Methanol
MDS	Myelodysplastic syndrome
MDT	Mean dissolution time
mg	Milligram
mg day^{-1}	Milligram per day
mg mL^{-1}	Milligram per milliliter
MGMT	O6-methylguanine-DNA methyltransferase
mL	Milliliter
mL min^{-1}	Milliliter per minute
mM	Millimolar
mm	Millimeter
mm sec^{-1}	Millimeter per second
MMR	Mismatch repair
MTIC	Monomethyl triazeno-imidazole carboxamide
MQC	Medium quality control
MRI	Magnetic resonance imaging
MRP	Multidrug resistance associated protein
MRT	Mean residence time
MSC	Model selection criterion
MW	Molecular weight
MWNT	Multiwalled carbon nanotubes
N	Number of theoretical plates
n	Diffusional exponent indicative of release mechanism in Korsmeyer-Peppas model
NDDS	Novel drug delivery systems
ng mL^{-1}	Nanogram per milliliter
NHL	Non-Hodgkin's lymphoma
NIR	Near infra-red
NLC	Nanostructured lipid carriers
nm	Nanometer
N7-MeG	N^7 position on guanine
N3-MeA	N^3 position in adenine
OA	Oleic acid

O3-MeA	O^3 on adenine
O6-MeG	O^6 on guanine
O/W	Oil-in-water
O/F/W	Oil-in-fat-in-water
OSN	Olfactory sensory neurons
PARP	Poly ADP ribose polymerase
PB	Phosphate buffer
PBCA	Polybutyl cyanoacrylate
PCL	Poly-ε-caprolactone
PCS	Photon correlation spectroscopy
PCP	*Pneumocystis carinii* pneumonia
PD	Parkinson's disease
PDI	Polydispersity index
PEG	Polyethylene glycol
P-gp	P-glycoprotein
pH	Negative log to the base 10 of hydrogen ion concentration
pKa	Acid dissociation constant
p-value	Significance level in statistical tests (probability of a type I error)
$P_{o/w}$	Equilibrium partition coefficient
PLA	Poly(D,L-lactide)
PLGA	D,L-lactide-co-glycolide
PNLC	TMZ loaded Precirol nanostructured lipid carriers
PRC	Precirol ATO 5
PVA	Poly vinyl alcohol
QC	Quality control
QELS	Quasi-elastic light scattering
QLS	Quasi light scattering
R	Mean $AUC_{0\text{-}24h}$ ratio
R^2	Regression coefficient
R_f	Retention factor
RES	Reticuloendothelial system
RH	Relative humidity
RMT	Receptor mediated transport
RP-HPLC	Reverse phase-high performance liquid chromatography
rpm	Revolutions per minute
R_s	Resolution
RSD	Relative standard deviation

R_t	Retention time
S	Slope of the least square regression line
SA	Stearic acid
SANS	Small angle neutron scattering
SAXS	Small angle X-Ray scattering
SD	Standard deviation
SDC	Sodium deoxy cholate
SDS	Sodium dodecyl sulfate
Sec	Seconds
SEM	Scanning electron microscopy
SLN	Solid lipid nanoparticles
SPE	Solid phase extraction
SS	Sample and separate method
NMR	Nuclear magnetic resonance spectroscopy
SWNT	Single walled carbon nanotubes
T	Temperature
TEM	Transmission electron microscopy
T_f	Tailing factor
Tf_R	Transferrin receptor
$t_{1/2}$	Half-life
TJ	Tight junction
$t_{50\%}$	Time to reach 50% of initial concentration
$t_{90\%}$	Time to reach 90% of initial concentration
TDW	Triple distilled water
T_m	Melting temperature
T_{max}	Time taken to reach maximum concentration
TMZ	Temozolomide
USA	United States of America
USFDA	United States Food and Drug Administration
USP	United States Pharmacopoeia
UV	Ultra Violet
VEGF	Vascular endothelial growth factor
Vd	Apparent volume of distribution
Vis	Visible
v/v	Volume by volume
w/w	Weight by weight
WHO	World Health Organization

WGA-HRP	Wheat germ agglutinin-horseradish peroxidase
XRD	X-ray diffraction method
ZP	Zeta potential

Table of Content

1. Introduction

1.1. Cancer and Brain Tumors

Cancer is world's second leading cause of mortality after cardiovascular diseases. It is a group of diseases which can affect any organ of the body where the body's cells deviate from the normal cellular processes leading to unregulated division. These unregulated masses of cells, commonly known as tumors may remain within the tissue of origin (in-situ cancer) or may begin to invade neighboring tissues (invasive cancer). Invasive tumors are malignant and the cells shed can travel through blood or lymph to various other organs and establish new tumors, a phenomenon known as metastasis. There are more than hundred different types of cancer and each type has its own unique features with respect to behavior and response to treatment. However, there are a number of biological and biochemical features which are common to all cancers [1,2]. The following characteristics have been identified which enable the cancer to proliferate and metastasize. They are

1. Self-sufficiency in generating many of the growth signals, thereby unlike normal cells are not dependent on exogenous growth signals for cell growth and division cycle.
2. Insensitivity to anti-growth signals by disrupting and/or evading anti-proliferative signals.
3. Resisting apoptosis by inactivating the p53 function, overexpressing anti-apoptotic regulators or survival signals, downregulating pro-apoptotic factors or by disrupting the extrinsic-ligand induced death pathway.
4. Capability to infinitely replicate by upregulation of telomerase enzyme which prevents telomerase deterioration over replication cycles besides preventing cellular senescence.
5. Inducing angiogenesis by upregulating angiogenesis inducers such vascular endothelial growth factor (VEGF) expression and countervailing inhibitors.
6. Initiating invasion of tissues and metastasis by altering gene expressions which results in cell migration and metastasis.
7. Initiation and development of genomic instability in cancer cells, which generates random mutations including chromosomal rearrangements besides activating characteristics.

8. Inflammation promoted by the tumor which activates a number of other hallmarks such as supplying bioactive molecules to the tumor microenvironment, survival factors which prevent cell death, pro-angiogenic factors etc. Furthermore, inflammatory cells release reactive oxygen species which can further cause mutations.
9. Modifying the energy metabolism mainly to glycolysis even in the presence of oxygen leading to a state of "aerobic glycolysis" and upregulating glucose transporters, mainly GLUT1, which increases the transport of glucose to tumor cell cytoplasm.
10. Avoiding detection and destruction by immune cells by disabling them.
11. Losing the ability of cell differentiation [3-5].

The term "brain tumors" implies to a collection of neoplasms which originate within the brain (primary tumors) or from cells in the brain metastasized from systemic tumors (secondary tumors) (Fig.1.1) [6]. Each type of tumor has characteristic histopathology, molecular and genetic profile, clinical spectrum, patient prognosis and treatment possibilities. According to the Central Brain Tumor Registry of the United States (CBTRUS), the age adjusted overall annual average incidence rate for brain tumors from 2007 to 2011 was 21.42 per 100,000 persons. Brain tumors are also the most common form of cancer amongst children. Although, brain tumors account for only 2% of all cancers they cause disproportionately high morbidity and mortality irrespective of gender, racial or other demographic differences. The approximate 5-year survival rate for all malignant brain tumors is around 33% [7] .

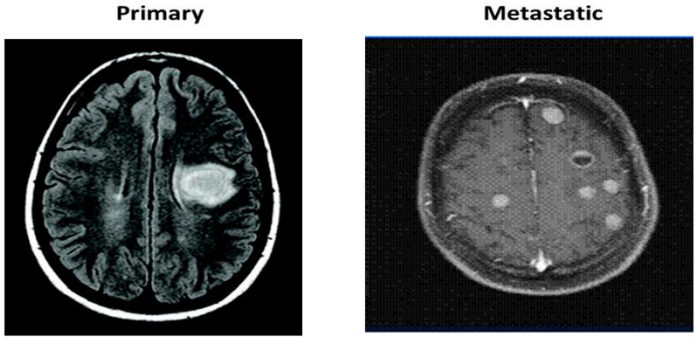

Fig. 1.1. MRI scan of primary and metastatic brain tumors [8]

The diagnosis and classification of brain tumors follows the *World Health Organization* (*WHO) Classification of Tumors of the Central Nervous System* (CNS) which was first published in 1979. It classified CNS tumors based on histological parameters. It also included a grading system (Table 1.1) for tumors based on their microscopic appearance and malignancy scale. This classification was revised in 2016 and now includes both histological and molecular genetic parameters [8,9].

Table 1.1. WHO grading system of CNS tumors on malignancy scale

Grade I Tumor • Slow growing cells • Almost normal appearance under a microscope • Least malignant • Usually associated with long term survival	**Grade II Tumor** • Relatively slow growing cells • Slightly abnormal appearance under a microscope • Can infiltrate adjacent normal brain tissue • Can recur as a high grade tumor
Grade III Tumor • Actively reproducing abnormal cells • Abnormal appearance under a microscope • Infiltrate adjacent normal brain tissue • Tumor tends to recur, often as a higher grade	**Grade IV Tumor** • Abnormal cells which reproduce rapidly • Very abnormal appearance under a microscope • Form new blood vessels to maintain rapid growth • Areas of dead cells (necrosis) in center

The most frequently occuring brain tumors which account for more than 70% of all brain tumors are the gliomas of astrocytic, oligodendroglial and ependymal origin. The most frequent (65%) and most malignant type is glioblastoma multiforme (GBM), the grade IV astrocytoma. The prognosis for GBM patients is very poor with less than 3% surviving at 5 years after diagnosis [10,11].

Even with technological advances in conventional treatments of surgery and radiation, the first line of treatment, cure is not assured. Simultaneously chemotherapy is also necessary. However, majority of malignant tumors spread rapidly and lead to debilitating disease resulting in mortality. This is due to the diffuse infiltrative nature of the cancer, tumor heterogeneity and poor penetration of chemotherapeutic drugs across the blood brain barrier (BBB) [12].

Chemotherapy plays an important role in the treatment of brain cancer. Treatment of brain tumors with chemotherapeutic agents is a big challenge as the CNS is protected by the BBB, which controls the permeation of molecules including therapeutics, proteins and cells, making it highly selective. The BBB is composed of endothelial cells lacking intracellular fenestrations and linked by tight junctions (TJs) restricting the entry of various compounds from the bloodstream into the brain. Additionally, there exists a well characterized network of efflux transporters that actively substrates from the brain into the bloodstream. Thus, it is a big challenge to design a delivery system which will selectively deliver the drug to brain or CNS. The presence of tumors in the brain also causes changes in the BBB, which are highly variable and also highly changeable both within individual tumors as well as between distinct tumors [13].

1.2. Strategies for Delivery to the Brain

Despite the fact that the BBB poses challenges in achieving therapeutic concentrations in the brain, several strategies have been used to enhance delivery of therapeutics to the brain. The approaches are:

a) Modification of the drug molecule
b) Direct administration into the brain
c) BBB modification/disruption
d) Utilizing endogenous transport systems
e) Bypassing the BBB by intranasal administration

1.2.1. Modification of the Drug Molecule

The predominant mechanism of delivery of molecules across the BBB is passive diffusion which in turn is dependent on the lipophilicity and molecular size. Molecules

with high lipophilicity (which form less than 8 hydrogen bonds) and small molecular weight (preferably less than 500 Da) are able to cross the BBB [14]. Enhancement in passive diffusion can be achieved by chemical structure modification of molecules to improve their unfavorable physicochemical properties like solubility and membrane permeation [15]. To improve the BBB permeability drug molecules can be designed as lipophilic analogs, prodrugs and chemical delivery systems.

In lipidization, the drug moiety is converted into a more lipophilic form by introduction of lipophilic groups like methyl- or chlorine-, esters. The classic example of enhanced BBB permeability by increasing lipophilicity is that of morphine and heroin. Modification of morphine to heroin by acetylation of 3- and 6- hydroxy groups results in >100 fold increase in lipophilicity resulting in 100 fold more uptake in the brain. Once in the brain, it gets hydrolyzed back into morphine, which being more hydrophilic diffuses slowly out of the brain, thereby prolonging the residence time and hence the time of action in the brain [16].

Prodrugs are inactive or less active derivatives of drug molecules that undergo chemical or enzymatic transformation in-vivo to release the active drug moiety responsible for eliciting pharmacological effects. Depending on the purpose for which the prodrug has been designed, the transformation into active moiety may occur prior to, during, or after absorption or into a specific tissue or organ [17]. Temozolomide is a prodrug which under physiological pH undergoes hydrolytic ring opening to monomethyl triazeno-imidazole carboxamide (MTIC). MTIC further undergoes fragmentation to give methyl-diazonium ions which methylates the DNA [18,19].

Chemical delivery system (CDS) involves the introduction of two types of moieties to a molecule of therapeutic importance, both of which are removed biologically in-vivo. One being a targetor is responsible for site-specific action, targeting and lock-in and the other/s are modifier functions which increase the lipophilicity of the compound. Estradiol CDS (Estredox) is a lipophilic drug with a Log P value of 3.3 and its derivatization with bio-removable lipophilic targetor moiety dihydrotrogonelline, resulted in enhanced permeation in the brain [20].

1.2.2. Direct Administration into the Brain

Direct delivery of drugs to the brain prevents the problems associated with the BBB permeation, systemic toxicity and the need for surface modification of the delivery vehicle. It includes administration of drugs directly into the brain, via injections, infusions, implants as well as convection enhanced delivery, therefore higher concentrations of the drug are achieved at the site. Furthermore, all types of therapeutic agents including macromolecules and nanocarriers can be administered by this route. This delivery method suffers from various limitations such as limited drug permeation distance because of slow diffusion and high elimination rate of the drug besides the highly invasive nature which increases the risk of infections, inflammation, edema and damage to the brain tissue. It is most often used for treating malignant gliomas such as GBM where effective treatment is a huge challenge and if the target is close to the ventricles. [21,22]

1.2.3. Drug Delivery by BBB Disruption

Under normal conditions the presence of TJs restricts the paracellular diffusion of molecules in the BBB. Various modulators ranging from chemical and biological substances to physical stimuli such as focused ultrasound and electromagnetic fields cause temporary alteration of the TJs leading to an increase in the permeability of the BBB and providing access to a wide range of compounds. TJ opening or BBB leakage is associated with many pathological conditions of the CNS such as ischemic stroke, brain tumors, epilepsy and many neurodegenerative diseases also [23].

Hyperosmotic disruption of the BBB follows the mechanism of drawing out water from the endothelial cells into the blood vessel lumen, leading to shrinkage of the endothelial cells. The resultant loss of water from the brain leads to vasodilation and stretching the endothelial cells. Furthermore, the endothelial cell cytoskeleton contracts via a calcium dependent mechanism resulting from interactions between actin and cadherin. As a result of all these mechanisms, the TJs widen and allow paracellular transport into the brain. Commonly used osmotic agents are mannitol, urea and arabinose. Intracarotid infusion of mannitol maintains the permeable state of the BBB for 15 minutes to 4h depending on the size of the molecule.

Chemical BBB disruptors include intraarterial vasoactive agents which cause temporary inflammation in the endothelial cells. Alkylglycerols destabilize the endothelial cell

membrane leading to BBB opening for 3-15 minutes. Other agents that have been explored include cytokine, interleukin, leukotriene c4, bradykinin, Cereport (RMP-7), nitric oxide, 5-hydroxytryptamine (5-HT), histamine and surfactants such as Tween 80 or sodium dodecyl sulfate [24-26].

Focused ultrasound (FUS) mediated delivery is a targeted, non-invasive and repeatable potential way to introduce transient BBB opening for the delivery of therapeutics to the brain with minimal side effects. FUS concentrates acoustic energy and deposits it in a small target region in the brain with minimal effect on the surrounding tissue. The focal point is contained at that small region at a specific distance from the transducer surface. When electrical energy is applied, the transducer converts that energy into mechanical motion, generating ultrasound which propagates through the skull and the brain causing several effects such as pressure variation, acoustic fluid streaming, cavitation and local hyperthermia. These effects enhance BBB permeability probably by causing shear in the cells activating pathways associated with permeability and disruption of TJ proteins. The magnetic resonance imaging (MRI) assisted FUS helps in better targeting and assessment of BBB opening in addition to providing enhanced diagnostic and therapeutic capabilities [27-29].

1.2.4. Strategies Utilizing Endogenous Transport Systems

The BBB is reported to express several influx and efflux transporters which control the permeability of various molecules including therapeutics into the brain. The transport systems can be classified into five broad categories, namely, 1) carrier-mediated transport (CMT); 2) ion-transport; 3) receptor-mediated transport (RMT); 4) adsorption-mediated transport (AMT) 5); cell-mediated transport and 6) active efflux transport.

1.2.4.1. Inhibition of Efflux Transporters

Efflux transporters like P-glycoprotein (P-gp) and members of the multidrug resistance associated protein (MRP) family which are involved in actively pumping substrates from the cerebral capillary endothelium back into the bloodstream before they cross the brain parenchyma. This makes the achievement of therapeutic concentrations of many drugs including vinca alkaloids, cyclosporine, daunomycin, verapamil, nifedipine, progesterone and taxol a challenge [30,31]. Furthermore, they play an important role in conferring multi-drug resistance, especially to tumor cells. The uptake of therapeutics can be achieved by P-

gp modulation at several levels: 1) downregulation of P-gp expression at the transcriptional or translational levels; 2) alteration of membrane targeting after P-gp synthesis and 3) use of P-gp transport inhibitors. Tariquidar, a third generation inhibitor is the most promising drug candidate which sufficiently inhibits P-gp at the BBB in-vivo by non-competitively binding to P-gp in nanomolar concentrations. The drug has shown dose linear responses and acceptable tolerability profile [32].

1.2.4.2. Delivery via Endogenous Mediated Transport Systems

CMT is responsible for transport of nutrients like hexoses (glucose, galactose), neutral amino acids (phenylalanine, DOPA, methionine), basic amino acids (lysine), acidic amino acids (glutamate), purines, nucleosides, monocarboxylic acids (lactate, pyruvate, ketone bodies), amines (neuropeptides, thyroid hormones, thiamine) and vitamins from blood to the brain [33,34]. RMT involves transport of endogenous large molecules to the brain such as iron, insulin, insulin-like growth factors, leptin, angiotensin II and brain natriuretic peptide. The most commonly known receptors involved in RMT are: i) Transferrin receptor (TfR) ii) Insulin receptor iii) Lipoprotein receptor and iv) Diphtheria toxin receptor (D_TR) [35,36]. AMT is a non-selective transport system involving interactions based on charge which can also be utilized for transport of therapeutics. Both AMT and RMT are saturable transport processes. AMT has lower binding affinity but higher binding capacity than RMT as it gets saturated at higher concentrations than the latter [37]. It is now known that the BBB allows selective entry of immune cells such as lymphocytes (monocytes, neutrophils and lymphocytes) into three distinct anatomical compartments i.e. cerebrospinal fluid (CSF), meninges and parenchyma of the brain that have an bearing on the CNS under physiological conditions as well as disease states. Some pathogens such as *Cryptococcus neoformans* and the human immunodeficiency virus (HIV) also rely on the monocytes or macrophages to cross the intact BBB. Apart from the immunocytes, stem cells also act as Trojan horses carrying hidden therapeutic cargoes across the BBB and thus have emerged as a novel delivery system for therapeutics to combat pathological conditions of the CNS including glioma [38].

The various transporters in the BBB are shown in Fig. 1.2.

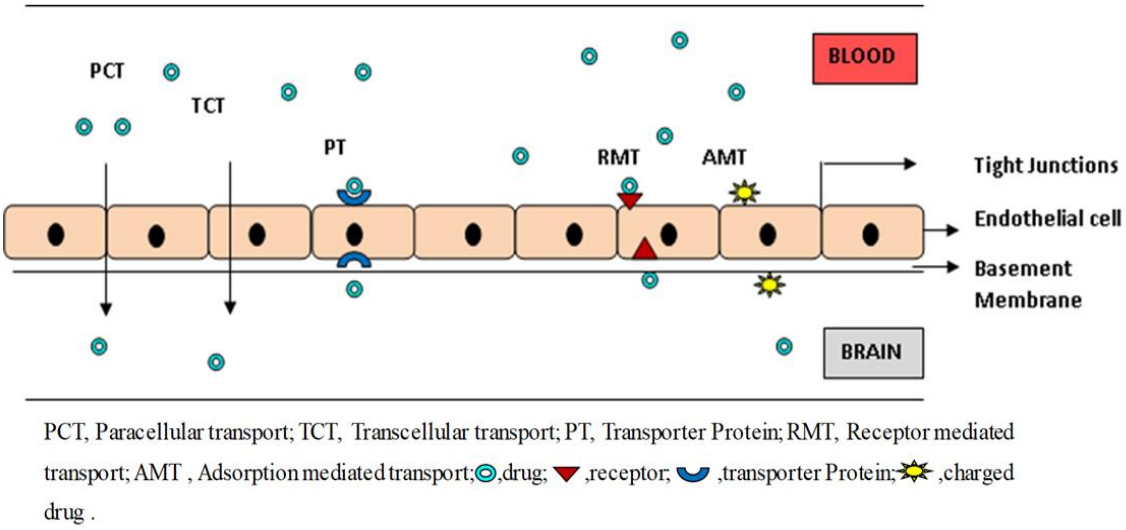

PCT, Paracellular transport; TCT, Transcellular transport; PT, Transporter Protein; RMT, Receptor mediated transport; AMT , Adsorption mediated transport; ,drug; ,receptor; ,transporter Protein; ,charged drug .

Fig. 1.2. Schematic diagram of the blood-brain barrier (BBB) and its transport mechanisms

The delivery via transport system has the following characteristics:

i. The drug is modified, for instance conjugated to a ligand or polymer which acts as a homing device and masks the intrinsic properties of the molecule.

ii. The drug is encapsulated in a delivery system, like nanoparticles, liposomes or niosomes, the surface of which is modified with a homing device and a hydrophilic polymer like polyethylene glycol to prolong the circulation time.

iii. The homing device and the delivery system should be non-immunogenic and capable of interacting with receptors at the BBB.

iv. The homing device must be target specific so as to avoid adverse effects and increase in transporter efficiency.

v. All systems must have a uniform and controlled size to control their biological fate.

The system should fulfill all the above criteria and for best response the target should be upregulated by the pathological condition [24].

1.2.5. Delivery by Bypassing the BBB via Intranasal Administration

Intranasal delivery has emerged as a potential route for delivery to the brain in a non-invasive manner. It not only circumvents the BBB but also provides rapid absorption of the therapeutics due to high surface area, minimizes effects of systemic administration such as hepatic first pass metabolism, systemic dilution, need for higher doses in addition to being a safer alternative [39]. Drugs administered by intranasal route can reach the brain using three main pathways: i) absorption across the nasal epithelium into the systemic circulation, from where it can reach the CNS via BBB, ii) transport via olfactory neurons or iii) trigeminal nerve pathway [40]. Transport of drugs to the brain intranasally can occur by both intracellular and extracellular pathways. Intracellular pathways include endocytosis into olfactory sensory neurons (OSN) and subsequent intra neuronal transport to the olfactory bulb. OSN have been shown to endocytose viruses, for instance, herpes, poliomyelitis, rhabdoviruses as well as large molecules such as horseradish peroxidase (HRP), wheat germ agglutinin-horseradish peroxidase (WGA-HRP) and albumin from the nasal passage. However, this process is very slow. Extracellular pathway which involves paracellular diffusion is much faster and is responsible for the rapid onset of action [41,42].

The physicochemical characteristics of the drug has an impact on the delivery of therapeutics with only small molecules of size > 500 Da and log P < 3.5 easily crossing the BBB via systemic circulation. Larger molecules can travel via the olfactory trigeminal pathway [43]. This route has been successfully used as a potential drug delivery route for delivery of challenging drugs which do not easily cross the BBB, such as polar low molecular weight molecules, peptides, proteins, vaccines, genes, DNA and plasmids. Nasal mucociliary clearance limits the time of absorption of drugs as does the low permeability of the nasal mucosa. However, inclusion of mucoadhesives like chitosan, various thermosensitive and ionic gelling systems in the formulations can help in enhancing absorption of therapeutics by retaining the drug in the nasal epithelium for longer periods, protecting the drug from nasal enzymes, increasing drug load and controlling the rate of drug release [44]. Many therapeutic proteins are also prone to enzymatic degradation in the nasal cavity. Nanocarriers have provided an alternative as they protect the drug from degradation and have been reported to enhance delivery to the brain utilizing transocytotic mechanisms. At the cellular level, size of the particles play an important role in internalization with particles below the

size of 50-100 nm showing rapid internalization as compared to 200 nm particles transcellularly [45].

1.3. Nanocarriers for Drug Delivery

Nanocarriers have shown promise in the delivery of therapeutics across the BBB in a controlled and non-invasive manner without interfering with the normal functioning of the brain. Nanoparticles are solid colloidal particles ranging in size from 1 to 1000 nm (1μm) consisting of macromolecular materials in which the active principle (drug or biologically active material) is dissolved, entrapped or encapsulated, or to which the active principle is adsorbed or attached. Depending on the method of preparation, nanospheres, nanoparticles or nanocapsules can be fabricated which display different properties and release kinetics optimal for delivery of the encapsulated drug [46].

Nanocarriers in the form of inorganic, polymeric and lipid nanoparticles, liposomes, micelles, nanogels, nanoemulsions, carbon nanotubes, dendrimers, polymerosomes and exosomes have led to significant advances with regard to:

i. Encapsulation of different types of molecules, ranging from high to low molecular weight, hydrophilic, lipophilic, proteins and genetic material.
ii. Modification of in vivo release, pharmacokinetic profile and biodistribution of the loaded molecules.
iii. Preferential targeting of otherwise inaccessible organs such as the brain.
iv. Selective targeting at the desired diseased sites including the subcellular organelles.
v. Broad spectrum of applications ranging from therapy for diseases such as cancers, neurological disorders, better vaccines, gene therapy and improved diagnostic imaging systems.
vi. Administration by all routes (oral, nasal, pulmonary, topical, ophthalmic, intracarotid and intravenous) [47].

For increased stability and half-life, the nanocarrier should stay in the circulation for longer periods by avoiding glomerular filtration and uptake by the reticuloendothelial system (RES). Size, surface charge, surface properties, morphology and composition of the matrix plays an important role in their fate in-vivo. In general, neutral particles and those that have

a particle size of approximately 100 nm show prolonged blood circulation and low uptake by the RES. Furthermore, modification of the surface with certain hydrophilic polymers such as polyethylene glycols (PEGs) sterically stabilize the nanocarriers and increase their circulation time [48,49].

Nanoparticles can be targeted to the tumor both actively and passively. In passive targeting the nanoparticles accumulate in the tumors by the enhanced permeation and retention (EPR) effect taking advantage of the leaky vasculature. In active targeting the surface of nanoparticles can be modified by conjugation with ligands such as proteins, antibodies, peptides that have an affinity for cellular receptors or components overexpressed and/or present at the target site [50,51].

The field of nanotechnology is rapidly growing and novel nanocarriers are being introduced as carriers for therapeutics. They include nanocrystals, liposomes, polymeric nanoparticles, lipid nanoparticles, polymer drug conjugates, hydrogels, dendrimers, polymeric micelles, nanoemulsions and a range of inorganic nanoparticles such as carbon nanotubes, gold nanoparticles, supramagnetic nanoparticles, quantum dots and ceramic nanoparticles. The various types of nanoparticles are shown in Fig. 1.3 [52]

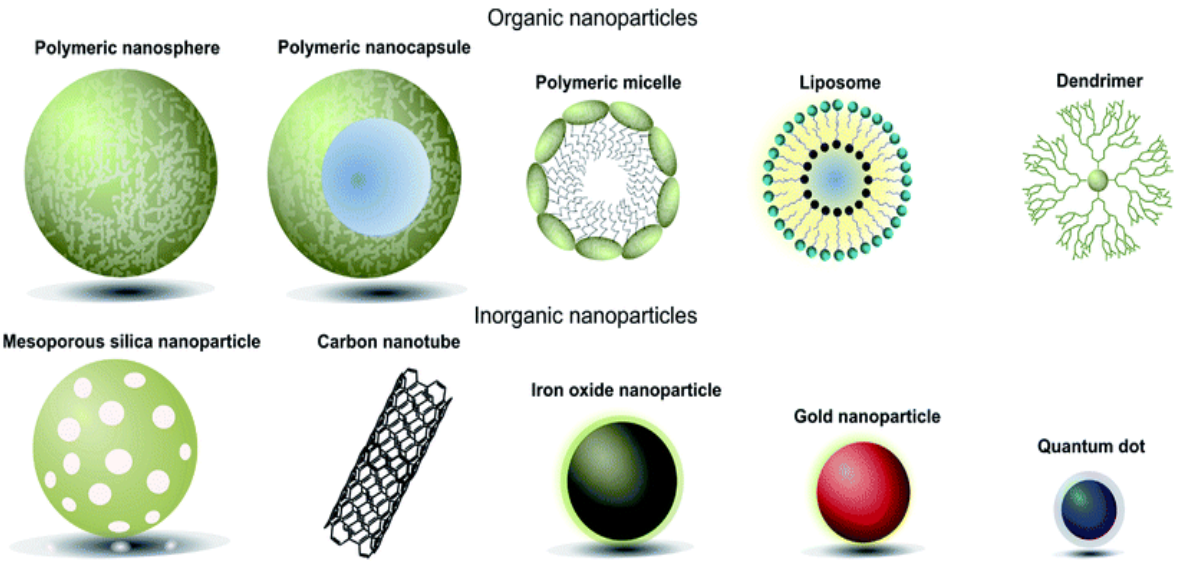

Fig. 1.3. Types of nanocarriers used in biomedical applications [52]

1.3.1. Nanocarriers for Delivery to the Brain

The types and characteristics of various nanocarriers that have been extensively used for delivery of drugs to the brain are summarized in Table 1.2.

Nanocarriers enhance delivery of therapeutics to the CNS possibly involving the following mechanisms:

i. Enhanced retention of the nanoparticles in the endothelial microvessel cells at the BBB by adsorption, creating a higher drug concentration gradient that increases the transport across the BBB.

ii. Inhibition of the efflux transport systems especially P-gp.

iii. A general toxic effect on the brain vasculature.

iv. Surfactant effect characterized by solubilisation of the endothelial cell lipids leading to membrane fluidization and enhanced BBB permeation.

v. Opening of the TJs at the BBB.

vi. Endocytosis by endothelial cells followed by release within these cells.

vii. Transcytosis through the endothelial cell layer.

viii. A combination of above effects [53].

Furthermore, enhanced delivery of nanocarriers to the brain can be achieved in combination with various other strategies such as cationization, use of pharmacological efflux inhibitors, vasoactive agents, hyperosmotic approach, olfactory delivery via intranasal route, focused ultrasound and microbubbles [51]. A wide range of polymers, both natural and synthetic can be utilized for the fabrication of nanoparticles. However, biodegradability and biocompatibility are critical parameters to be taken into consideration when selecting polymers. The choice of polymers also influences the characteristics of the formulation, especially the drug loading efficiency and drug release kinetics [54].

1.4. Nanostructured Lipid Carriers

Nanostructured lipid carriers (NLC) are new generation of lipid nanoparticles which were developed to overcome the limitations of solid lipid nanoparticles (SLN). NLC also exists as a solid matrix of lipids at room and body temperature. However, instead of using only a solid lipid, a portion is replaced by an oil, which results in a less ordered lipid matrix

providing increased drug loading and preventing leaching out of the drug during storage [97,98].

Based on the variation in the composition of lipid and oil mixtures in addition to the various fabrication methods, NLC can be categorized into three types.

1) Imperfect type NLC: Spatially different lipids are blended such as glycerides, which are composed of number of fatty acids. This results in imperfections in the crystal order. The drug loading can be further increased by increasing imperfections by using a mix of various glycerides, varying in saturation and length of C-chains.
2) Amorphous type NLC: A structureless amorphous matrix is formed by mixing special lipids such as hydroxyoctacosanyl hydroxystearate or iso-propyl myristate with the solid lipid. As the NLC exists in an amorphous state rather than an ordered state, drug expulsion resulting from β-modification during storage is prevented.
3) Multiple O/F/W type contains numerous nanosized liquid oil compartments distributed in the solid matrix. Drug solubility is higher in these nanosized compartments resulting in increased drug loading. However, the release is still prolonged because the compartments are surrounded by a solid lipid matrix [99-101].

Fig. 1.4 illustrates the various types of NLC in comparison to SLN.

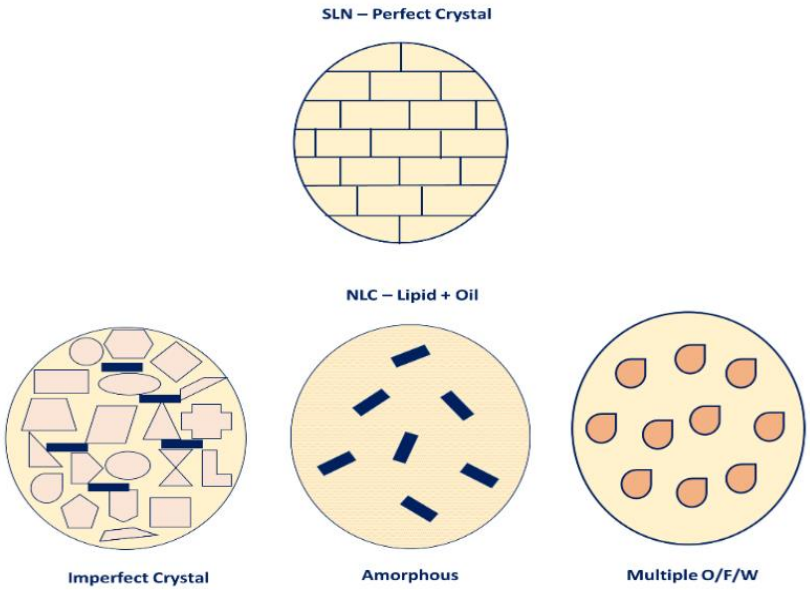

Fig.1.4. Types of NLC compared to crystalline SLN [102]

Table 1.2. Nanocarriers for delivery to the brain

Nanocarriers	Characteristics	Therapeutics Investigated
Liposomes	Vesicular bilayers composed of amphiphilic lipids. Cholesterol and phospholipids are important components Classified into unilamellar and multilamellar vesicles Hydrophilic drugs are entrapped in the aqueous core whereas hydrophobic drugs are entrapped in the lipids. Biocompatible, biodegradable, low toxicity, targeted delivery and controlled release. Leaching out of hydrophilic drugs take place. Phospholipids are prone to oxidation and hydrolysis Rapid removal from circulation by RES [55,56]	Amphotericin B (AmBisome®) Daunorubicin (DaunoXome®) Cytarabine (DepoCyt®) Doxorubicin (Doxil®) [55] 5-Fluorouracil [57] Methylprednisolone [58] Rivastigmine [59]
Polymeric Nanoparticles	Prepared from biodegradable and biocompatible polymers such as polycaprolactone (PCL) poly (D,L-lactide-co-glycolide)(PLGA),poly(D,L-lactide) (PLA), polybutyl cyanoacrylates (PBCA), chitosan. Easy to prepare and have better control over drug release. Due to toxicity, residual solvents, cost and difficulty in scale up. [25,60,61]	Olanzapine [62] Rivastigmine [63] Tacrine [64] Doxorubicin [65] siRNA [66]
Lipid Nanocarriers	Include SLN, NLC and lipid drug conjugates Composed of biocompatible and biodegradable lipids Scale up feasibility Degradation mainly occurs by lipases Poor encapsulation for hydrophilic drugs	Camptothecin [67] Baicalein [68] Risperidone [69] Quinine hydrochloride [70] Olanzapine [71]
Dendrimers	Highly branched, monodisperse macromolecules with a large number of functional groups to which a variety of molecules can be attached. Hydrophobic drugs are complexed within the hydrophobic core enhancing solubility or attached covalently or non-covalently to the surface Difficult to control release, possible cytotoxicity Defects in higher generation dendrimers due to steric hindrance [72-74]	Methotrexate [75] Tamoxifen [76] siRNA [77] 5-Fluorouracil [78] Haloperidol [79]

Nanocarriers	Characteristics	Therapeutics Investigated
Polymeric Micelles	Formed by amphiphilic block copolymers which aggregate in aqueous phase to form micelles with a hydrophobic core and hydrophilic surface. Can be tuned to render them sensitive to stimulus such as temperature, pH, light, and ultrasound. Due to small size evade uptake by RES Issues in stability at physiological pH especially at dilutions below their critical micelle concentration (CMC) Limited polymers in use Poor scale up feasibility [80,81]	Amphotericin B [82] Paclitaxel [83] Doxorubicin [84] Adriamycin [85] Cyclosporin A [86]
Nanoemulsions	Consist of two immiscible liquids usually an oil and aqueous phase stabilized by surfactants and co surfactant. Scale up feasibility High drug loading can be achieved Poor stability in blood Difficult to control release Tendency to coalesce and flocculate [81]	Risperidone [87] Olanzapine [88] Saquinavir [89] Curcumin [90] Resveratrol [91]
Carbon Nanotubes (CNT)	Fabricated by rolling up a single sheet of graphene (single walled carbon nanotubes; SWNT) or multiple layers to form concentric cylinders (multi walled carbon nanotubes; MWNT). Their needle shape facilitates transmembrane permeation and intracellular accumulation of drugs via 'nanoneedle' mechanism. High drug loading and fast cellular uptake Toxicity issues [92,93]	Doxorubicin[94] siRNA [95] Angiopep-2 [96]

1.4.1. Methods of Production

1.4.1.1. Formulation Ingredients

Like lipid nanoemulsions which are usually oil-in-water (O/W) type, the major components of NLC are also lipids, surfactants and water. However, in NLC a proportion of oil is replaced by a solid lipid resulting in a solid lipid matrix at room temperature. The solid lipids are blended with oils preferably in the ratio ranging from 70:30 to 99.9:0.1. In multiple emulsion NLC, higher proportion of oils can be used. The system is stabilized with the help

of 0.5% to 5% surfactant solutions. Various lipids, oils and surfactants commonly used in formulation of NLC is enlisted in Table 1.3.

Table 1.3. Formulation ingredients for NLC preparation ([102]

Formulation Ingredients	Examples
Solid Lipids	Stearic acid Glyceryl Monostearate (GMS) Carnauba wax Cetyl palmitate Glyceryl Palmitostearate (Precirol® ATO 5 Glyceryl Behenate (Compritol 888 ATO®) Grades of Witepsol® Grades of Softisan® Gelucire® [105]
Liquid lipids/Oils	Soyabean oil Medium chain triglycerides (MCT)/caprylic and capric triglycerides Oleic Acid (OA) Isopropyl Myristate α-tocopherol/ Vitamin E Corn oil Squalene
Surfactants	Poloxamer 188 Tween 20 & 80 Myverol 18-04K Sodium dodecyl sulfate (SDS) Sodium deoxy cholate (SDC) Poly vinyl Alcohol (PVA) Lecithin Solutol HS 15® Polyoxyl castor oil

1.4.1.2. Fabrication Techniques

The fabrication methods for NLC preparation include high pressure homogenization (HPH), microemulsion, emulsification-sonication, solvent emulsification-evaporation, solvent diffusion, phase inversion, solvent injection and membrane contractor techniques. The methods are summarized in Table 1.4. However, the preferred method is HPH due to the fact that the method is cost efficient and is already used in the pharmaceutical industry for preparation of emulsions for nutrition and hence feasible for large scale production [106].

Table 1.4. Fabrication methods for production of NLC [102]

Method	Procedure	Advantages and Limitations
HPH **a) Hot homogenization** b) **Cold homogenization**	In hot method the drug-lipid melt is emulsified with an aqueous stabilizer solution maintained at the same temperature under high shear resulting in a hot pre-emulsion. The pre-emulsion is then processed in a HPH maintaining the temperature above lipid melting point. The nanoemulsion formed recrystallizes to form NLC when cooled at room temperature. In cold HPH, drug-lipid melt is solidified and milled rapidly under liquid nitrogen resulting in microparticles. The formed microparticles are dispersed in a cold surfactant solution before subjecting it to HPH at or below room temperature. Usually, 3-5 homogenization cycles at 500-1500 bar are sufficient for nanoemulsion formation.	Simple and cost effective Well established on large scale Avoidance of organic solvent in manufacture. Thermolabile drug can be processed by cold method. Increase in temperature during homogenization cannot be avoided. Dispersion quality is often compromised by the presence of microparticles
Microemulsion	Drug-lipid melt is emulsified with hot aqueous surfactant solution at the same temperature. The hot microemulsion formed is poured immediately into cold water resulting in a nanoemulsion which upon recrystallization forms NLC.	Scale up feasible Uses high concentration of surfactants Strong dilution of particles due to use of high volumes of water.
Solvent Diffusion	Lipids are dissolved in solvent such as benzyl alcohol, tetrahydrofuran. Organic solvents are saturated with water for thermodynamic equilibrium. The transient oil-in-water emulsion is diffused into water under continuous stirring leading to solidification of the dispersed phase.	Water immiscible solvents used Use of Organic solvents Ultrafiltration/ lyophilization required
Emulsification-Sonication	Procedure is same as HPH, however the preemulsion is ultra-sonicated using probe sonicator.	High shear mixing. Metallic contamination from the probe during sonication may occur

Method	Procedure	Advantages and Limitations
Solvent emulsification-Evaporation	Involves use of water-immiscible organic solvents like chloroform, cyclohexane to dissolve the lipids. The lipid solution is then emulsified in an aqueous surfactant solution under continuous stirring. The organic phase is evaporated, resulting in lipid precipitation.	Suitable for thermosensitive drugs as it avoids any thermal stress Use of organic solvents Additional step of evaporation required
Phase Inversion	A mix of lipid, drug, water and surfactant is formed under stirring and exposed to 3 heating and cooling cycles(85–60–85°C) after which the shock is induced by diluting with cold water (0°C) resulting in NLC formation by phase inversion	Suitable for thermosensitive drugs Avoids use of organic solvents Tedious process
Solvent injection/ Solvent displacement	Lipids are dissolved in a water-miscible solvent and quickly injected into an aqueous solution of surfactants through an injection needle	Easy handling and fast production process Use of organic solvents
Membrane Contractor	Lipid melt is passed under pressure through a porous membrane resulting in small lipid droplets. Simultaneously, aqueous phase is circulated inside the membrane module, and sweeps away lipid droplets from the pore. Lipid NPs are formed after cooling at room temperature	Simple methodology and equipment

1.4.2. Characterization of NLC

Characterization of NLC like all other colloidal carriers is a critical requirement for assessing quality, stability and release kinetics of the delivery system. For SLN and NLC, it is quite a challenging task as apart from being of extremely small size, the system is also dynamic due to complex nature of the lipids. The important characterization methods are measurement of particle size and its distribution, structural properties, surface charge and morphology, crystallinity and polymorphism and thermal behavior [107].

1.4.2.1. Particle Size and Zeta Potential

Particle size and its distribution is an important characteristic which has an influence on the stability, solubility, release rate and biological performance of the NLC. The usual diameter of NLC ranges from 10-1000 nm. However, for site specific delivery a 50-300 nm range is preferred especially for central nervous system disorders and chemotherapeutic agents. Size in the range of 50-300 nm provides easier permeation of barriers, enhanced cell uptake and rapid action whereas size above 300 nm provides sustained drug delivery. Further, particle size is an indicator of stability and during storage NLC should maintain a narrow size range. Increase in particle size during storage indicates agglomeration and physical instability.

A number of factors influencing particle size and its distribution include composition of the formulation (properties of lipids and drugs added, type of surfactants), manufacturing process such as choice of process, equipment used, processing temperature, pressure and number of cycles during HPH, sterilization and lyophilization [108]. Photon correlation spectroscopy (PCS), Dynamic light scattering (DLS), Quasi light scattering (QLS), Quasi-elastic light scattering (QELS) and Multi-angle light scattering (MALS) are the commonly used non-destructive techniques, which give information about the size based on the equivalent hydrodynamic diameter in liquid dispersions. DLS works by measuring the intensity of light scattered from the sample and size distribution is based on the back scattered light intensity. It is usually capable of measuring particle diameters in the range of a few nanometers to about 3 µm. The presence of particles larger than 3 µm in the NLC formulation can be excluded by DLS. PCS also measures the polydispersity represented as polydispersity index (PDI) provided by the particle size distribution of the sample. Low PDI (0.1-0.25) indicates narrow size distribution whereas PDI above 0.5 indicates a broad size distribution hence more polydispersity. PCS shows that NLC being non-spherical particles

differ from a nanoemulsion with respect to Brownian motion. This asymmetry of particles also leads to higher PDI in NLC as compared to nanoemulsions. It is always preferable to use both PCS and DLS method simultaneously for particle size determination [110-112].

Zeta potential (ZP) gives important information on the long term stability of nanoparticles and their tendency to agglomerate. In general, a ZP of ± 60 mV indicates excellent stability. However, for good stability of electrostatically stabilized nanodispersion a minimum of ± 30 mV is desired and for cases where stability is resultant of both electrostatic and steric stabilization, a minimum ZP of ± 20 mV is desirable. High negative potential or positive potential on all the particles will result in repulsion of particles, decreasing the tendency to aggregate. ZP can easily be measured using analytical instruments based on the principle of electrophoretic/electroacoustic mobility. In commercial instruments, a ZP measurement unit is integrated with the DLS instrument so as to measure particle charge and particle size using the same instrument [100,112].

1.4.2.2. Particle Morphology

Morphology refers to the external characteristics such as shape and surface structure of particles. Anisometric particles have high surface area in addition to short diffusion pathways as compared to spherical particles [112]. Due to higher surface area, non-spherical particles also require higher amounts of surfactants for stabilization. Further, morphology significantly influences drug loading, encapsulation efficiency, drug release characteristics, pharmacokinetics, biodistribution and targeted delivery of the NLC. It also plays an important role in cell uptake and receptor binding and interaction with cells [113,114]. PCS and DLS analyze the particle size assuming that the particles are spherical in shape. However, NLC are not spherical solid lipid particles embedded with oil droplets, rather they are solid platelets with the oil present between the solid platelet and the surfactant layer [115]. Electron microscopy techniques like scanning electron microscopy (SEM), transmission electron microscopy (TEM) and atomic force microscopy (AFM) are extremely useful in determining the particle size, state of aggregation, morphology, surface topography and even the internal structure of the NLC [98].

1.4.2.3. Crystallinity and Lipid Modification

Characterization of crystallinity and degree of lipid modification is necessary as it influences entrapment efficiency, release characteristics and stability of the NLC. Thermodynamic stability as well as packing density of the lipid increases whereas drug incorporation rate decreases in the following order [107]

Supercooled melt > α-modification > β` modification > β modification

Most of the processes for NLC production involve formation of a hot microemulsion, by heating the lipid above its melting point and then solidifying it by dispersing in the aqueous stabilizer solution. Mostly the lipid mix of NLC results in melting point depression leading to crystallization of the lipids at a temperature much below its melting point. Crystallization and solidification of lipids occur only when the blend is cooled below its critical crystallization temperature (CCT). The CCT if it not achieved, results in a supercooled emulsion instead of a solid. It is dependent on the production method, type of lipid and stabilizer used, the proportion of liquid lipid, drug incorporation and also the particle size of the formulation [100,112]. After solidification, ageing and polymorphic transformations can be observed in the lipids [116].

Differential scanning calorimetry (DSC) and X-Ray diffraction (XRD) are commonly used techniques for structural characterization of particles and provide valuable information with respect to crystallinity and polymorphism. Furthermore, techniques like Raman spectroscopy, small-angle X-Ray scattering (SAXS), small-angle neutron scattering (SANS) and neutron diffraction have also been used to determine crystal structure, particle size and shape, polymorphism and quantitation of crystalline component in a sample [102].

1.4.2.4. Other Colloidal Forms and Dynamic Phenomena

The presence of various colloidal forms such as supercooled melts, micelles, mixed micelles, liposomes etc. are an important factor which can affect the stability, drug incorporation capacity and drug release of NLC. These supercooled melts, micelles, mixed micelles and liposomes are alternative sites for drug incorporation and are of profound importance in drug release and formulation stability. Magnetic resonance techniques such as nuclear magnetic resonance (NMR) and electron spin resonance (ESR) are important tools to evaluate the presence of other colloidal structures and understand the dynamic phenomena [107].

1.4.2.5. Encapsulation Efficiency and Drug Loading

Encapsulation efficiency (EE) is a critical factor which needs to be optimized during formulation design as it has an impact on the drug release and also on the cost-effectiveness of the formulation. It is the percentage amount of drug that gets entrapped in the nanoparticle and reflects the efficiency of the formulation. In NLC, the presence of liquid lipids leads to increased imperfections in the crystal structure of the lipids increasing the EE [117].

Drug loading expresses the amount of drug in nanoformulation divided by the weight of the polymer/lipid used. The drug content and entrapment efficiency can be determined directly by digesting the NLC in a suitable organic solvent or indirectly by estimating free drug in the supernatant obtained after separating the nanoparticles from the aqueous dispersion by centrifugation.

1.4.2.6. In Vitro Drug Release

The drug release behavior of NLC is dependent on the proportion of oil, production temperature and emulsifier concentration. The controlled release of drug from the NLC can result in extended half-life and protection from enzymatic degradation. Drug release from NLC can either be controlled by diffusion of the drug or erosion of the matrix depending upon whether the drug is entrapped in the core of the NLC, in the shell or in the matrix. In most of the cases release of the drug is controlled by slow dissolution rate in the aqueous environment and the degradation rate of the lipids. The release profile is usually biphasic with an initial burst release due to the drug present on the surface of the nanoparticles followed by prolonged release of the drug from the core. The drug release behavior of NLC is dependent on the type of solid lipid used, proportion of oil, production temperature and emulsifier concentration. Stabilizers also play an important role as these control the attachment of the lipase/co-lipase to the nanoparticle [117-119]. Drug release can be assessed using one of the following methods, namely, sample and separate (SS), continuous flow (CF), and dialysis membrane (DM) methods. However, dialysis membrane method is the most commonly used method [120].

1.4.2.7. Stability of NLC

NLC may contain various other colloidal structures, such as micelles, mixed micelles, liposomes and nanoemulsions which have an impact on the formulation stability. During

long term stability aggregation may occur due to collision leading to perikinetic flocculation. In highly concentrated NLC dispersions, a pearl like effect is observed resulting in a network formation which prevents collision and perikinetic flocculation. After administration, upon dilution with the gastric fluids or blood this network is disturbed releasing discrete nanoparticles.

Physical instability of NLC in terms of aggregation or gelling during storage is also a major concern. All NLC formulations should maintain their nanoparticle properties such as particle size during storage and preserved from any bacterial growth in the aqueous phase. Two approaches can be utilized to ensure physical stability of the NLC during storage: i) removal of water from the nanoparticle dispersion by freeze drying; and ii) addition of a preservative to the dispersion.

A freeze-dried product should maintain adequate appearance and be easily resuspended in water with a short reconstitution time. Further, it should not induce any changes in the particle size of nanoparticles and maintain the encapsulated drug activity. However, aggregation has been observed in freeze dried formulations without cryoprotectants. Various carbohydrate and polymeric cryoprotectants have been studied and used for NLC preservation such as trehalose, sucrose, sorbitol, mannitol, Microcelac®, Avicel RC591®, lactose and dextrose [121,122].

Preservatives are used to maintain physical stability especially in dermal products which are majorly fluid or semisolid preparations containing water as the dispersion media. However, preservatives can also destabilize NLC. The destabilizing effect of preservatives is dependent on number of factors such as hydrophobicity of the particles, attachment of preservative to the particle surface, ability to reduce zeta potential, nature of particle stabilizer and its interaction with the preservative. To have a stable and preserved NLC the preservative should be as hydrophilic in nature in addition to being non- ionic so as to have minimal interaction with the particle surface and not significantly affect the zeta potential [123].

1.4.2.8. Applications of NLC

NLC are new generation lipid nanoparticles which have found wide application as carriers for various therapeutics besides delivery via different routes of administration including topical, pulmonary, ocular, oral and intranasal route. Further, NLC have shown promise in cosmetic formulations and a number of products are available in the market also.
In dermal products especially cosmetics, NLC have been reported to protect the actives from degradation, prevent transepidermal water loss, enhance skin occlusion, enhance skin permeation and drug targeting, flexibility to modulate drug release and enhance sunblock activity of Ultraviolet (UV) blockers [124,125].

NLC have been specifically used for oral administration with the aim to enhance oral bioavailability by enhancing the uptake of drug by lymphatic system via microfold cells (M cells) in the intestinal membrane and bypassing the first pass metabolism. Inside the gastrointestinal tract the lipids in the NLC are digested partially in the stomach and then in the small intestines into diglycerides and free fatty acids. The presence of lipids also decreases transit and thus increases the residence time in stomach and upper small intestine resulting in enhanced absorption. Moreover, due to the nanoscale surface area is considerably increased which enhances the adhesion of NLC to the gut walls. Furthermore, NLC also stimulate the release of bile which facilitates formation of micelles and solubilisation of drugs besides increasing the carrier transport across the stagnant layer, existing between the intestinal bulk fluid and brush border membrane of enterocytes, enhancing drug absorption [126,127].

Lipid nanocarriers offer many advantages in pulmonary drug delivery such as: a) uniform distribution of the drug dose in the alveoli; b) enhanced solubility, c) protection from degradation, d) sustained release which prolongs therapeutic efficacy and also reduces dosing frequency e) potential to deliver macromolecules. The NLC can be delivered to the lower respiratory tract effectively as the lower particle size below 500 nm leads to enhanced deposition in all parts of lungs due to enhanced diffusional movement. Further, NLC possess bioadhesive properties due to their small size and lipophilic nature in addition to evading clearance by alveolar macrophages resulting in prolonged residence time in the lungs. NLC need to meet the requirements like other inhalational formulations for pulmonary delivery

such as biocompatibility, non-toxicity, non-irritating, sterility, isotonicity, pH in the range of 3-8.5 in addition to stability in propellants [128].

In the recent years, NLC formulations have been investigated for their potential as a ocular delivery system as they can enhance corneal permeation of therapeutics and thereby improve bioavailability, in addition to being safe, non-invasive and patient compliant. Further, the mucoadhesive nature of NLC improves their interaction with the corneal membrane resulting in prolonged residence time, enhanced bioavailability and lesser systemic and local side effects. NLC formulations have been investigated for the treatment of various disorders of the eye such as inflammation, infections, glaucoma and also disorders affecting the posterior segment of the eye [129].

Lipid nanoparticles including liposomes and solid lipid nanoparticulate formulations have been shown to have enhanced delivery of therapeutics to the brain which otherwise were unable to cross the BBB in therapeutic concentrations. The olfactory bulb pathway and trigeminal nerve system pathways bypass the BBB and have gained importance in targeted delivery of a variety of therapeutics ranging from small molecules, proteins and peptides, stem cells and even plasmids to the brain. NLC formulations due to their smaller particle size and higher drug loading appear to be superior to SLNs, and demonstrated enhanced cytotoxicity, cellular uptake and BBB permeability. NLC formulations by the intranasal route have been explored exhaustively for enhanced delivery to the brain. Intranasal delivery has been shown to be a reliable, safe and non-invasive method for delivery of CNS drugs in addition to higher concentrations achieved in the brain, lesser side effects and prolonged residence time and enhanced targeting efficiency [25,130,131].

1.5. Objective of the Current Research Work

Temozolomide is an anti-cancer drug approved for the treatment of brain tumors especially refractory anaplastic astrocytoma and newly diagnosed GBM. It is an oral prodrug which is completely absorbed in the body and because of its small size and lipophilic nature, it readily crosses the BBB. Studies have shown that approximately 30 to 40% of the plasma concentration levels are achieved in the brain, which reaches a maximum in about 1h. At physiological pH of the blood and tissues, temozolomide spontaneously undergoes hydrolysis to the active metabolite [5-(3-dimethyl-1-triazenyl) imidazole-4-carboxamide]

(MTIC), which rapidly breaks down to form the reactive methyldiazonium ion. MTIC has poor permeability in the brain due to its more hydrophilic nature. Due to its short half-life of 1.8h in plasma and spontaneous degradation at physiological pH higher doses of the drug need to be administered to achieve therapeutic concentrations in the brain. This leads to various dose dependent effects such as cardiomyopathy, bone marrow depression and oral ulcerations, nausea and vomiting [132,133].

Designing a nanoparticulate delivery system will provide an effective system for enhancing delivery of temozolomide to the brain by protecting the drug from degradation, prolonging its circulation time and modifying the distribution leading to achievement of higher concentration of temozolomide in the brain, possible dose reduction and reduced side-effects.

NLC are lipid nanocarriers which in addition to providing the above properties are known to be less toxic, biocompatible and biodegradable. Further, they are capable of high drug loading, providing controlled release of the drug and enhanced targeting efficiency.

Considering, these benefits offered by NLC, the present research purpose was to develop and optimize a delivery system which will protect the drug from degradation in the blood or reduce the conversion to MTIC and thereby enhance permeability of the drug to the brain with reduction of side-effects.

To achieve this, the following objectives were laid down:

- Design and development of novel, nanostructured delivery systems of temozolomide with enhanced permeation to the brain.
- Characterization of the developed nanoformulations and optimization of various design parameters.
- To carry out the pharmacokinetic and biodistribution studies of the developed nanoformulations.
- Analysis plays a critical role in meeting the above objectives of successful formulation development and in vivo studies. Therefore, the work objective also includes the development and validation of simple, rapid and sensitive analytical (UV & HPLC) methods and bioanalytical (HPLC) methods for quantification of temozolomide during various phases of development such as preformulation, formulation development and characterization, stability and animal studies.

References

1 Cooper, G.M (2000) The development and causes of cancer. In *The Cell: A Molecular Approach.*, Boston University, Sunderland (MA),Sinauer Associates. https://www.ncbi.nlm.nih.gov/books/NBK9839/. Content accessed in March 2018

2 United States National Institute of Health (2007) Biological sciences curriculum study. NIH Curriculum Supplement Series [Internet]. *Understanding Cancer. https://www.ncbi.nlm.nih.gov/books/NBK20362/* . Content accessed in March 2018

3 Hanahan, D. and Weinberg, R.A. The hallmarks of cancer. *Cell* 100 (1), 57-70

4 Hanahan, D. and Weinberg, Robert A. Hallmarks of cancer: the next generation. *Cell* 144 (5), 646-674

5 Floor, S.L. et al. (2012) Hallmarks of cancer: of all cancer cells, all the time? *Trends in Molecular Medicine* 18 (9), 509-515

6 DeAngelis, L.M. (2001) Brain tumors. *New England Journal of Medicine* 344 (2), 114-123

7 Butowski, N.A. (2015) Epidemiology and diagnosis of brain tumors. *CONTINUUM: Lifelong Learning in Neurology* 21 (2, Neuro-oncology), 301-313

8 American Brain Tumor, A. (2015) About brain tumors: A primer for patients and caregivers. Chicago. https://www.abta.org/wp-content/uploads/2018/03/about-brain-tumors-a-primer-1.pdf . Content accessed in March 2018

9 Louis, D.N. et al. (2016) The 2016 World Health Organization classification of tumors of the central nervous system: a summary. *Acta Neuropathologica* 131 (6), 803-820

10 Ohgaki, H. and Kleihues, P. (2005) Epidemiology and etiology of gliomas. *Acta Neuropathologica* 109 (1), 93-108

11 Marie, S.K.N. and Shinjo, S.M.O. (2011) Metabolism and brain cancer. *Clinics* 66 (Suppl 1), 33-43

12 Lu, C.-T. et al. (2014) Current approaches to enhance CNS delivery of drugs across the brain barriers. *International Journal of Nanomedicine* 9, 2241-2257

13 Serwer, L.P. and James, C.D. (2012) Challenges in drug delivery to tumors of the central nervous system: An overview of pharmacological and surgical considerations. *Advanced Drug Delivery Reviews* 64 (7), 590-597

14 Begley, D.J. (2004) Delivery of therapeutic agents to the central nervous system: the problems and the possibilities. *Pharmacology & Therapeutics* 104 (1), 29-45

15 Pavan, B. et al. (2008) Progress in drug delivery to the central nervous system by the prodrug approach. *Molecules* 13 (5), 1035-1065

16 Rautio, J. et al. (2008) Prodrug approaches for CNS delivery. *The AAPS Journal* 10 (1), 92-102

17 M Huttunen, K. and Rautio, J. (2011) Prodrugs-an efficient way to breach delivery and targeting barriers. *Current Topics in Medicinal Chemistry* 11 (18), 2265-2287

18 Moody, C.L. and Wheelhouse, R.T. (2014) The medicinal chemistry of imidazotetrazine prodrugs. *Pharmaceuticals* 7 (7), 797-838

19 Agarwala, S.S. and Kirkwood, J.M. (2000) Temozolomide, a novel alkylating agent with activity in the central nervous system, may improve the treatment of advanced metastatic melanoma. *The Oncologist* 5 (2), 144-151

20 Bodor, N. and Buchwald, P. (1999) Recent advances in the brain targeting of neuropharmaceuticals by chemical delivery systems. *Advanced Drug Delivery Reviews* 36 (2–3), 229-254

21 Orive, G. et al. (2010) Biomaterial-based technologies for brain anti-cancer therapeutics and imaging. *Biochimica Et Biophysica Acta-Reviews on Cancer* 1806 (1), 96-107

22 Allhenn, D. et al. (2012) Drug delivery strategies for the treatment of malignant gliomas. *International Journal of Pharmaceutics* 436 (1–2), 299-310

23 Obermeier, B. et al. (2013) Development, maintenance and disruption of the blood-brain barrier. *Nature Medicine* 19 (12), 1584-1596

24 Chen, Y. and Liu, L. (2012) Modern methods for delivery of drugs across the blood–brain barrier. *Advanced Drug Delivery Reviews* 64 (7), 640-665

25 Joseph, E. and Saha, R.N. (2013) Advances in brain targeted drug delivery: nanoparticulate systems. *Journal of PharmaSciTech* 3 (1), 1-8

26 Hersh, D.S. et al. (2016) Evolving drug delivery strategies to overcome the blood brain barrier. *Current Pharmaceutical Design* 22 (9), 1177-1193

27 Burgess, A. and Hynynen, K. (2013) Noninvasive and targeted drug delivery to the brain using focused ultrasound. *ACS Chemical Neuroscience*. 8588, 1-7

28 Azad, T.D. et al. (2015) Therapeutic strategies to improve drug delivery across the blood-brain barrier. *Neurosurgical Focus* 38 (3):E9

29 Sirsi, S.R. and Borden, M.A. (2014) State-of-the-art materials for ultrasound-triggered drug delivery. *Advanced Drug Delivery Reviews* 72, 3-14

30 Cordon-Cardo, C. et al. (1989) Multidrug-resistance gene (P-glycoprotein) is expressed by endothelial cells at blood-brain barrier sites. *Proceedings of the National Academy of Sciences of the United States of America* 86 (2), 695-698

31 Pardridge, W.M. (2007) Blood-brain barrier delivery. *Drug Discovery Today* 12 (1-2), 54-61

32 Su, Y. and Sinko, P.J. (2006) Drug delivery across the blood–brain barrier: why is it difficult? how to measure and improve it? *Expert Opinion on Drug Delivery* 3 (3), 419-435

33 Shah, G.N. and Mooradian, A.D. (1997) Age-related changes in the blood-brain barrier. *Experimental Gerontology* 32 (4-5), 501-519

34 Zlokovic, B.V. (2008) The blood-brain barrier in health and chronic neurodegenerative disorders. *Neuron* 57 (2), 178-201

35 Klerk, O.L. (2014) The Role of P-Glycoprotein in Psychiatric Disorders and in Psychiatric Treatment,Editor Dierckx, R.A.J.O. et al. In *PET and SPECT in Psychiatry*, Springer, 65-90

36 Mei, X.G., Yang, M.Y., Editor Prakash, S. (2007) Drug delivery system for active brain targeting in *Artificial Cells, Cell Engineering and Therapy*, Woodhead Publishing, CRC Press 404-423

37 Wei, L. (2012) Adsorptive-mediated brain delivery systems. *Current Pharmaceutical Biotechnology* 13 (12), 2340-2348

38 Zhang, F. et al. (2015) Drug delivery strategies to enhance the permeability of the blood–brain barrier for treatment of glioma. *Drug Design, Development and Therapy* 9, 2089-2100

39 Miyake, M.M. and Bleier, B.S. (2015) The blood-brain barrier and nasal drug delivery to the central nervous system. *American Journal of Rhinology and Allergy* 29 (2), 124-127

40 Illum, L. (2015) Intranasal delivery to the central nervous system. In *Blood-Brain Barrier in Drug Discovery*, pp. 535-565, John Wiley & Sons, Inc

41 Chapman, C.D. et al. (2013) Intranasal treatment of central nervous system dysfunction in humans. *Pharmaceutical Research* 30 (10), 2475-2484

42 Lochhead, J.J. and Thorne, R.G. (2012) Intranasal delivery of biologics to the central nervous system. *Advanced Drug Delivery Reviews* 64, 614-628

43 Quintana, D.S. et al. (2016) The promise and pitfalls of intranasally administering psychopharmacological agents for the treatment of psychiatric disorders. *Molecular Psychiatry* 21 (1), 29-38

44 Mittal, D. et al. (2014) Insights into direct nose to brain delivery: current status and future perspective. *Drug Delivery* 21 (2), 75-86

45 Mistry, A. et al. (2009) Nanoparticles for direct nose-to-brain delivery of drugs. *International Journal of Pharmaceutics* 379 (1), 146-157

46 Singh, R. et al. (2009) Nanoparticle-based targeted drug delivery. *Experimental and Molecular Pathology* 86

47 Grabrucker, A.M. et al. (2014) Nanoparticles as blood–brain barrier permeable CNS targeted drug delivery systems. In *The Blood Brain Barrier (BBB)* (Fricker, G. et al., eds.), pp. 71-89, Springer Berlin Heidelberg

48 Davis, M.E. et al. (2008) Nanoparticle therapeutics: an emerging treatment modality for cancer. *Nature Reviews Drug Discovery* 7, 771-782

49 Kumari, A. et al. (2010) Biodegradable polymeric nanoparticles based drug delivery systems. *Colloids and Surfaces B: Biointerfaces* 75 (1), 1-18

50 Craparo, E.F. et al. (2011) Nanoparticulate systems for drug delivery and targeting to the central nervous system. *CNS Neuroscience & Therapeutics* 17 (6), 670-677

51 Wong, H.L. et al. (2012) Nanotechnological advances for the delivery of CNS therapeutics. *Advanced Drug Delivery Reviews* 64 (7), 686-700

52 Richards, D.A. et al. (2017) Antibody fragments as nanoparticle targeting ligands: a step in the right direction. *Chemical Science* 8 (1), 63-77

53 Kreuter, J. (2014) Drug delivery to the central nervous system by polymeric nanoparticles: What do we know? *Advanced Drug Delivery Reviews* 71, 2-14

54 Wohlfart, S. et al. (2012) Transport of drugs across the blood?brain barrier by nanoparticles. *Journal of Controlled Release* 161 (2), 264-273

55 Vieira, D.B. and Gamarra, L.F. (2016) Getting into the brain: liposome-based strategies for effective drug delivery across the blood–brain barrier. *International Journal of Nanomedicine* 11, 5381-5414

56 Allen, T.M. and Cullis, P.R. (2013) Liposomal drug delivery systems: From concept to clinical applications. *Advanced Drug Delivery Reviews* 65 (1), 36-48

57 Soni, V. et al. (2005) Transferrin coupled liposomes as drug delivery carriers for brain targeting of 5-florouracil. *Journal of Drug Targeting* 13 (4), 245-250

58 Gaillard, P.J. et al. (2012) Enhanced brain delivery of liposomal methylprednisolone improved therapeutic efficacy in a model of neuroinflammation. *Journal of Controlled Release* 164 (3), 364-369

59 Arumugam, K. et al. (2008) A study of rivastigmine liposomes for delivery into the brain through intranasal route. *Acta Pharmaceutica* 58 (3), 287-297

60 Patel, T. et al. (2012) Polymeric nanoparticles for drug delivery to the central nervous system. *Advanced Drug Delivery Reviews* 64 (7), 701-705

61 Desai, N. (2012) Challenges in development of nanoparticle-based therapeutics. *The AAPS Journal* 14 (2), 282-295

62 Joseph, E. and Saha, R.N. (2017) Investigations on pharmacokinetics and biodistribution of polymeric and solid lipid nanoparticulate systems of atypical antipsychotic drug: effect of material used and surface modification. *Drug Development and Industrial Pharmacy* 43 (4), 678-686

63 Wilson, B. et al. (2008) Poly (n-butylcyanoacrylate) nanoparticles coated with polysorbate 80 for the targeted delivery of rivastigmine into the brain to treat Alzheimer's disease. *Brain Research* 1200, 159-168

64 Wilson, B. et al. (2008) Targeted delivery of tacrine into the brain with polysorbate 80-coated poly(n-butylcyanoacrylate) nanoparticles. *European Journal of Pharmaceutics and Biopharmaceutics* 70 (1) 75-84

65 Gulyaev, A.E. et al. (1999) Significant transport of doxorubicin into the brain with polysorbate 80-coated nanoparticles. *Pharmaceutical Research* 16 (10), 1564-1569

66 Kozielski, K.L. et al. (2014) Bioreducible cationic polymer-based nanoparticles for efficient and environmentally triggered cytoplasmic siRNA delivery to primary human brain cancer cells. *ACS Nano* 8 (4), 3232-3241

67 Yang, S.C. et al. (1999) Body distribution in mice of intravenously injected camptothecin solid lipid nanoparticles and targeting effect on brain. *Journal of Controlled Release* 59 (3), 299-307

68 Tsai, M.-J. et al. (2012) Baicalein loaded in tocol nanostructured lipid carriers (tocol NLCs) for enhanced stability and brain targeting. *International Journal of Pharmaceutics* 423 (2), 461-470

69 Patel, S. et al. (2011) Brain targeting of risperidone-loaded solid lipid nanoparticles by intranasal route. *Journal of Drug Targeting* 19 (6), 468-474

70 Gupta, Y. et al. (2007) Transferrin-conjugated solid lipid nanoparticles for enhanced delivery of quinine dihydrochloride to the brain. *Journal of Pharmacy and Pharmacology* 59 (7), 935-940

71 Joseph, E. et al. (2017) Design and in vivo evaluation of solid lipid nanoparticulate systems of Olanzapine for acute phase schizophrenia treatment: Investigations on antipsychotic potential and adverse effects. *European Journal of Pharmaceutical Sciences* 104, 315-325

72 Nanjwade, B.K. et al. (2009) Dendrimers: emerging polymers for drug-delivery systems. *European Journal of Pharmaceutical Sciences* 38 (3), 185-196

73 Somani, S. and Dufès, C. (2014) Applications of dendrimers for brain delivery and cancer therapy. *Nanomedicine* 9 (15), 2403-2414

74 Cheng, Y. et al. (2008) Dendrimers as drug carriers: applications in different routes of drug administration. *Journal of Pharmaceutical Sciences* 97 (1), 123-143

75 Wu, G. et al. (2006) Targeted delivery of methotrexate to epidermal growth factor receptor–positive brain tumors by means of cetuximab (IMC-C225) dendrimer bioconjugates. *Molecular Cancer Therapeutics* 5 (1), 52-59

76 Li, Y. et al. (2012) A dual-targeting nanocarrier based on poly (amidoamine) dendrimers conjugated with transferrin and tamoxifen for treating brain gliomas. *Biomaterials* 33 (15), 3899-3908

77 Serramía, M.J. et al. (2015) In vivo delivery of siRNA to the brain by carbosilane dendrimer. *Journal of Controlled Release* 200, 60-70

78 Ren, Y. et al. (2010) Co-delivery of as-miR-21 and 5-FU by poly (amidoamine) dendrimer attenuates human glioma cell growth in vitro. *Journal of Biomaterials Science, Polymer Edition* 21 (3), 303-314

79 Katare, Y.K. et al. (2015) Brain targeting of a water insoluble antipsychotic drug haloperidol via the intranasal route using PAMAM dendrimer. *Molecular Pharmaceutics* 12 (9), 3380-3388

80 Nishiyama, N. and Kataoka, K. (2006) Current state, achievements, and future prospects of polymeric micelles as nanocarriers for drug and gene delivery. *Pharmacology & Therapeutics* 112 (3), 630-648

81 Lu, Y. and Park, K. (2013) Polymeric micelles and alternative nanonized delivery vehicles for poorly soluble drugs. *International Journal of Pharmaceutics* 453 (1), 198-214

82 Shao, K. et al. (2010) Angiopep-2 modified PE-PEG based polymeric micelles for amphotericin B delivery targeted to the brain. *Journal of Controlled Release* 147 (1), 118-126

83 Zhang, P. et al. (2012) Transferrin-conjugated polyphosphoester hybrid micelle loading paclitaxel for brain-targeting delivery: synthesis, preparation and in vivo evaluation. *Journal of Controlled Release* 159 (3), 429-434

84 Inoue, T. et al. (2009) Therapeutic efficacy of a polymeric micellar doxorubicin infused by convection-enhanced delivery against intracranial 9L brain tumor models. *Neuro-Oncology* 11 (2), 151-157

85 Yokoyama, M. et al. (1998) Characterization of physical entrapment and chemical conjugation of adriamycin in polymeric micelles and their design for in vivo delivery to a solid tumor. *Journal of Controlled Release* 50 (1-3), 79-92

86 Aliabadi, H.M. et al. (2005) Polymeric micelles for the solubilization and delivery of cyclosporine A: pharmacokinetics and biodistribution. *Biomaterials* 26 (35), 7251-7259

87 Kumar, M. et al. (2008) Intranasal nanoemulsion based brain targeting drug delivery system of risperidone. *International Journal of Pharmaceutics* 358 (1-2), 285-291

88 Kumar, M. et al. (2008) Mucoadhesive nanoemulsion-based intranasal drug delivery system of olanzapine for brain targeting. *Journal of Drug Targeting* 16 (10), 806-814

89 Vyas, T.K. et al. (2008) Improved oral bioavailability and brain transport of Saquinavir upon administration in novel nanoemulsion formulations. *International Journal of Pharmaceutics* 347 (1), 93-101

90 Sood, S. et al. (2014) Optimization of curcumin nanoemulsion for intranasal delivery using design of experiment and its toxicity assessment. *Colloids and Surfaces B: Biointerfaces* 113, 330-337

91 Pangeni, R. et al. (2014) Vitamin E loaded resveratrol nanoemulsion for brain targeting for the treatment of Parkinson's disease by reducing oxidative stress. *Nanotechnology* 25 (48), 485102

92 Wong, B.S. et al. (2013) Carbon nanotubes for delivery of small molecule drugs. *Advanced Drug Delivery Reviews* 65 (15), 1964-2015

93 Bianco, A. et al. (2005) Applications of carbon nanotubes in drug delivery. *Current Opinion in Chemical Biology* 9 (6), 674-679

94 Zhang, X. et al. (2009) Targeted delivery and controlled release of doxorubicin to cancer cells using modified single wall carbon nanotubes. *Biomaterials* 30 (30), 6041-6047

95 Varkouhi, A.K. et al. (2011) SiRNA delivery with functionalized carbon nanotubes. *International Journal of Pharmaceutics* 416 (2), 419-425

96 Ren, J. et al. (2012) The targeted delivery of anticancer drugs to brain glioma by PEGylated oxidized multi-walled carbon nanotubes modified with angiopep-2. *Biomaterials* 33 (11), 3324-3333

97 Weber, S. et al. (2014) Solid lipid nanoparticles (SLN) and nanostructured lipid carriers (NLC) for pulmonary application: A review of the state of the art. *European Journal of Pharmaceutics and Biopharmaceutics* 86 (1), 7-22

98 Iqbal, M.A. et al. (2012) Nanostructured lipid carriers system: Recent advances in drug delivery. *Journal of Drug Targeting* 20 (10), 813-830

99 Müller, R.H. et al. (2002) Nanostructured lipid matrices for improved microencapsulation of drugs. *International Journal of Pharmaceutics* 242 (1), 121-128

100 Üner, M. (2006) Preparation, characterization and physico-chemical properties of Solid Lipid Nanoparticles (SLN) and Nanostructured Lipid Carriers (NLC): Their benefits as colloidal drug carrier systems. *Die Pharmazie- An International Journal of Pharmaceutical Sciences* 61 (5), 375-386

101 Jaiswal, P. et al. (2016) Nanostructured lipid carriers and their current application in targeted drug delivery. *Artificial Cells, Nanomedicine, and Biotechnology* 44 (1), 27-40

102 Khosa, A. et al. (2018) Nanostructured lipid carriers for site-specific drug delivery. *Biomedicine & Pharmacotherapy* 103, 598-613

103 Ghate, V.M. et al. (2016) Nanostructured lipid carriers for the topical delivery of tretinoin. *European Journal of Pharmaceutics and Biopharmaceutics* 108, 253-261

104 Hu, F.-Q. et al. (2005) Preparation and characterization of stearic acid nanostructured lipid carriers by solvent diffusion method in an aqueous system. *Colloids and Surfaces B: Biointerfaces* 45 (3), 167-173

105 Mendes, A.I. et al. (2013) Miconazole-loaded nanostructured lipid carriers (NLC) for local delivery to the oral mucosa: Improving antifungal activity. *Colloids and Surfaces B: Biointerfaces* 111 (Supplement C), 755-763

106 Pardeike, J. et al. (2009) Lipid nanoparticles (SLN, NLC) in cosmetic and pharmaceutical dermal products. *International Journal of Pharmaceutics* 366 (1), 170-184

107 Mehnert, W. and Mäder, K. (2001) Solid lipid nanoparticles: Production, characterization and applications. *Advanced Drug Delivery Reviews* 47 (2), 165-196

108 Üner, M. (2016) Characterization and Imaging of Solid Lipid Nanoparticles and Nanostructured Lipid Carriers. In *Handbook of Nanoparticles* (Aliofkhazraei, M., ed.), pp. 117-141, Springer International Publishing

109 Shete, H. and Patravale, V. (2013) Long chain lipid based tamoxifen NLC. Part I: Preformulation studies, formulation development and physicochemical characterization. *International Journal of Pharmaceutics* 454 (1), 573-583

110 Jores, K. et al. (2004) Investigations on the structure of solid lipid nanoparticles (SLN) and oil-loaded solid lipid nanoparticles by photon correlation spectroscopy, field-flow fractionation and transmission electron microscopy. *Journal of Controlled Release* 95 (2), 217-227

111 Galyean, A.A. et al. (2015) Using light scattering to evaluate the separation of polydisperse nanoparticles. *Analytica Chimica Acta* 886, 207-213

112 Tamjidi, F. et al. (2013) Nanostructured lipid carriers (NLC): A potential delivery system for bioactive food molecules. *Innovative Food Science & Emerging Technologies* 19 (Supplement C), 29-43

113 Moghimi, S.M. et al. (2012) Factors controlling nanoparticle pharmacokinetics: an integrated analysis and perspective. *Annual Review of Pharmacology and Toxicology* 52 (1), 481-503

114 Truong, N.P. et al. (2015) The importance of nanoparticle shape in cancer drug delivery. *Expert Opinion on Drug Delivery* 12 (1), 129-142

115 Jores, K. et al. (2005) Solid lipid nanoparticles (SLN) and oil-loaded SLN studied by spectrofluorometry and Raman spectroscopy. *Pharmaceutical Research* 22 (11), 1887-1897

116 Shah, R. et al. (2015) Lipid nanoparticles: production, characterization and stability, *Springer Briefs in Pharmaceutical Science and Drug Development* Springer, 1-7

117 Fang, C.-L. et al. (2013) Nanostructured lipid carriers (NLCs) for drug delivery and targeting. *Recent Patents on Nanotechnology* 7 (1), 41-55

118 Olbrich, C. et al. (2002) Lipase degradation of Dynasan 114 and 116 solid lipid nanoparticles (SLN)—effect of surfactants, storage time and crystallinity. *International Journal of Pharmaceutics* 237 (1), 119-128

119 Müller, R.H. et al. (2002) Solid lipid nanoparticles (SLN) and nanostructured lipid carriers (NLC) in cosmetic and dermatological preparations. *Advanced Drug Delivery Reviews* 54 (Supplement), S131-S155

120 D'Souza, S. (2014) A review of in vitro drug release test methods for nano-sized dosage forms. *Advances in Pharmaceutics* 2014

121 Zhuang, C.-Y. et al. (2010) Preparation and characterization of vinpocetine loaded nanostructured lipid carriers (NLC) for improved oral bioavailability. *International Journal of Pharmaceutics* 394 (1), 179-185

122 Varshosaz, J. et al. (2012) Freeze-drying of nanostructure lipid carriers by different carbohydrate polymers used as cryoprotectants. *Carbohydrate Polymers* 88 (4), 1157-1163

123 Obeidat, W.M. et al. (2010) Preservation of nanostructured lipid carriers (NLC). *European Journal of Pharmaceutics and Biopharmaceutics* 76 (1), 56-67

124 Müller, R.H. et al. (2007) Nanostructured lipid carriers (NLC) in cosmetic dermal products. *Advanced Drug Delivery Reviews* 59 (6), 522-530

125 Purohit, D.K. et al. (2016) Nano-lipid carriers for topical application: Current scenario. *Asian Journal of Pharmaceutics* Jan-March Suppl 9(5) S1-S9

126 Lin, C.-H. et al. (2017) Recent advances in oral delivery of drugs and bioactive natural products using solid lipid nanoparticles as the carriers. *Journal of Food and Drug Analysis* 25 (2), 219-234

127 Desai, P.P. et al. (2012) Overcoming poor oral bioavailability using nanoparticle formulations – opportunities and limitations. *Drug Discovery Today: Technologies* 9 (2), e87-e95

128 Pardeike, J. et al. (2011) Development of an Itraconazole-loaded nanostructured lipid carrier (NLC) formulation for pulmonary application. *International Journal of Pharmaceutics* 419 (1), 329-338

129 Sánchez-López, E. et al. (2017) Lipid nanoparticles (SLN, NLC): overcoming the anatomical and physiological barriers of the eye–Part II-ocular drug-loaded lipid nanoparticles. *European Journal of Pharmaceutics and Biopharmaceutics* 110, 58-69

130 Chen, Y. et al. (2016) Nanostructured lipid carriers enhance the bioavailability and brain cancer inhibitory efficacy of curcumin both in vitro and in vivo. *Drug Delivery* 23 (4), 1383-1392

131 Song, S. et al. (2016) Novel RGD containing, temozolomide-loading nanostructured lipid carriers for glioblastoma multiforme chemotherapy. *Drug Delivery* 23 (4), 1404-1408

132 Koukourakis, G.V. et al. (2009) Temozolomide with radiation therapy in high grade brain gliomas: pharmaceuticals considerations and efficacy; a review article. *Molecules* 14 (4), 1561-1577

133 Huang, G. et al. (2008) Solid lipid nanoparticles of temozolomide: Potential reduction of cardial and nephric toxicity. *International Journal of Pharmaceutics* 355 (1), 314-320

2. Drug Profile

2.1. Introduction

Temozolomide is an imidazotetrazine derived methylating agent approved as an orphan drug by the United States Food and Drug Administration (USFDA) for the treatment of refractory anaplastic astrocytoma in the year 1999 and for newly diagnosed glioblastoma multiforme in the year 2005. It was synthesized at Aston University by Malcolm Stevens and his team in the early 80's as one of the series of novel imidazotetrazinones. Later, the molecule was licensed to Schering Plough (USA) [1,2]. The agents of the series have unique physicochemical properties and improved antitumor activity because of the presence of three adjacent nitrogen atoms compared to two nitrogens of bicyclic triazines. Temozolomide is an oral prodrug which is completely absorbed in the body and because of its small size and lipophilic nature, it readily crosses the BBB. It spontaneously converts to its active metabolite 5-(3-methyl) 1-triazen-1-yl-imidazole-4-carboxamide (MTIC) at physiological pH which further fragments to generate the reactive methyl-diazonium ion [3-5]. Temozolomide has also been reported to show promising activity against malignant melanoma [6-8], intracranial ependymoma [9,10], medullablastoma [11,12], other CNS tumors [13] and mycosis fungoides with CNS progression [14].

2.2. Drug Properties

Name :	Temozolomide
Chemical name :	4-methyl-5-oxo- 2,3,4,6,8-pentazabicyclo [4.3.0] nona-2,7,9-triene- 9-carboxamide
CAS number :	85622-93-1
Molecular formula :	$C_6H_6N_6O_2$
Structure :	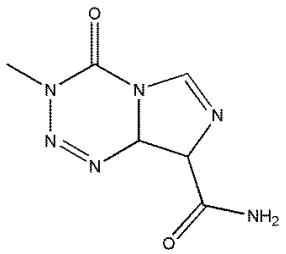

Molecular weight :	194.15
Therapeutic class :	Anti-neoplastic
Chemical class :	Alkylating agent
Description :	White to light tan/light pink non-hygroscopic powder
Solubility :	At 25^0C, solubility is pH independent; in water (~3.1mg mL^{-1}) methanol (~4.4 mg mL^{-1}), dimethyl sulfoxide (~30mg mL^{-1}) and ethanol (<1mg mL^{-1})
Melting point :	212^0C
pKa :	No pKa
Partition coefficient :	- 1.153
BCS classification :	Class I
Optical activity :	Achiral
Polymorphism :	Nine polymorphic forms identified
Stability :	Stable in acid pH (<5) and labile at pH > 7
Proprietary names :	Temodal, Temodar (Schering-Plough Corporation, USA) Temomedac (Alfred E. Tiefenbacher GmbH & Co)
Marketed as :	5mg, 20mg, 100mg, 140mg, 180mg, and 250mg hard capsules. 100 mg/vial Lyophilized powder for intravenous infusion.

2.3. Therapeutic Indications and Dosage

Temozolomide is indicated for the treatment of adult patients with newly diagnosed glioblastoma multiforme concurrently with radiotherapy and subsequently as monotherapy. It is also indicated for treatment of children from the age three years, adolescents and adults diagnosed with malignant glioma such as glioblastoma multiforme or refractory anaplastic astrocytoma i.e. patients who have experienced progression of disease on a drug regimen of

procarbazine and nitrosourea. It has also been proposed as a first line treatment for advanced metastatic malignant melanoma [15].

During concomitant therapy in patients with newly diagnosed high grade glioma, temozolomide is administered at a dose of 75 $mg.m^{-2}$ for 42 days concomitant with focal radiotherapy. No dose reductions are recommended during the concomitant phase. However, dose interruptions or discontinuation may occur based on the haematological and nonhaematological toxicity criteria. Treatment with concomitant temozolomide can be continued when all of the following conditions are met: absolute neutrophil count (ANC) $\geq$ 1.5 x 10^9 L^{-1}; platelet count $\geq$ 100 x 10^9 L^{-1}; common toxicity criteria (CTC) non-haematological toxicity less than or equal to Grade I (except for alopecia, nausea and vomiting). The maintenance phase starts after four weeks of concomitant therapy and temozolomide is administered for an additional 6 cycles. Maintenance dosage in cycle I is 150 $mg.m^{-2}$ once daily for 5 days followed by 23 days without treatment. At the start of cycle 2, dosage is usually increased to 200 $mg.m^{-2}$, if toxicity criteria are met. The dose is kept at 200 $mg.m^{-2}$ per day for the first 5 days of each subsequent cycle except if toxicity occurs. If the dose was not escalated at cycle 2, escalation should not be done in subsequent cycles.

During treatment, a complete blood count should be obtained on Day 22 (21 days after the first dose of temozolomide) or within 48 hours of that day, and weekly until the ANC is above 1.5 x 10^9 L^{-1} (1500 μL^{-1}) and platelet count exceeds 100 x 10^9 L^{-1} (100,000 μL^{-1}).

For adults with refractory anaplastic astrocytoma, the initial dose is 150 $mg.m^{-2}$ once daily for 5 consecutive days per 28 day treatment cycle. For adult patients, if both the nadir and day of dosing (Day 29, Day 1 of next cycle) ANC are greater than or equal to 1.5 x 10^9 L^{-1} (1500 μL^{-1}) and both the nadir and Day 29, Day 1 of next cycle platelet counts are greater than or equal to 100 x 10^9 L^{-1} (100,000 μL^{-1}), the dose may be increased to 200 $mg.m^{-2}$ per day for 5 consecutive days per 28 day treatment cycle. The next cycle of temozolomide should not be started until the ANC and platelet count exceed the recommended levels. If the ANC falls below the required level the next cycle should be reduced by 50 $mg.m^{-2}$, but not below 100 $mg.m^{-2}$, the lowest recommended dose. The therapy can be continued until disease progression [16,17].

2.4. Mechanism of Action

Temozolomide undergoes spontaneous chemical conversion, in presence of water, at physiologic pH to the active compound MTIC. MTIC further degrades to generate a very reactive methyldiazonium ion. They are base selective DNA alkylating agents and preferentially bind to the middle guanine residue of a GGG sequence. The sites and percentage of methylation adduction on DNA are the N^7 position on guanine (N7-MeG; 70%), N^3 position in adenine (N3-MeA; 9%), O^3 on adenine (O3-MeA), and O^6 on guanine (O6-MeG; 6%)[18]. O6-MeG plays a critical role in cytoxicity although it does not inhibit processes such as DNA replication and transcription. However, during base pairing phase of DNA replication, thymine is preferentially incorporated instead of cytosine opposite O^6-MeG. The mismatch repair pathway of the cell recognises this aberration. However, unless the methyl adduct is removed from the guanine, thymine will most likely be reinserted instead of cytosine. The MutS branch of the mismatch repair pathway has a key role in signalling the initiation of apoptosis in response to repetitive failure to repair this aberration results in a state of chronic strand breaks, which triggers an apoptotic response [16,19,20].

2.5. Resistance Mechanisms

Resistance to temozolomide is thought to be mediated by two independent repair mechanisms i.e. the enzyme O^6-alkylguanine transferase (AGT) and DNA mismatch repair proteins. The O^6-MeG reverses the damage by a single step error free reaction in which the methyl group is transferred to cysteine residue on AGT. The concentration of AGT is the major determinant of sensitivity of tumour cell lines to temozolomide and other alkylating agents, carmustine and dacarbazine. Patients with low concentration of AGT have better survival than those with high concentration of the enzyme. Furthermore, transfer of AGT gene via retrovirus to cells devoid of endogenous AGT activity resulted in conferring a high level of resistance on temozolomide and other methylating and chloroethylating agents [21]. Resistance to temozolomide was observed in some cells despite low AGT levels indicating that some other mechanisms of resistance might be involved. A deficiency in the mismatch repair (MMR) pathway due to mutations in any one or more of the protein complexes that detect and repair DNA can render cells resistant to methylation and thereby to cytotoxic effects of temozolomide. This deficiency results in a failure to recognise and repair O^6 MG adducts produced by methylating agents resulting in continuation of replication without cell

cycle arrest or apoptosis. Resistance in tumours due to the MMR deficiency are unaffected by AGT inhibitors.

Another possible mechanism of resistance for temozolomide is the base excision repair (BER) pathway. BER involves number of DNA repair proteins to mend damage in the DNA due to oxidation, alkylation, deamination and single strand breaks. Methylation induced by temozolomide at N^7 of guanine and N^3 at adenine activates the BER pathway and repair is initiated. Studies have shown that treatment with temozolomide in tumour cells induced an increase in the activity of poly ADP ribose polymerase (PARP) involved in the nucleotide excision repair and its inhibition potentiates the cytotoxicity of methylating agents. Studies with PARP inhibitors and with cell lines deficient in either MMR or excision repair have indicated of a role in the repair of N^7-MeG and O^3-MeA adducts in the resistance to temozolomide and other alkylating agents. However, the importance of these adducts in the antitumor activity of drug may be secondary to that of O^6-MeG except in tumours deficient in base excision repair [18, 21-23].

2.6. Pharmacokinetics

2.6.1. Absorption

Temozolomide shows schedule dependent anti-tumour activity and is rapidly and completely absorbed after oral administration with peak plasma concentration (C_{max}) achieved in a median T_{max} of 1h. Food reduces the rate and extent of temozolomide absorption. Mean peak plasma concentration and AUC decreased by 32% and 9%, respectively and median T_{max} increased two fold from 1 to 2.25h, when temozolomide was administered after a modified high-fat breakfast [24].

A pharmacokinetic study showed that the oral and intravenous formulations are bioequivalent. Following a single oral dose of 150 $mg.m^{-2}$, the geometric mean C_{max} values for temozolomide and MTIC were 7.5 $\mu g.mL^{-1}$ and 282 $ng.mL^{-1}$, and geometric mean AUC values were 23.4 $\mu g.h.mL^{-1}$ and 864 $ng.h.mL^{-1}$ respectively.

Studies indicate that temozolomide exhibits linear pharmacokinetics over single oral doses of 100-1000 $mg.m^{-2}$ and over the daily oral doses of 100-250 $mg.m^{-2}$ administered for 5 consecutive days which covers the therapeutic range of the drug [17].

2.6.2. Distribution

Temozolomide has a mean apparent volume of distribution of 0.4 $L.kg^{-1}$ (% CV=13%). It is weakly bound to human plasma proteins; the mean percent bound is 15%. It is extensively distributed to all organs including the brain. Studies in rats and rhesus monkeys showed that the levels of the drug in the brain and CSF are approximately 30-40% of the plasma concentration. However, the metabolite MTIC does not effectively penetrate the CNS. Concentrations of temozolomide in brain and testes appeared to be highest at 1h post-dose then decreased slowly; higher concentrations remained in the kidneys, liver, large and small intestinal wall, salivary gland and testes [15].

2.6.3. Metabolism and Elimination

Temozolomide undergoes spontaneous hydrolysis at physiological pH to generate its active metabolite MTIC and its temozolomide acid metabolite. MTIC further degrades to 5-amino-imidazole-4-carboxamide (AIC), known to be an intermediate in purine and nucleic acid biosynthesis and to methylhydrazine ions, the active alkylating species. Cytochrome P450 (CyP450) does not play any role in the metabolism of temozolomide, thereby avoiding interpatient variability in bioavailability. Systemic exposure to MTIC and AIC is low. Compared to the AUC of temozolomide, the AUC of MTIC and AIC is 2.4% (% CV = 59%) and 23% (% CV = 15%) respectively. The elimination of MTIC and AIC is parallel to that of temozolomide indicating a formation related elimination of both the metabolites [2,17].

2.6.4. Excretion

About 38% of the administered temozolomide dose is recovered over 7 days: 37.7% in urine and 0.8% in faeces indicating that renal excretion is the major pathway for elimination. Majority of the recovery is in urine and includes temozolomide acid metabolite (2.3%), AIC (12%), unchanged temozolomide (5.6%) and unidentified polar metabolite(s) (17%). The incomplete recovery is perhaps due to conversion of temozolomide to AIC, which in turn is known to be an intermediate in the purine and nucleic acid synthesis. A portion may also be eliminated as carbon dioxide [25].

Overall clearance of temozolomide is about 5.5 $L.h^{-1}.m^{-2}$. It is rapidly eliminated with a mean elimination half-life of 1.8h and exhibits linear kinetics over the therapeutic dosing range of 75 to 250 $mg.m^{-2}$ per day [15,19].

Accumulation of temozolomide has not been observed on multiple dosing as the mean $AUC_{0\text{-}24h}$ ratio (R) is approximately equal to one. No changes were observed in oral clearance (CL/F) and apparent volume of distribution (V_d/F) across doses or between days 1 to 5 indicating that temozolomide exhibits both dose and time independent kinetics. Interpatient variability was also very low.

2.6.5. Special Populations

A population pharmacokinetic analysis of temozolomide indicates that there is no influence of age (19 to 78 years) on the pharmacokinetics [15]. Furthermore, reports have indicated that women have an approximately 5% less clearance for temozolomide than men. The oral clearance is similar in smokers and non-smokers. Safety of temozolomide for paediatric population of age 3 years and below has not been studied. For children above three years, it is recommended for use only in recurrent or progressive malignant glioma.

Population pharmacokinetic studies also indicated that creatinine clearance over the range of 36 to130 $mL.min^{-1}.m^{-2}$ has no effect on the clearance of temozolomide after oral administration. Studies have not been carried out in patients with severely impaired renal function ($CL_{cr} < 36\ mL.min^{-1}.m^{-2}$), hence caution should be exercised.

A study showed that pharmacokinetics of patients with mild to moderate hepatic impairment (Child-Pugh Class I - II) were similar to those observed in patients with normal hepatic function. However, caution should be exercised when administering temozolomide to patients with severe hepatic impairment. Temozolomide treatment can reactivate hepatitis B which might hamper the treatment and reduce patient survival. Therefore, it is recommended to screen the patient for hepatitis and viral infections before the commencement of therapy [26].

2.7. Preclinical Toxicity

Temozolomide is a mutagenic, teratogenic and genotoxic agent which is more toxic to rats and dogs than humans. It has been reported to induce mammary carcinomas in rats irrespective of gender after 6 cycles of oral administration of 0.13 to 0.63 times the maximum human dose (25-125 $mg.m^{-2}$) on 5 consecutive days every 28 days. Temozolomide dose 0.5 times of the maximum daily dose also induced fibrosarcomas of the heart, eye, seminal vesicles, salivary glands, abdominal cavity, uterus, and prostate, carcinomas of the seminal

vesicles, schwannomas of the heart, optic nerve and harderian gland, adenomas of the skin, lung, pituitary and thyroid.

Preclinical studies have also shown that temozolomide primarily causes toxicity of the haematopoietic and lymphoreticular systems, gastrointestinal tract and testes. All the effects are usually reversible except for the effect on the testes. Irreversible reticular degeneration was observed at very high and lethal doses [15,17].

2.8. Adverse Reactions

Temozolomide is generally well tolerated and safe. The most common adverse reactions reported during therapy are fatigue, dyspnoea, alopecia, rash, nausea, vomiting, anorexia, headache and constipation. Myelosuppression including thrombocytopenia and neutropenia, a dose-limiting toxicity of most of the cytotoxic drugs is dose dependent, non-cumulative and usually reversible. Bone marrow recovery usually occurs within 28 days. Studies have reported that temozolomide therapy has an overall incidence of 5-8% of 3/4 grade myelosuppression. Females have been reported to have 1.5 to 1.7 fold higher risk of adverse effects with temozolomide therapy due to pharmacokinetic and pharmacodynamic differences [27]. Patients treated with temozolomide may also experience prolonged pancytopenia which can progress to aplastic anaemia and in some cases has fatal outcome. Dose dense and continuous temozolomide regimens can also induce severe lymphopenia and decrease the $CD4^+$ cells count both of which increase the risk of opportunistic infections like immunosuppression-related tumors, *Pneumocystis carinii* pneumonia (PCP) and cytomegalovirus (CMV) [19,28].

Exposure to alkylating agents results in higher risk of developing myelodysplastic syndrome (MDS) characterized by bone marrow failure with morphologic dysplasia and peripheral cytopenia. However, with temozolomide therapy only a few cases of MDS have been reported. This is probably because MDS develops 2-5 years after the beginning of therapy with alkylating agents while the median survival of patients with recurrent malignant glioma is less than 2 years [29,30]. Exposure to temozolomide appears to also be associated with development of other secondary hematologic neoplasms such as acute lymphoblastic leukemia (ALL) and non-Hodgkin's lymphoma (NHL), although only few cases have been reported. Other adverse effects reported post-marketing are elevation of liver enzymes, fatal

and severe hepatotoxicity, hyperbilirubinemia, cholestasis, hepatitis, pulmonary fibrosis, pneumonitis and diabetes insipidus [17].

2.9. Drug Interactions

There are not many drug interaction studies reported for temozolomide and drugs used in treatment and management of brain tumors. Leviteracetam, an anti-epileptic drug prescribed to glioma patients for treatment of seizures, is a potent O^6-methylguanine-DNA methyltransferase (MGMT) inhibitor and has been reported to inhibit glioma cell proliferation and increase sensitivity of the glioma cells to temozolomide [31]. Co-administration with ranitidine does not affect the bioavailability of temozolomide [24]. It is reported that commonly administered drugs such as ondansetron, phenytoin, phenobarbital, dexamethasone, carbamazepine, H_2 antagonists and prochlorperazine have no effect on oral clearance of temozolomide. Valproic acid reduces the clearance of temozolomide by 5% [32]. A synergistic effect was seen when temozolomide was coadministered with perifosine in cell culture and animal studies [33]. Studies have shown that dihydroartemisinin in low concentrations potentiate the anti-tumor effects of temozolomide in rat C6 glioma cells [34]. Resveratrol, an antioxidant has also been indicated to enhance the therapeutic effect of temozolomide by reducing autophagy and increasing apoptosis [35]. Further, no interaction between temozolomide and cisplatin, carmustine, domperidone, haloperidol has been reported [20].

2.10. Marketed Formulations

Temozolomide is available as following dosage forms and strengths

- Hard gelatin capsules for oral use containing 5 mg, 20 mg, 100 mg, 140 mg, 180 mg or 250 mg of temozolomide. The inactive ingredients in the formulation are lactose anhydrous, colloidal silicon dioxide, sodium starch glycolate, tartaric acid and stearic acid.
- Injection available as a sterile pyrogen free lyophilized powder containing 100 mg of temozolomide per vial for intravenous administration. The inactive ingredients in the formulation are mannitol, L-threonine, polysorbate 80, sodium citrate dehydrate and hydrochloric acid.

Each vial is reconstituted with 41mL Sterile Water for Injection and the resultant solution will contain 2.5 $mg.mL^{-1}$ temozolomide. Reconstituted product must be used within 14h including infusion time. The formulation should be infused intravenously using a pump over a period of 90 minutes.

References

1 Wesolowski, J.R. et al. (2010) Temozolomide (Temodar). *American Journal of Neuroradiology* 31 (8), 1383-1384

2 Schwenka, J. and Ignoffo Robert, J. (2008) Temozolomide. *Cancer Practice* 8 (6), 311-313

3 Newlands, E.S. et al. (1997) Temozolomide: a review of its discovery, chemical properties, pre-clinical development and clinical trials. *Cancer Treatment Reviews* 23 (1), 35-61

4 Stevens, M.F.G. (2014) Chapter 5 - Temozolomide: from cytotoxic to molecularly targeted agent A2 - Neidle, Stephen. In *Cancer Drug Design and Discovery (Second Edition)*, Academic Press pp. 145-164,

5 Stevens, M.F.G. and Newlands, E.S. (1993) From triazines and triazenes to temozolomide. *European Journal of Cancer* 29 (7), 1045-1047

6 Quirbt, I. et al. (2007) Temozolomide for the treatment of metastatic melanoma. *Current Oncology* 14 (1), 27-33

7 Ueno, T. et al. (2006) Modulation of chemotherapy resistance in regional therapy: a novel therapeutic approach to advanced extremity melanoma using intra-arterial temozolomide in combination with systemic O6-benzylguanine. *Molecular Cancer Therapeutics* 5 (3), 732-738

8 Agarwala, S.S. and Kirkwood, J.M. (2000) Temozolomide, a novel alkylating agent with activity in the central nervous system, may improve the treatment of advanced metastatic melanoma. *The Oncologist* 5 (2), 144-151

9 Rudà, R. et al. (2016) Temozolomide as salvage treatment for recurrent intracranial ependymomas of the adult: a retrospective study. *Neuro-Oncology* 18 (2), 261-268

10 Soffietti, R. et al. (2014) Temozolomide for recurrent intracranial ependymoma of the adult: patterns of response, survival and correlations with mgmt promoter methylation. *Neuro-Oncology* 16 (Suppl 3), iii50-iii51

11 Cefalo, G. et al. (2014) Temozolomide is an active agent in children with recurrent medulloblastoma/primitive neuroectodermal tumor: an Italian multi-institutional phase II trial. *Neuro-Oncology* 16 (5), 748-753

12 Durando, X. et al. (2007) Temozolomide treatment of an adult with a relapsing medulloblastoma. *Cancer Investigation* 25 (6), 470-475

13 Nicholson, H.S. et al. (2007) Phase 2 study of temozolomide in children and adolescents with recurrent central nervous system tumors. *Cancer* 110 (7), 1542-1550

14 Bird Thomas, G. et al. (2016) Temozolomide for central nervous system involvement in mycosis fungoides. *International Journal of Dermatology* 55 (7), 751-756

15 European Medicines Agency (2010) Assessment report for Temomedac. Doc. Ref.: EMA/51724/2010,1-19. http://www.ema.europa.eu/docs/en_GB/document_library//EPAR_Public_assessment_report/human/001124/. Contents accessed in March 2018.

16 Stupp, R. et al. (2001) Current and future developments in the use of temozolomide for the treatment of brain tumours. *The Lancet Oncology* 2 (9), 552-560

17 Merck & Co., I. (2008) Label TEMODAR (Temozolomide) capsules and powder for injection, submitted to USFDA, Centre for Drug Evaluation and Research.https://www.accessdata.fda.gov/drugsatfda_docs/label/2015/021029s029lbl.pdf. Contents accessed in March 2018

18 Jihong, Z. and Malcolm, F.G.S.a.T.D.B. (2012) Temozolomide: mechanisms of action, repair and resistance. *Current Molecular Pharmacology* 5 (1), 102-114

19 Trinh, V.A. et al. (2009) The safety of temozolomide in the treatment of malignancies. *Expert Opinion on Drug Safety* 8 (4), 493-499

20 Darkes, M.J.M. et al. (2002) Temozolomide. *American Journal of Cancer* 1 (1), 55-80

21 Friedman, H.S. et al. (2000) Temozolomide and treatment of malignant glioma. *Clinical Cancer Research* 6 (7), 2585-2597

22 Yoshimoto, K. et al. (2012) Complex DNA repair pathways as possible therapeutic targets to overcome temozolomide resistance in glioblastoma. *Frontiers in Oncology* 2, 186

23 Johannessen, T.-C.A. and Bjerkvig, R. (2012) Molecular mechanisms of temozolomide resistance in glioblastoma multiforme. *Expert Review of Anticancer Therapy* 12 (5), 635-642

24 Beale, P. et al. (1999) Effect of gastric pH on the relative oral bioavailability and pharmacokinetics of temozolomide. *Cancer Chemotherapy and Pharmacology* 44 (5), 389-394

25 Baker, S.D. et al. (1999) Absorption, metabolism, and excretion of 14C-temozolomide following oral administration to patients with advanced cancer. *Clinical Cancer Research* 5 (2), 309-317

26 Grewal, J. et al. (2007) Fatal reactivation of hepatitis B with temozolomide. *New England Journal of Medicine* 356 (15), 1591-1592

27 Armstrong, T.S. et al. (2009) Risk analysis of severe myelotoxicity with temozolomide: the effects of clinical and genetic factors. *Neuro-Oncology* 11 (6), 825-832

28 Villano, J.L. et al. (2009) Temozolomide in malignant gliomas: current use and future targets. *Cancer Chemotherapy and Pharmacology* 64 (4), 647-655

29 Scaringi, C. et al. (2013) Temozolomide-related hematologic toxicity. *Oncology Research and Treatment* 36 (7-8), 444-449

30 Su, Y.-W. et al. (2005) Treatment-related myelodysplastic syndrome after temozolomide for recurrent high-grade glioma. *Journal of Neuro-Oncology* 71 (3), 315-318

31 Bobustuc, G.C. et al. (2010) Levetiracetam enhances p53-mediated MGMT inhibition and sensitizes glioblastoma cells to temozolomide. *Neuro-Oncology* 12 (9), 917-927

32 Schering Corporation (1998) Clinical pharmacology/ biopharmaceutics review submitted to USFDA, Centre for Drug Evaluation and Research (NDA 21-029). https://www.accessdata.fda.gov/drugsatfda_docs/nda/99/21029_Temodar_clinphrmr.pdf. Contents accessed in March 2018.

33 Momota, H. et al. (2005) Perifosine inhibits multiple signaling pathways in glial progenitors and cooperates with temozolomide to arrest cell proliferation in gliomas in vivo. *Cancer Research* 65 (16), 7429-7435

34 Huang, X.J. et al. (2008) Dihydroartemisinin potentiates the cytotoxic effect of temozolomide in rat C6 glioma cells. *Pharmacology* 82 (1), 1-9

35 Lin, C.-J. et al. (2012) Resveratrol enhances the therapeutic effect of temozolomide against malignant glioma in vitro and in vivo by inhibiting autophagy. *Free Radical Biology and Medicine* 52 (2), 377-391

3. Analytical and Bioanalytical Methods

3.1. Introduction

Analytical methods play a pivotal role in the discovery, development and manufacture of pharmaceuticals. They are used during screening of potential drug molecules, drug design and synthesis, formulation development, stability studies, evaluation of in vitro release and in vivo efficacy of the drug. Therefore, it is important to develop an analytical method which is accurate, reliable and reproducible. Further, the method should be specific and sensitive to assess the quality, safety and performance attributes in a simple and cost effective manner. A developed method can show variation in results due to changes in instrument, analyst and laboratories. Validation of the developed method plays an important role in minimizing these method problems [1]. Guidelines for developing and validating analytical methods laid down by regulatory bodies such as International Conference on Harmonization (ICH), US Food and Drug administration (USFDA) lay emphasis on suitability of the method for intended use and compliance with the standards set for accuracy, precision, sensitivity and specificity [2-4].

3.2. Analytical Methods for Estimation of Temozolomide

Temozolomide (TMZ) is official in USP 40-NF35 and the monograph describes quantification of TMZ by HPLC method (USP, 2014). Few analytical and bioanalytical methods have been reported for the estimation of TMZ in bulk, formulations and biological samples. An ultraviolet (UV) spectroscopy method [5] has been reported for determination of TMZ in capsule dosage forms, however the method is not fully validated as per the ICH guidelines. Few methods by high-performance liquid chromatography (HPLC) using UV detector have also been reported for bulk and formulations [6,7] and biological samples [8-13]. All the reported methods are of low sensitivity, use higher proportions of organic solvents for the mobile phase composition and for biological samples involve tedious and time consuming techniques for extraction of TMZ from biological matrices.

For biological samples a few methods have also been reported by liquid chromatography tandem mass spectroscopy (LC-MS/MS) [12,14,15] and micellar electrokinetic capillary chromatography (MEKC) [16]. However, these methods are very expensive and not all moderately funded laboratories have access to the facility.

For the present work, quantitative estimation of TMZ was required at various stages such as preformulation studies, evaluation and screening of in-house developed nanoparticulate formulations and for pharmacokinetic and biodistribution studies of the optimized formulations. So, as an antecedent to formulation development HPLC methods customized to our needs were developed for both formulations and biological matrices and validated appropriately. Further, a simple, rapid and economical UV-vis spectroscopy method was also developed for routine analysis for quantifying TMZ such as estimation of entrapment efficiency and drug loading of in-house developed nanoformulations.

Extensive literature survey did not reveal any rapid, sensitive and fully validated HPLC method for the estimation of TMZ in rat biomatrices which can be useful for in vivo evaluation of delivery systems of TMZ. Therefore, to meet the requirement a simple, rapid, sensitive, accurate and reliable HPLC method for estimation of TMZ in rat plasma and tissues was developed. All the methods developed and validated were in compliance with the ICH and USFDA guidelines.

3.3. Chemicals and Reagents

Temozolomide was obtained as a gift sample from Neon Laboratories Ltd, India. Ultrapure water from MilliQ plus facility procured from Millipore®, India was used throughout the analysis. Methanol and acetonitrile (HPLC grade) was purchased from Merck India Ltd. Analytical grade hydrochloric acid (37%), glacial acetic acid, ethylene diamine tetra acetic acid disodium (Na EDTA), formic acid (98-100%) and perchloric acid (70%) was purchased from Merck India Ltd. Excipients such as sucrose and mannitol were procured from SD Fine-Chem Limited, India. Poly-ε-caprolactone (PCL), polyvinyl alcohol (PVA), stearic acid, polysorbate 80 and poloxamer 188 (Pluronic-F68) used in the preparation of TMZ nanoparticles in the laboratory were purchased from Sigma Aldrich Corporation, India. Gift samples of Glyceryl monostearate (GMS), Compritol® 888ATO (glyceryl behenate) and Precirol® ATO5 (glyceryl palmitostearate) were received from Gattefosse India Ltd. Soy lecithin (Lipoid® S75) was obtained as gift sample from Lipoid GmbH, Germany. TMZ loaded nanoparticles were fabricated in-house.

3.4. Ultraviolet (UV) Spectrophotometric Method for Determination of TMZ

3.4.1. Instrumentation

A Shimadzu double beam UV-Vis-NIR spectrophotometer (UV-3600, Shimadzu Corporation, Kyoto, Japan) connected to a computer loaded with UV probe software (Version 2.42) was used for absorbance measurements. For intermediate precision study a double-beam UV-Vis-NIR spectrophotometer (V-570, Jasco Inc., Japan) connected to a computer loaded with spectra manager software was used. Both the instruments have an automatic wavelength accuracy of 0.1 nm and matched quartz cells of 10 mm path length.

3.4.2. Method Development

For media optimization, various aqueous media like 100 mM hydrochloric acid medium (pH 1.2), acetate buffer (pH 4.5), phosphate buffers (pH 5-8) were investigated. Further, effect of addition of solvents like acetonitrile/methanol in various proportions was also investigated on the solubility of the drug. Other factors considered were sensitivity, stability, ease of sample preparation and applicability of the method. Spectrophotometric scanning from 700 to 200 nm was carried out with the reference solution to determine the λ_{max} for the detection of TMZ using the diluent as blank. Apparent molar absorptivity and Sandell's sensitivity were calculated according to the standard formulae.

3.4.3. Preparation of Stock and Calibration Standards

A stock solution of TMZ (100 $\mu g.mL^{-1}$) was prepared by dissolving 5 mg of drug in 50 mL of the selected solvent media i.e. 100 mM hydrochloric acid medium (pH 1.2). Six solutions at different concentrations in the range of 3-25 $\mu g.mL^{-1}$ were prepared by transferring six different aliquots of the stock solution into a series of 10 mL volumetric flasks and diluting them to the mark with selected media.

3.4.4. Method Validation

To establish selectivity and specificity, TMZ solutions (5 $\mu g.mL^{-1}$) prepared from the stock solution and a placebo mix solution containing common excipients used for preparation of nanoparticles such as PCL, PVA, poloxamer 188, stearic acid, polysorbate 80, GMS, Precirol, Compritol, mannitol and sucrose were prepared. The solutions were scanned from 700 to 200 nm and checked for change in the absorbance at respective wavelengths.

Considering the fact that TMZ is stable at acidic pH and undergoes decomposition at neutral and alkaline pH, a sample solution of 14 $\mu g.mL^{-1}$ concentration was also prepared in buffer at pH 1.2, 4.5, 6.8 and 8.0. The samples were kept for 24h in order to verify that none of the degradation products interfered with the quantification of the drug.

To establish linearity of the proposed method, nine separate series of solutions of the drug (3-25 $\mu g.mL^{-1}$ in selected media) were prepared from the stock solutions and analyzed. The data was subjected to least square regression analysis. Limit of detection (LOD) and limit of quantification (LOQ) was determined using the calibration standards and calculated as $3.3\sigma/S$ and $10\sigma/S$ respectively, where S is the slope of the calibration plot and σ is the standard deviation of y-intercept of regression equation.

For determining accuracy of the proposed method, different quality control (QC) levels of drug concentrations, namely, low quality control (LQC; 5$\mu g.mL^{-1}$), medium quality control (MQC; 14 $\mu g.mL^{-1}$) and high quality control (HQC; 22 $\mu g.mL^{-1}$) were prepared from independent stock solution and analyzed. Accuracy was assessed as the percentage relative error and mean percentage recovery. To support the accuracy of the developed method, placebo spiking method was carried out. In this method, LQC, MQC and HQC were added to the placebo solution and the total drug concentration was determined using the proposed methods. Accuracy was assessed as the percentage relative error and mean percentage recovery.

Precision was determined by using different QC levels of drug concentrations, prepared from independent stock solution and analyzed for inter-day variation, intra-day variation and instrument variation. For intraday variation, different levels of drug concentrations in triplicates were prepared three different times in a day and studied. Same protocol was followed for three different days to study inter-day variation. One set of different levels of the concentrations were re-analyzed using Jasco instrument by the proposed methods. Precision was reported as the relative standard deviation (% RSD).

Robustness was examined by evaluating the effect of small variation in the experimental parameters on the analytical performance of the method. It was determined by (a) changing pH of the medium by ± 0.2 units and (b) stability of TMZ in the selected diluent at room temperature for 24h. Three different QC standards (LQC, MQC, and HQC) were prepared

in the media with different pH, and mean percentage recovery was determined for each sample.

3.4.5. Results and Discussion

TMZ exhibited pH independent UV absorption in all the media with three absorption bands with maxima at λ = 212, 252 and 329 nm respectively as reported in literature [17] However, during short term stability studies in various media of different pH, a new absorption band with maxima at 272 nm appeared whereas a reduction in absorption band at maxima 329 nm was observed. The increase in absorbance at 272 nm and reduction in absorbance at 329 nm after 24h became more significant as the pH of the media increased from 6.8 to 8.0. This shift in absorption maxima from 329 nm to 272 nm indicates degradation of TMZ to 5-aminoimidazole-4-carboxamide (AIC) at pH 5 and above (Fig. 3.1). The results conform to the reports that TMZ is stable in acidic pH (<5) and undergoes conversion which increases as the pH increases from neutral to basic pH [17,18]. Hence pH of the solvent media is critical for the estimation of TMZ. Further, for selection of suitable solvent media, the criteria employed apart from stability was sensitivity of the method, ease of preparation, economy and wider application of the method for routine analysis of TMZ. Addition of acetonitrile/methanol in various proportions with various aqueous media did not improve the sensitivity of the method. Thus, 100 mM hydrochloric acid (pH 1.2) as a media was finally selected based on criteria like; stability of drug, sensitivity of the method, cost, ease of preparation and applicability of the method.

TMZ was found to exhibit maximum absorption at a wavelength (λ_{max}) at 329 nm in the selected medium (pH 1.2). The spectrum is shown in Fig.3.2. Apparent molar absorptivity of TMZ was found to be 9.749 × 103 $L.mol^{-1}.cm^{-1}$ in hydrochloric acid medium. Sandell's sensitivity of drug was found to be 0.003 $\mu g.cm^{-2}$/ 0.001A^{o} in the selected media.

The method was validated by testing linearity, sensitivity, limit of detection, limit of quantitation, specificity, accuracy, precision, and robustness.

The UV spectrum of TMZ was not changed in the presence of the placebo mix containing excipients used for preparation of nanoparticles. Further, the placebo mix did not show any

significant absorbance at the selected wavelength of 329 nm (Fig.3.2). Therefore, the proposed method is specific and selective for TMZ.

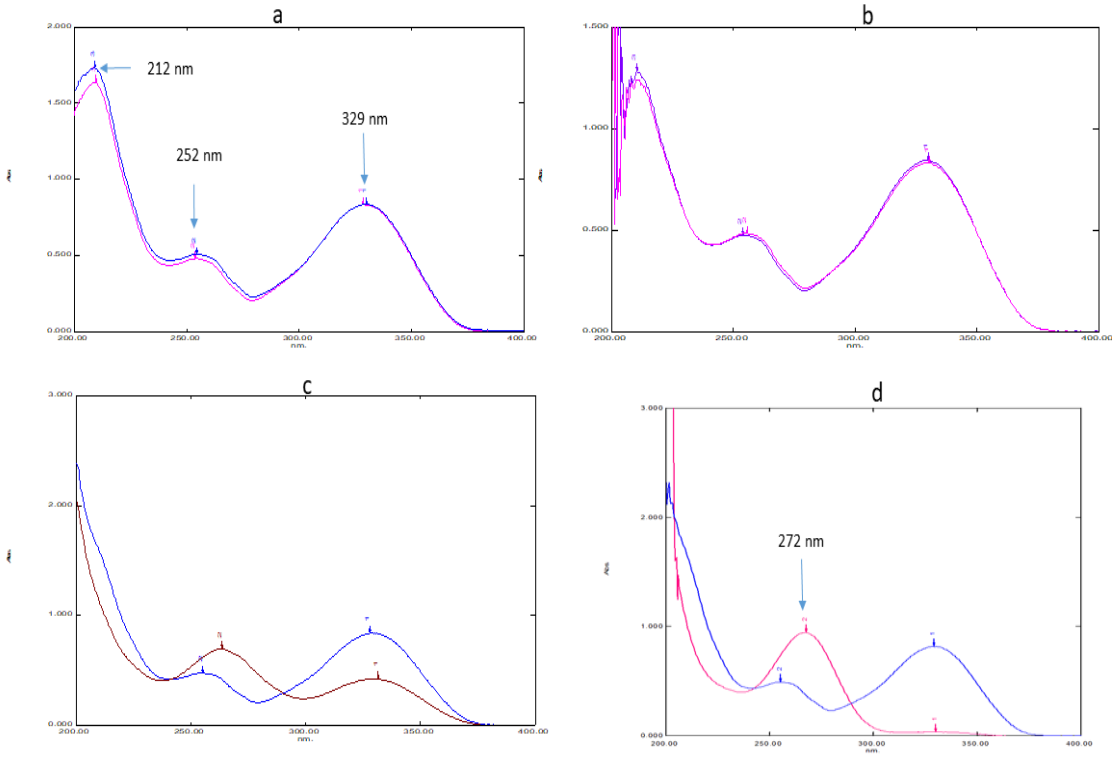

Fig. 3.1. Stability of TMZ solution (14 µg.mL^{-1}) after 24h (pink/red) in a) 100 mM hydrochloric acid (pH 1.2) b) ph.4.5 acetate buffer c) pH 6.8 phosphate buffer and d) pH 8.0 phosphate buffer

The calibration curve constructed by plotting the absorbance against the concentrations of TMZ (Table 3.1) was linear within the range of 3-25 µg.mL^{-1}. The calibration curves for TMZ were evaluated by a linear regression analysis and the regression equation obtained was absorbance at 329 nm = 0.0503 x (concentration of TMZ in µg.mL^{-1}) + 0.0002 with a regression coefficient (R^2) equal to 1. The statistical data summary is given in Table 3.2. The LOD and LOQ were found to be 0.170 µg.mL^{-1} and 0.510 µg.mL^{-1} respectively.

Accuracy (as % relative error) ranged from 0.01% to 0.02% (Table 3.3). The excellent mean % recovery values ranging from 99.60 -100.90% and their low % RSD values (<1.42) represent the accuracy of proposed method. The accuracy of the proposed methods was also

evaluated by placebo spiking method (Table 3.4). The mean percentage recoveries (% RSD) for the LQC, and HQC were found to be 99.34 (1.27), 100.58 (0.90) and 100.15 (1.37), respectively. These results demonstrate the validity and reliability of the proposed method for estimation of TMZ.

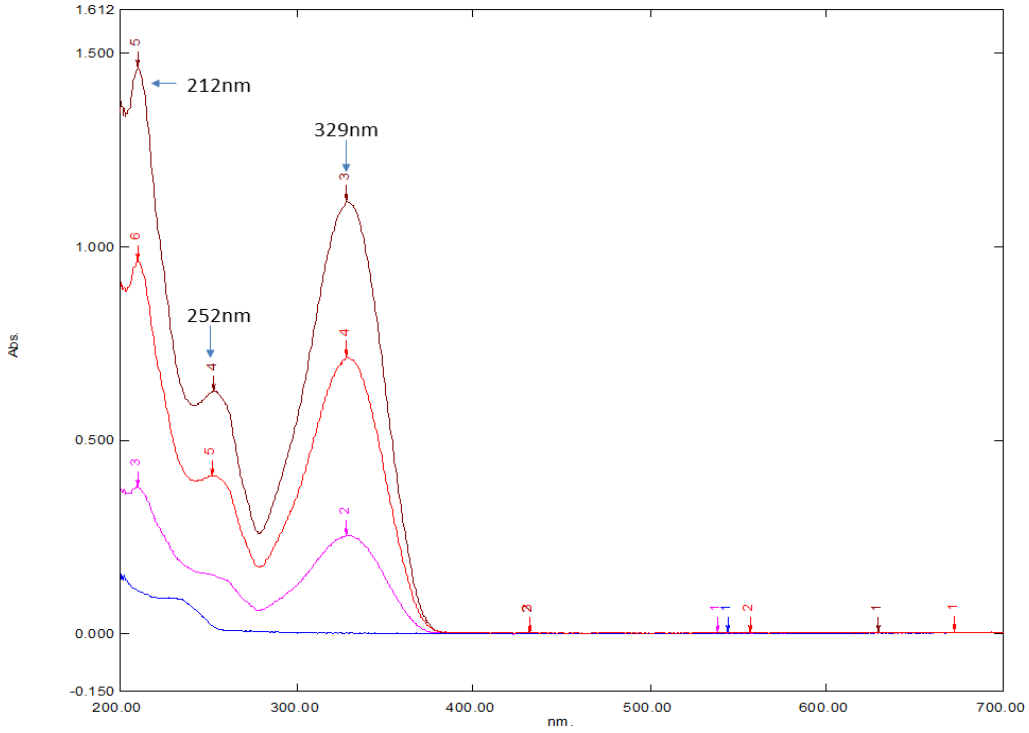

Fig. 3.2. UV spectrum of temozolomide with placebo (blue) overlaid with standards (LQC; pink, MQC; red and HQC; brown) in 100 mM hydrochloric acid medium (pH 1.2)

Table 3.1. Calibration data of the developed UV spectroscopy method

TMZ conc. (µg.mL^{-1})	Absorbance at 329 nm ± SD[a]	% RSD[b]
3.00	0.151±0.002	1.33
9.00	0.452 ± 0.005	1.20
13.00	0.656±0.006	0.88
17.00	0.846±0.004	0.44
21.00	1.071±0.003	0.25
25.00	1.250±0.0032	0.20

[a] Standard deviation. [b] Relative standard deviation.

Each absorbance value is a result of nine separate determinations

Table 3.2. Statistical data summary for the UV spectroscopy method

Parameters	**Results**
Calibration range (µg,.mL^{-1})	3 to 25
Linearity (Regression coefficient)	1
Regression equation	Y = 0.0503*X + 0.0002
Slope (S.E. [a])	0.05028 ± 0.0005
Confidence interval of slope [b]	0.049 to 0.052
Intercept (S.E .[a])	0.0002 ± 0.009
Confidence interval of intercept [b]	-0.024 to 0.024
Standard error of estimate	0.0095
Limit of detection (µg.mL^{-1})	0.170
Limit of quantification (µg.mL^{-1})	0.510
Absolute recovery (Accuracy)	99.60 to 100.90%
Precision (% RSD [c])	Repeatability: > 1.28% (Intraday) Intermediate precision: > 0.76 % (Interday)

[a] Standard error of mean; [b] Calculated at 0.05 level of significance; [c] % Relative standard deviation

Precision of the method was determined by studying repeatability and intermediate precision. Repeatability results indicate the precision under the same operating conditions over a short interval of time. Intermediate precision expresses within-laboratory variations on different days and in different instruments. In precision study, % RSD values were not more than 1.5% in all the cases (Table 3.5) indicating that these methods have excellent repeatability and intermediate precision.

Variation of pH of the selected media by ± 0.2 did not have any significant effect on the absorbance as the recovery values were found to be from 99.4% to 100.35%. The TMZ solution in the selected diluent did not exhibit significant changes for 24 h when kept at room temperature with the recovery values from 98.01 to 99.81% (Table 3.6). This provides an indication of the reliability and stability of the proposed method during routine analysis.

Table 3.3. Accuracy data of the proposed UV method for determination of TMZ

QC Standard	Predicted concentration (µg.mL^{-1})[a]			Mean % Recovery ± SD	Accuracy[b] (%)
	Range	Mean ± SD	%RSD		
LQC	4.95-5.09	5.03 ± 0.07	1.43	99.60 ± 1.42	0.01
MQC	14.08 -14.47	14.27 ± 0.20	1.40	100.90± 1.41	0.02
HQC	22.01-22.45	22.21 ± 0.22	0.99	99.97± 0.99	0.01

LQC, MQC and HQC for UV method are 5, 14 and 22 µg.mL^{-1} respectively.
Each value is result of six separate determinations.
[a]Predicted concentration of TMZ calculated by linear regression equation.
[b]Accuracy is given in % bias (= 100 × [(predicted concentration – nominal concentration)/nominal concentration)].

Table 3.4. Results of placebo spiking method by the proposed UV method

QC Standard	Predicted concentration (µg.mL^{-1})[a]			Mean% recovery ± SD	Accuracy[b] (%)
	Range	Mean ± SD	%RSD		
LQC	4.97-5.09	5.02 ± 0.06	1.27	99.34 ± 1.27	0.00
MQC	14.08-14.31	14.22 ± 0.13	0.90	100.58 ± 0.90	0.02
HQC	21.91-22.49	22.25± 0.30	1.37	100.15 ± 1.37	0.01

Each result is the average of three separate determinations
[a]Predicted concentration of TMZ calculated by linear regression equation.
[b]Accuracy is given in % bias (= 100 × [(predicted concentration – nominal concentration)/nominal concentration)].

Table 3.5. Precision study results for the UV method

QC Standard	Intraday repeatability % RSD (n=9)			Interday repeatability % RSD (n = 27)	Inter-instrument repeatability % RSD (n = 6)
	Day 1	Day 2	Day 3		
LQC	1.28	0.91	1.23	0.76	0.70
MQC	1.11	1.06	1.03	0.30	0.92
HQC	0.74	0.79	1.06	0.17	1.11

Table 3.6. Robustness data for the proposed UV method

QC Standard	pH 1.1		pH 1.3		Stability data (24h)	
	Mean % recovery ± SD	%RSD	Mean % recovery ± SD	%RSD	Mean % recovery ± SD	%RSD
LQC	99.40 ± 0.80	0.80	100.07± 0.61	0.61	98.01 ± 2.37	2.42
MQC	100.35± 0.86	0.85	100.21± 1.08	1.07	98.08± 1.28	1.30
HQC	99.67 ± 0.48	0.48	99.83± 0.59	0.59	98.11 ± 0.40	0.41

Each result is the average of three separate determinations

In summary, the results demonstrate that the proposed UV spectrophotometric method is cost effective, simple, rapid, sensitive, accurate and precise and can be used for the routine analysis of TMZ either in bulk or in the formulations, without interference of commonly used excipients for nanoformulations.

3.5. HPLC Analytical Method for Determination of TMZ

3.5.1. Instrumentation and Chromatographic Conditions

The HPLC system (LC-2010HT, Shimadzu Corporation, Japan) consisted of a pulse-free solvent delivery system comprising two pumps, high-efficiency 5-line degasser, block heating-type column oven, sample cooler (LC-2010CHT), intelligent autosampler and dual wavelength UV-visible detector. Chromatographic peaks were collected and analyzed using LCsolutions software loaded on a computer system. Chromatographic separations were carried out on Hypersil Gold aQ C18 column (4.6 x 150 mm, 5 µm particle size; Thermoscientific, India) with mobile phase composition of methanol-0.5% acetic acid (10:90, v/v) at a flow rate of 1.0 $mL.min^{-1}$. The aqueous phase was filtered through a 0.22 µm nylon membrane filter and ultrasonically degassed prior to use. The column oven temperature was maintained at 25ºC. The detector was operated at a wavelength of 329 nm for data acquisition. The volume injected was 30 µL and the run time was 9 minutes under isocratic elution.

3.5.2. Method Development

Different buffers (phosphate, formic acid, acetic acid) of pH range 3.0-5.0 were tried as mobile phases with different proportions of organic solvents methanol and acetonitrile for development of the HPLC method with the objective of achieving high sensitivity in terms of high peak height to area ratio, good peak symmetry, optimum resolution and minimal column damage.

3.5.3. Preparation of Stock and Calibration Standards

Primary stock solution of TMZ was prepared by dissolving 5mg of TMZ in methanol and making up the volume to 50 mL to obtain a concentration of 100 $\mu g.mL^{-1}$. A secondary stock of 10$\mu g\ mL^{-1}$ was prepared using 0.5% acetic acid solution as the diluting solvent. For calibration curve, six different concentrations of 40, 100, 150, 250, 500 and 1000 $ng.mL^{-1}$ were prepared by taking appropriate aliquots of the secondary stock solution in a 2ml centrifuge tube and making up the volume with the diluting solvent. The calibration standards were prepared in triplicate.

3.5.4. Method Validation

The method developed was validated as per the ICH guidelines [4] for selectivity, sensitivity, linearity, accuracy, precision and robustness.

Selectivity was determined by placebo spiking method wherein a known concentration of TMZ was spiked in a placebo mix containing excipients used for the in house nanoformulation as detailed in Section 3.4.4. The chromatograms of the TMZ spiked in placebo was compared with TMZ standard prepared without placebo mix. A blank sample of the placebo mix was also injected to assess any interference at the retention time of TMZ due to the excipients.

To establish linearity, calibration standards in the range of 40-1000 $ng.mL^{-1}$ were prepared in triplicate and analyzed on three different days. The calibration data was analyzed by least squares linear regression and a calibration equation was generated.

Sensitivity, was determined in terms of LOD and LOQ, which were calculated using the standard formula of $3.3\sigma/S$ and $10\sigma/S$ respectively where σ is the standard deviation of the response and S is the slope of the calibration curve.

Accuracy was determined by analysis of QC standards (LQC=50 ng.mL^{-1}, MQC=450 ng. mL^{-1} and HQC=950 ng.mL^{-1}) prepared and represented in terms of % bias and % recovery. Further, accuracy was confirmed by placebo spiking method wherein the QC standards were spiked into the placebo mix and the results of accuracy reported as % recovery.

For precision studies, repeatability and intermediate precision was determined by evaluating intra and inter day variation in analysis. QC standards were prepared in triplicates thrice a day for intraday variation and the same protocol was followed for three consecutive days for inter day variation. Precision was calculated as % RSD values of the predicted concentration derived from the regression equation.

Robustness studies are carried out to evaluate the impact of slight variations in chromatographic conditions which can occur during routine analysis. Robustness of the developed method was assessed by introducing small changes in chromatographic conditions such as change in % of methanol in the mobile phase (5 and 15%), pH of the mobile phase (2.5 and 3.5), column temperature (20 and 30ºC) and flow rate (0.8 and 1.2 mL). QC standards were analyzed in triplicates and the results reported as the mean of % recovery and % RSD at all QC levels. Further, solution stability of TMZ was carried out by leaving the QC standard solutions in a tightly stoppered volumetric flasks at room temperature for 24h. Long term stability of the stock solution was also determined by storing the stock solution at 4ºC and assay was determined at regular intervals over a period of 1 month.

System suitability parameters were also evaluated. A TMZ solution of concentration 1000 ng.mL^{-1} was injected six times and the system suitability parameters were recorded. These included injection precision and chromatographic factors such as capacity factor (k'), resolution (R_s), tailing factor (T_f), number of theoretical plates (N) and injection precision.

Further, to evaluate the stability indicating potential of the method forced degradation studies were also carried out. TMZ was subjected to acidic, alkaline, oxidative and thermal stress conditions. TMZ solution (50 µg.mL^{-1}) were prepared on 0.1N hydrochloric acid (HCl), 0.1 N sodium hydroxide (NaOH) and 5% hydrogen peroxide and refluxed for 6h at 60ºC. For thermal degradation, sample of the drug was placed in a temperature controlled

oven at 80ºC for 6h. For photostability, TMZ solution was exposed to both solar and UV radiation in a UV chamber for 12h each. All the samples were then cooled to room temperature, suitably diluted with the diluting solvent and analyzed by the proposed method.

3.5.5. Results and Discussion

The main consideration during method optimization was given to peak properties such as retention time, peak shape and symmetry, in addition to higher sensitivity in terms of high peak to area ratio. These parameters were set by studying effects of various buffers (formic, acetic, phosphate) pH of buffers (pH 3-5), choice of organic solvent (methanol and acetonitrile). Various buffers and the pH variation had minimal effect on the peak properties of TMZ probably due to the unionized nature of TMZ. However, 0.5% acetic acid solution was used as it resulted in good peak properties and high peak to area ratio. Use of acetonitrile resulted in faster elution and poor resolution. Methanol was selected for the mobile phase composition as it gave satisfactory peak properties, good resolution and is comparatively economical. A mobile phase composition of methanol: 0.5% aqueous acetic acid (10:90, v/v), pH 3.0, was found to be optimal for good peak resolution and peak properties. During robustness studies, it was observed that the flow rate varying from 0.8 - 1.2 $mL.min^{-1}$ had an impact on the retention time as well as the peak area. A flow rate of 1.0 $mL.min^{-1}$ was selected as optimum for the method. Retention time of TMZ was obtained at 4.1 ± 0.25 min in the selected mobile phase (Figure 3.3a). The peak had good resolution and asymmetric factor of ~1.2. The run time for single injection was 9 minutes for the proposed method.

The method was selective as no interference from the placebo mix was observed in the vicinity of the drug peak. This indicated that the method was selective and suitable for quantification of TMZ in formulations in presence of excipients (Figure 3.3 b & c). Further, no significant change in TMZ recovery and peak properties was observed in TMZ spiked placebo mix in comparison to QC standards. Least square regression analysis indicated linearity between peak area and concentrations over the range of 40 -1000 $ng.mL^{-1}$ with R^2 value equal to 1. The best fit linear equation was average peak area = [87.467 x TMZ concentration in $ng.mL^{-1}$] - 10.05. The low value of standard error of estimates (145.5) indicates the goodness of fit of regression analysis.

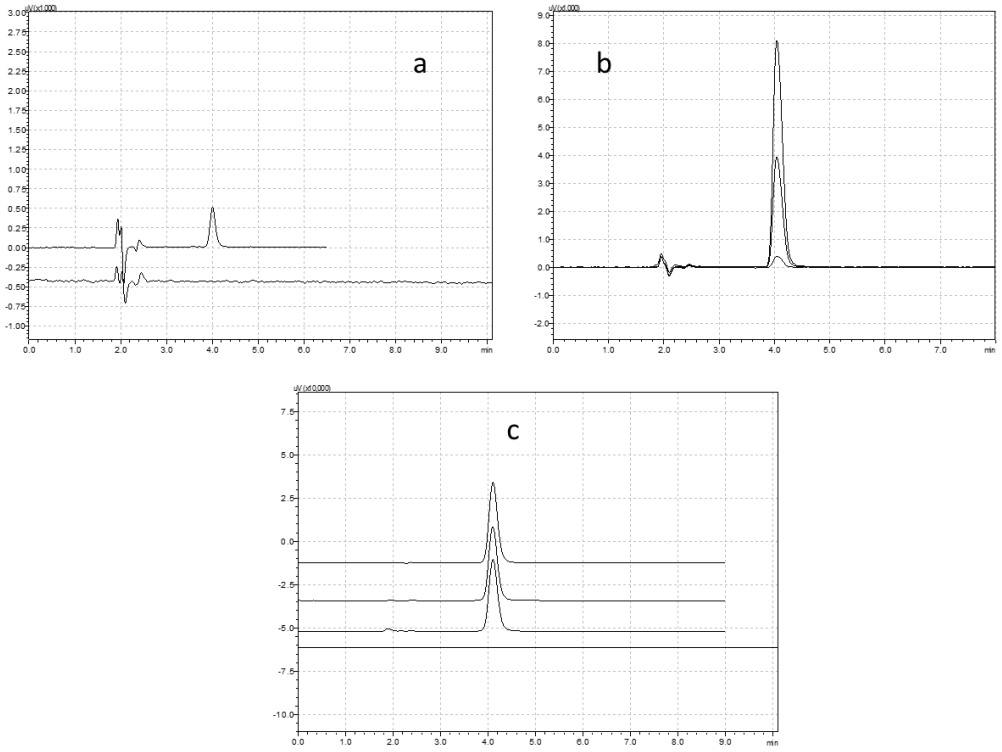

Fig. 3.3. Representative chromatograms of temozolomide indicating selectivity of the HPLC method: a) placebo overlaid with calibration standard (40 ng.mL^{-1}); b) placebo overlaid with QC standards (LQC, MQC, HQC) and c) placebo overlaid with in-house developed NLC formulations

At all concentration levels the SD was very low and % RSD did not exceed 1.91%. The calibration data is as given in Table 3.7.

The LOD and LOQ values calculated from the standard formula was found to be 2.97 and 9.00 ng.mL^{-1} respectively.

The proposed method was found to be accurate and precise with % bias and % RSD values at all QC levels, for both inter and intraday, in the range of -1.98 to 0.36 % and < 2% respectively. Furthermore, high recovery values (98.02 -100.36%) and SD < 1.6 indicates accuracy and precision of the method. The data for interday and intraday accuracy and precision is tabulated in Table 3.8. Accuracy was further confirmed by placebo spiking and

the results (Table 3.9) of high recovery of almost 100% and low % bias (-0.40 to 0.82) indicating suitability of the method for quantification of TMZ in presence of formulation excipients.

Table 3.7. Calibration data for the determination of TMZ by HPLC

TMZ conc. (ng.mL^{-1})	**Peak Area ± SD**	**% RSD**
40	3540 ± 45.08	1.27
100	8756 ± 97.20	1.11
150	13260 ± 114.72	0.87
250	21622 ± 413.79	1.91
500	43680 ± 451.57	1.03
1000	87504 ± 905.92	1.04

Each peak area value represents average of nine individual determinations

The method was found to be robust and the peak area as tabulated in Table 3.10 did not vary significantly when chromatographic conditions deviated from the optimized ones with respect to methanol percentage in the mobile phase (5-15%), pH of the mobile phase (2.5 - 3.5), column temperature (20-30°C) and flow rate (0.8-1.2 mL.min^{-1}). The recovery of TMZ was in the range of 98.21 to 100.26 and % RSD was < 2.0. Further, the variations did not significantly affect the system suitability parameters indicating the potential of the method to quantify TMZ accurately and precisely.

Stability studies of QC standards at RT for 24h demonstrated that TMZ was stable at room temperature for 24h and the stock solution in methanol was stable for 1 month at 4°C. Results calculated in terms of recovery were in the range of 97.64 – 99.93%.

The method was also found to be suitable with respect to system performance as the values obtained for system suitability parameters such as capacity factor (k' ~ 1.3), resolution (R_s ~ 9.0), number of theoretical plates (~ 5650) were within acceptable limits. Injection

precision (% RSD) was 0.36 and the peak symmetry was also good (T_f ~ 1.2). The results confirmed that the method was specific, precise and suitable for determination of TMZ.

Table 3.8. Accuracy and precision data for the HPLC analytical method

QC Standard	Predicted Conc. (ng.mL^{-1})		% Recovery ± S.D	% Bias[#]
	Mean ± S.D	% RSD		
Intraday (n=9)				
LQC	49.53 ± 0.97	1.95	98.76± 0.76	-0.94
MQC	443.31 ± 5.22	1.18	98.51± 1.16	-1.49
HQC	953.39 ± 11.40	1.20	100.36± 1.20	0.36
Interday (n=27)				
LQC	49.01 ± 0.51	1.03	98.02± 1.01	-1.98
MQC	446.48 ± 7.05	1.58	99.22± 1.57	-0.78
HQC	949.89± 12.61	1.33	99.99± 1.33	-0.01

[#]Accuracy is given as % bias (= 100 × [(predicted concentration – nominal concentration)/nominal concentration)].

Table 3.9. Accuracy studies for HPLC analytical method by placebo spiking method

Amount of TMZ added (ng)	Recovered TMZ ± SD (ng)	% Recovery ± SD	% Bias
50	50.41 ± 0.76	100.82 ± 1.53	0.82
450	448.19 ± 3.80	99.60 ± 0.85	-0.40
950	946.85 ± 11.83	99.67 ± 1.24	-0.33

Each result is the average of three separate determinations

[b] Accuracy is given as % bias (= 100 × [(predicted concentration – nominal concentration)/nominal concentration)].

Table 3.10. Robustness data of developed HPLC analytical method

Parameter Changed		**% Recovery ± SD**	**% RSD**
Ratio of Methanol : 0.5% acetic acid solution (pH 2.9 ± 0.1)	5:95	99.44 ± 1.17	1.18
	15:85	99.74 ± 1.38	1.39
pH of buffer	2.5	99.65 ± 1.79	1.80
	3.5	99.79 ± 1.58	1.58
Column temperature (°C)	20	100.26 ± 1.83	1.83
	30	98.47 ± 1.57	1.78
Flow rate ($mL.min^{-1}$)	0.8	99.23 ± 1.19	1.20
	1.2	98.21 ± 1.58	1.61

Each result is the average of three separate determinations at all QC levels.

The results of forced degradation study are summarized in Table 3.11. In all stress conditions except base hydrolysis, the recovery was in the range of 95.14 - 97.03%. In base hydrolysis, no peak of TMZ was observed indicating complete degradation of the drug. These results are in accordance with the reports that TMZ is stable at pH < 5, but undergoes rapid degradation as the pH increases from neutral to alkaline [17,18]. The results indicated possible degradation except photostability. However, no interference at the retention time of the drug or any additional peaks were observed. The probable reason for no degradation peaks is that the degradation products are hydrophilic in nature and eluted out quite early in the chromatogram and merged with the mobile phase peak. Further, there is a possibility that the degradant/s do not absorb at or near 329 nm resulting in no detection. The degradation

was indicated by decrease in the peak area or no peak at all, as observed in the base hydrolysis. The representative chromatograms are as shown in Figure 3.4.

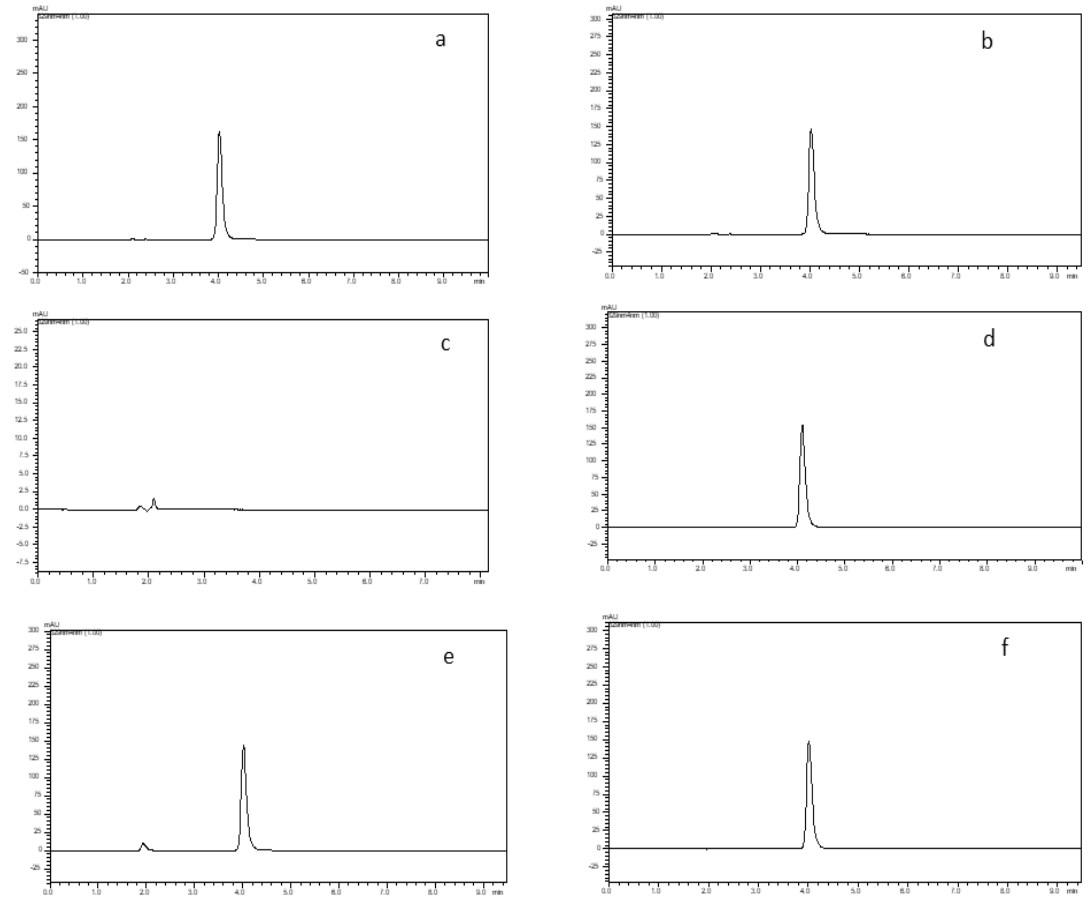

Fig. 3.4. Representative peaks of forced degradation study of TMZ; a) TMZ; b) acid hydrolysis; c) base hydrolysis; d) photostability; e) oxidation and f) thermal stress

Table 3.11. Results of forced degradation studies of TMZ by HPLC

Stress condition	**% Recovery ± SD (n=3)**
Acid hydrolysis (0.1N HCl at 60°C, 4h)	95.14 ± 2.41
Base hydrolysis (0.1N NaOH at 60°C, 4h)	No TMZ peak detected
Photostability (Solar energy+ UV lamp; 12h each)	97.03 ± 1.42
Oxidation (5% hydrogen peroxide, at 60°C, 4h)	95.69 ± 3.43
Thermal (80°C, 4h)	96.43 ± 2.32

The method was successfully used to determine drug content in house developed nanoformulations. The results will be discussed in Chapter 5.

3.6. HPLC Method for Quantification of TMZ in Rat Plasma and Tissues

3.6.1. Instrumentation and Chromatographic Conditions

The HPLC instrument used is same as described in section 3.5.1. Chromatographic separations were carried out on a C-18 Oyster BDS Premium column (4.6 × 150 mm, 5 µm particle size, Merck, India) with mobile phase composition of 0.5% acetic acid - methanol in the ratio of 98:2% v/v at a flow rate of 1.0 $mL.min^{-1}$. The buffer was filtered through a 0.22µm nylon membrane filter and ultrasonically degassed prior to use. The column oven temperature was maintained at 35^0 C. The detector was operated at a dual wavelength of 310 and 329 nm for data acquisition of the internal standard (IS) and TMZ respectively. The volume injected was 50 µL and the run time was 15 minutes under isocratic elution.

3.6.2. Collection of Plasma and Tissue Homogenates

Study protocols (Protocol No. IAEC/RES/19/16 and IAEC/RES/23/07) were approved by the Institutional Animal Ethics Committee (IAEC), BITS Pilani prior to commencement of the work. Healthy male Wistar rats were obtained from Central Animal Facility, BITS, Pilani (Rajasthan, India). They were kept in standard plastic cages maintained under controlled conditions (23 ± 2°C, 60 ± 5% RH and 12h dark-light cycle) and provided standard laboratory pellet food with water ad libitum. Blood samples were collected from the retro-orbital sinus of male Wistar rats into 2mL polypropylene centrifuge tubes containing 100 µL of 10% w/v solution of EDTA. The blood EDTA mix was centrifuged at 8000 rpm for 30 minutes at 4ºC. The clear supernatant plasma was pooled into fresh tubes and stored at -20ºC till further use.

Tissues were collected from six healthy rats after a surgical procedure under anesthesia, where a midline incision was made in the abdomen and organs such as liver, heart, kidneys, brain, spleen and lungs were excised. The animal was then sacrificed using the standard protocol. These tissues were rinsed and cleaned gently with ice cold formic acid (4%) solution and then dried with Whatmann filter paper number 40. The organs were then

weighed individually, transferred to a pre chilled 50 mL centrifuge tube and two volumes (2mL for 1g tissue) of ice cold 4% formic acid solution was added. A fine tissue homogenate was obtained by homogenizing the same at 20,000 rpm using a Kinematica ™ Polytron ™ PT 1600E benchtop homogenizer (Thermo Fisher Scientific Inc., USA). The homogenate was then centrifuged at 8,000 rpm for 30 minutes and the supernatant was collected and stored in -80°C till further use.

3.6.3. Preparation of Stock Solutions, Calibration and Quality Control Standards

Primary stock solutions of TMZ and IS were prepared at a concentration of 1000 µg mL^{-1} by dissolving the compounds in methanol and water respectively. The TMZ and IS stock solutions were further diluted with 0.5% acetic acid solution and water to produce working standard solutions of 300 µg.mL^{-1} and 250 µg.mL^{-1} respectively. The TMZ standard solution was further diluted to give spiking standard solutions of 1, 2, 5, 10, 20, 50, 100, 150 and 200 µg.mL^{-1} respectively. Calibration samples (50,100, 250, 500, 1000, 2500, 5000, 7500 and 10000 ng.mL^{-1}) were prepared by spiking 10µL of spiking standard solutions into 200 µL of blank rat plasma. The plasma standards were prepared fresh in three replicates on three different days of validation. Quality control (QC) standards were independently prepared at limit of quantitation (LOQQC= 50ng.mL^{-1}), low (LQC= 150ng.mL^{-1}), medium (MQC= 4000ng.mL^{-1}) and high (HQC= 8000ng.mL^{-1}) concentration levels. The QC standards were prepared fresh in five replicates on each day of validation. TMZ in the calibration standadrds and QC standards was stabilized by addition of 90 µL of 1M formic acid. For tissue samples, acidification with formic acid was omitted. The calibration standards and the QC standards were processed as described in "Sample preparation" and analysed by the proposed method.

3.6.4. Sample Preparation

Protein precipitation procedure was used for the extraction of TMZ from the plasma and tissues. Prior to extraction, the plasma and tissue samples were spiked with 100µL of IS working standard equivalent to a concentration of 25 µg.mL^{-1}. For extraction, 100µL of perchloric acid solution (8.5%) was added to the control, calibration samples, QC samples and blank plasma and tissue sample (without TMZ and IS) to precipitate the proteins and vortex mixed for 5 minutes. The samples were centrifuged at 12,000 rpm for 15 minutes at

4ºC. The clear supernatant was transferred to autosampler and 50 µL was injected into the HPLC system for analysis.

3.6.5. Method Validation Parameters

The method in plasma was validated in terms of linearity, specificity, accuracy, precision (intraday and interday) and stability (stock solution, freeze-thaw, bench-top, long-term and post-preparative) in accordance to the US Food and Drug Administration (USFDA) guidelines for bioanalytical method validation [3]. The calibration samples were freshly prepared and analysed in triplicate on three consecutive days. Linearity of the calibration curve was obtained by plotting the peak area ratio (area of TMZ/area of IS) for plasma and as peak area for tissues against the corresponding concentration of TMZ. Selectivity, which assesses the method for any interferences from the sample matrix, endogenous substances, degradants and sample blank peaks due to the reagents added during sample processing, was investigated by processing six independent sources of rat plasma and analysing them with the proposed method. Accuracy, recovery and precison (interday and intraday) was determined on QC standards (50, 150, 4000 & 8000 $ng.mL^{-1}$) prepared freshly in five replicates on three consecutive days. Precision was calculated as percent relative standard deviation (% RSD) and accuracy was expressed as % bias which is the percent deviation from the nominal value. It is calculated using the following equation:

$$\%\ Bias = 100 \text{ x } \frac{\text{Observed Concentration} - \text{Nominal concentration}}{\text{Nominal concentration}}$$

Recovery (extraction efficiency) studies involved comparing the analytical results from the extracted QC standards (n=5) with the unextracted standards of the same concentration representing 100% recovery.

3.6.6. Stability Studies

To evaluate stability of TMZ under different working conditions required for analysis by the proposed method, short term and long term stability studies were carried out on three QC standards (LLOQ, MQC and HQC). The short term studies involved keeping the QC standards at controlled room tempertaure (CRT) of ~25ºC and analysing the same at 6, 12 and 18h. Long term stability was investigated in QC standards stored at -20ºC for 90 days.

In freeze-thaw stability studies, the QC standards were exposed to three alternate freeze (-20ºC) / thaw cycles. Furthermore, stability of the processed samples was evaluated in the autosampler at 4ºC for 24h. The stability was expressed in terms of accuracy as % bias and % RSD.

3.6.7. Analysis of In Vivo Samples

Samples of pharmacokinetic biodistribution studies for both pure drug and the in house developed nanoformulations were analysed by the above validated method. The proces and results are discussed in Chapter 6.

3.6.8. Results & Discussion

The prime consideration while developing a bioanalytical method is that the method should be specific and selective. Further, high height to area ratio and peak symmetry is important for improved sensitivity and resolution. To achieve rapid and efficient protein precipitation, minimal interference and good recovery, organic solvents such as methanol, acetone and acetonitrile, in addition to mineral acid perchloric acid were tried. The organic solvents were required in large volumes (700-1000 µL) to achieve protein precipitation which was not desired as our objective was to develop a green method with minimal use of solvents. Further, the sample processing was multi-step, tedious and a time consuming procedure. Perchloric acid was finally selected due to two reasons: one that it was a simple one step method with high and consistent recovery (>85%) and high throughput. Secondly, as discussed earlier that TMZ is stable under acidic conditions, addition of perchloric acid would contribute in maintaining stability of TMZ in the plasma.

The UV spectrum of TMZ showed a maximum absorbance (λ_{max}) at 329nm. However, The IS could not be detected at that wavelength. Therefore, a dual wavelength of 329 nm and 310 nm was selected for determination of TMZ and IS respectively depending on the absorbance and interference from the matrix. Peak properties and resolution of TMZ and IS from endogenous compounds were optimized by varying organic to aqueous phase ratio, buffer type, buffer strength and flow rate.

The blank plasma samples from six rats did not show any interference at the retention time of TMZ and IS indicating selectivity of the method. Representative chromatogram of the blank plasma sample, plasma sample spiked with IS and plasma spiked with both TMZ and

IS at 310 and 329 nm respectively is as shown in Fig. 3.5. The retention time of TMZ and IS was observed at approximately 8.9 and 4.7 min respectively.

The calibration curve obtained by plotting peak area ratios (TMZ/IS) and respective concentrations and subjected to linear regression analysis indicated that the calibration curve was linear in the range of 50-10000 $ng.mL^{-1}$ with $r^2 \geq 0.998$. The best fit linear equation for the calibration curve was peak area ratios = 0.0018 x concentration of TMZ in $ng.mL^{-1}$ + 0.0361 with low standard error of estimate 0.3174. The standard deviation of peak area ratios was significantly low across the concentration range and % RSD was less than 9.0. Back calculated values for the calibration standards were also determined. The bias ranged from -9.31 to 6.93.

The method showed high and consistent recovery at all concentration levels. The mean absolute recovery of TMZ from rat plasma over the calibration range was in the range of 90.55 to 94.10% with % RSD ranging from 1.27 to 3.13. The recovery results at all QC concentrations are given in Table 3.12. The IS also demonstrated a consistent recovery of 97.70 ± 6.45%.

TMZ concentration of 50 $ng.mL^{-1}$ was selected as the LLOQ as it demonstrated a peak response 6 times than that of the blank. Further, the % bias (accuracy) and precision of LLOQ samples analyzed independent of the calibration curve was -5.76% and 5.09% respectively, indicating sensitivity of the method.

The calibration curve equation and range for various tissues is given in Table 3.13.

Table 3.12. Recovery of TMZ from plasma quality control standards

QC Standard	Mean absolute recovery ± SD	%RSD
LOQQC	92.32 ± 1.55	1.67
LQC	90.55 ± 1.55	1.71
MQC	94.10 ± 2.94	3.13
HQC	92.72 ± 1.17	1.27

Each value is the average of fifteen separate determinations (n = 5 on three occasions);
Recovery = [(Peak area of serum standard / peak area of analytical standard) × 100].

Table 3.13. Calibration data for rat tissues

Tissue	Linearity range ($ng.mL^{-1}$)	Calibration Equation	R^2
Brain	100 - 10000	y = 49.507x + 1265.2	0.999
Spleen	50 -10000	y = 49.815x + 1385.3	1.000
Heart	50 -10000	y = 46.844x + 1061	0.996
Lungs	50 - 5000	y = 58.471x + 1581.1	0.999
Kidneys	50 -10000	y = 50.399x + 2307.6	0.999
Liver	100 -5000	y = 49.543x + 1657	0.9989

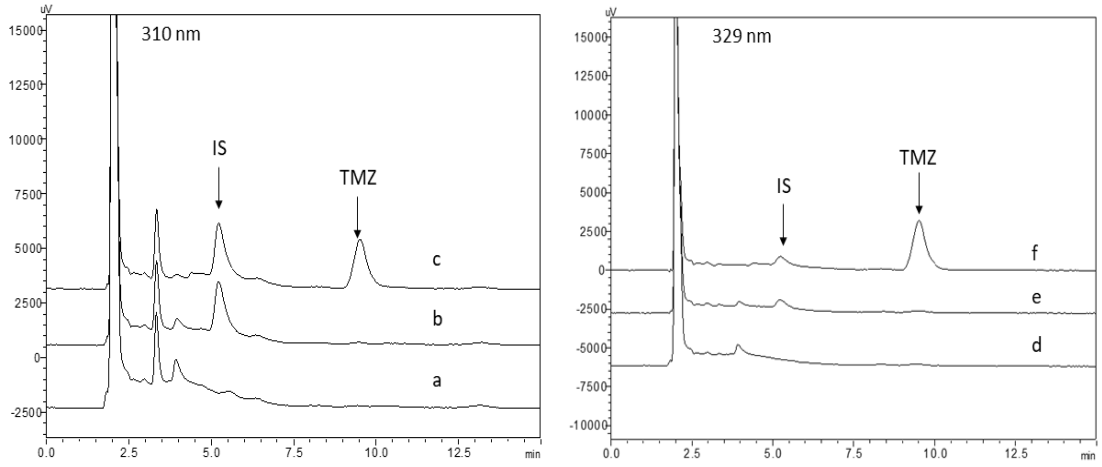

Fig. 3.5. Representative chromatograms of blank plasma (a & d), Plasma spiked with the IS (b & e) and plasma spiked with IS and TMZ (c & f) at 310nm and 329nm respectively

Accuracy and precision of the proposed method was confirmed as the percent deviation was very less. At all QC standard levels the intraday % bias ranged from -6.31 to - 3.13 and for interday the results were in the range of -5.07 to 3.46. The method was precise with % RSD < 4.50 for intraday and < 6.50 for interday at all concentrations including LLOQ. The method demonstrated excellent reproducibility and accuracy. The results of accuracy and precision obtained at each QC standard level are given in Table 3.14.

Table 3.14. Accuracy and precision data of the HPLC method in plasma standards

QC standard	Accuracy (% Bias)		Precision (% RSD)	
	Intraday $	Interday*	Intraday$	Interday*
LOQQC	-6.31	-3.95	2.63	6.27
LQC	-3.25	-2.45	4.20	4.43
MQC	-5.93	3.46	3.25	4.90
HQC	-3.13	-5.07	3.62	4.56

$ n= 5; * n=15;
Accuracy is given in % bias (= 100 × [(predicted concentration – nominal concentration)/nominal concentration)].

Stability studies indicated that TMZ was stable during short term stability study, long term stability study, freeze-thaw study and post preparative stability in autosampler. No significant change in the TMZ concentration was observed (% RSD >7.0) for 18h at RT indicating bench top stability. The % bias was in the range of -3.46 to 7.54. Similarly, in long term study where the plasma samples were stored at -20ºC for 3 months, freeze-thaw study in which the samples were subjected to three alternate freeze-thaw cycles and post preparative study in the autosampler at 4ºC, no significant difference between the freshly prepared standard and the samples at respective conditions was observed. The % RSD at all studied concentrations in all these studies was >6.0 and the % bias ranged from -0.63 to 8.56, indicating stability of the samples under various processing and storage conditions as mentioned in the method. The results of stability studies are tabulated in Table 3.15.

The dilution integrity of the method was used to investigate the dilution and ability of the method to analyze samples which exceed the upper limit of quantification of TMZ. The dilution integrity for plasma samples with TMZ at a concentration of 25000 $ng.mL^{-1}$ was found to be within acceptable limits with accuracy (% bias) of -2.35 and % RSD of 3.62. The results indicated that the method is accurate and precise for over-curve dilution up to 25000 $ng.mL^{-1}$.

Table 3.15. Stability studies of TMZ in rat plasma

Sample condition	TMZ conc. ($ng.mL^{-1}$)	% RSD			Accuracy (% Bias)		
		6h	12h	18h	6h	12h	18h
Short term stability [a]	LLOQ	2.76	3.92	3.23	3.19	7.54	2.49
	MQC	6.86	4.28	2.43	-3.46	-1.86	-0.15
	HQC	1.58	2.57	1.19	6.58	5.52	7.12
Freeze-thaw stability [b]	LLOQ	1.47			3.76		
	MQC	2.02			1.59		
	HQC	1.17			6.94		
Autosampler stability [c]	LLOQ	2.78			7.46		
	MQC	2.72			-0.63		
	HQC	1.79			6.27		
Long term stability [d]	LLOQ	3.87			8.56		
	MQC	5.62			6.09		
	HQC	3.13			5.12		

a-ambient temperature (25°C); b - after three freeze-thaw cycles; c - at 4°C for 24 h.; d - Stored at −20°C for 3 months. Each value is an average of five separate determinations

3.7. Conclusions

The developed UV spectrophotometric method for quantification of TMZ was selective, accurate, precise and robust. In addition to this, the method was rapid and cost effective. The method was successfully used for routine analysis of bulk, preformulation studies and also for nanoformulations.

The RP-HPLC method both analytical and bioanalytical were selective, sensitive, accurate and precise. The methods used simple procedures and were high throughput. The analytical method was successfully used for estimation of TMZ in various studies for development of nanoformulations including in vitro release study. The bioanalytical method in plasma and tissues was successfully utilized for pharmacokinetic and biodistribution studies of pure drug as well as the in house developed nanoformulations.

References

1 Green, J.M. (1996) Peer reviewed: a practical guide to analytical method validation. *Analytical Chemistry* 68 (9), 305A-309A

2 Food and Drug Administration (FDA) (2015) Guidance for industry: analytical procedures and methods validation for drugs and biologics. US Department of Health and Human Services, Food and Drug Administration, Center for Drug Evaluation and Research: Rockville, MD, USA.

3 Food and Drug Administration (FDA) (2013) FDA guidance for industry: bioanalytical method validation. US Department of Health and Human Services,Food and Drug Administration, Center for Drug Evaluation and Research: Rockville,MD,USA

4 ICH, Harmonized Tripartite Guideline (2005) Validation of analytical procedures: text and methodology Q2B (R1). ICH Steering Committee, Geneva,Switzerland pp. 11-12

5 Razak, A.A. et al. (2013) Development and validation of UV method of temozolomide in bulk and capsule formulation. *International Journal of Pharmaceutical Sciences and Research* 4 (4), 1419-1423

6 Khan, A. et al. (2016) Design of experiment based validated stability indicating RP-HPLC method of temozolomide in bulk and pharmaceutical dosage forms. *Beni-Suef University Journal of Basic and Applied Sciences* 5 (4), 402-408

7 Rao, A.L. et al. (2010) RP-HPLC analysis of temozolomide in pharmaceutical dosage forms. *Asian Journal of Chemistry* 22 (7), 5067-5071

8 Pallerla, S., Prabhakar, B. (2016). Bioanalytical method development and validation of temozolomide in rat plasma using RP-HPLC method. *International Journal of Pharmaceutical Sciences and Research*, 7(1), 1298-01

9 Shen, F. et al. (1995) Determination of temozolomide in human plasma and urine by high-performance liquid chromatography after solid-phase extraction. *Journal of Chromatography B: Biomedical Sciences and Applications* 667 (2), 291-300

10 Reyderman, L. et al. (2004) Disposition and pharmacokinetics of temozolomide in rat. *Xenobiotica* 34 (5), 487-500

11 Jain, D. et al. (2014) Double-salting out assisted liquid–liquid extraction (SALLE) HPLC method for estimation of temozolomide from biological samples. *Journal of Chromatography B* 970, 86-94

12 Diez, B.D. et al. (2010) Evaluation of the exposure equivalence of oral versus intravenous temozolomide. *Cancer Chemotherapy and Pharmacology* 65 (4), 727-734

13 Kim, H. et al. (2001) High-performance liquid chromatographic analysis and stability of anti-tumor agent temozolomide in human plasma. *Journal of Pharmaceutical and Biomedical Analysis* 24 (3), 461-468

14 Goldwirt, L. et al. (2013) Development of a new UPLC-MSMS method for the determination of temozolomide in mice: application to plasma pharmacokinetics and brain distribution study. *Biomedical Chromatography* 27 (7), 889-893

15 Peer, C.J. et al. (2016) Quantification of temozolomide in nonhuman primate fluids by isocratic ultra-high performance liquid chromatography-tandem mass spectrometry to study brain tissue penetration following intranasal or intravenous delivery. *Separations* 3 (1), 4

16 Andrasi, M. et al. (2010) Analysis and stability study of temozolomide using capillary electrophoresis. *Journal of Chromatography B* 878 (21), 1801-1808

17 Lopes, I.C. et al. (2013) Temozolomide chemical degradation to 5-aminoimidazole-4-carboxamide–Electrochemical study. *Journal of Electroanalytical Chemistry* 704, 183-189

18 Newlands, E.S. et al. (1997) Temozolomide: a review of its discovery, chemical properties, pre-clinical development and clinical trials. *Cancer Treatment Reviews* 23 (1), 35-61

4. Preformulation Studies

4.1. Introduction

Drug discovery and development is an expensive process, so it is necessary to evaluate and characterize the drug molecule in depth to successfully develop a commercially viable product with the desired characteristics of quality, safety and efficacy. Preformulation studies provide information on the physicochemical properties of the drug candidate and its interactions with various excipients, salt and polymorph screening which play a critical role in deciding on a suitable dosage form, selection of appropriate excipients for designing and developing a stable, safe and effective formulation of consistent quality and performance. This reduces the development time and cost considerably and reduces the possible challenges during formulation development. Preformulation studies include drug identification, powder characteristics such as particle size, crystallinity and polymorphism, solubility in various solvents and buffers, determination of pK_a, partition and distribution coefficients, stability in both solid and solution state and drug-excipient compatibility studies [1-3].

Temozolomide (TMZ) is a well-established anti-cancer drug for treatment of brain tumors, therefore, a lot of preformulation information is available. However, as our research objective involves formulation of nanostructured lipid carriers for TMZ, appropriate studies which can provide information about the drug characteristics and help in designing of the lipid nanoparticles were undertaken.

4.2. Experimental

4.2.1. Materials

Temozolomide was received as a gift sample from Neon Laboratories Ltd (Mumbai, India). Other formulation excipients were obtained from sources mentioned in section 3.3 of Chapter 3. Ultrapure water obtained from MilliQ Plus purification assembly, procured from Millipore®, was used for all the studies. Stearic acid, hydrochloric acid, potassium dihydrogen phosphate, disodium hydrogen phosphate, sodium hydroxide, sodium chloride, glycine, dimethyl sulfoxide (DMSO), sodium acetate, glacial acetic acid, methanol, isopropyl alcohol (IPA), ethanol, acetonitrile, acetone, polyethylene glycol 400 (PEG 400) were purchased from Merck India Ltd. All other chemicals used were of analytical grade and purchased from S.D. Fine Chemicals, India.

4.2.2. Instruments/Equipments

Digital analytical balance (Mettler-Toledo, Switzerland.) was used for all the weighing. An orbital shaker incubator (MAC instruments, India), vortex mixer (Spinix, India), magnetic stirrer with hot plate (Tarsons, India) and Remi cooling centrifuge was used for the solubility studies in various buffers, solvents and lipids. Humidity chamber (Thermotech, India) was used for stability studies at room temperature conditions. Frost free 200 liter refrigerator (LG India) was used for refrigerated conditions studies. All pH measurements were carried out using a portable pH meter (Hanna Instruments, USA) after calibration. Characterization and drug excipient compatibility studies were carried out using Fourier Transform Infrared (FTIR) spectrophotometer (model- IR Prestige 21; model software: IR Solutions ver.1.0; Shimadzu, Japan) and heat flux type differential scanning calorimeter (DSC-60 with TA-60WS thermal analyzer; integrating software: TA-60WS collection monitor, ver. 1.51; analysis software: TA-60; Shimadzu, Japan). UV spectrophotometer and HPLC system mentioned in chapter 3 were also used.

4.2.3. Bulk Characterization

Temozolomide was visually observed for physical characteristics such as color. Further, identification of TMZ was carried out by using the standard procedure of infrared (IR) spectrum as recommended in its USP monograph. Further, the UV spectrum and DSC thermogram was also generated. The UV spectrum was recorded as described earlier in Chapter 3.

For IR spectrum, TMZ was mixed with moisture free potassium bromide of spectroscopy grade and the mix was loaded into the IR holder. The spectrum was recorded in the range of 400 to 4000 nm^{-1} with a resolution of 4 cm^{-1}.

Thermal analysis by DSC was also carried out by taking around 2 mg of TMZ in a non-hermetic aluminum pan with lid in the sample holder, while an empty sealed pan was placed in the reference holder. Inert environment was maintained during the analysis by purging nitrogen gas at a flow rate of 30 $mL.min^{-1}$. The thermogram acquisition was carried out in the temperature range of 30°C to 300°C with a heating rate of 10°C min^{-1}.

4.2.4. Solubility Studies

Solubility of TMZ in various aqueous and non-aqueous solvents was determined by using the shake flask method. The aqueous solvents included water and buffers in the pH range of 1-8 whereas the non-aqueous solvents included dimethyl sulfoxide (DMSO), methanol, ethanol, acetone, acetonitrile, isopropyl alcohol and polyethylene glycol 400 (PEG 400). In microcentrifuge tubes 2mL of each solvent and an excess of TMZ were added and kept for shaking in orbital shaking incubator for 24 h at 37 ± 0.5°C. Throughout the study, an excess of TMZ was ensured in all the tubes. After 24h the centrifuge tubes were centrifuged for 15 minutes at 10,000 rpm and the supernatant collected was suitably diluted and analyzed by the proposed HPLC method.

The buffers were prepared (Table 4.1) as reported by Herzfeldt and Kummel [4].

Table 4.1. Composition of buffers from pH 1.0-9.0

Composition of Solution A	**Composition of Solution B**	**pH**	**Volume of Solution A**	**Volume of Solution B**
Hydrochloric acid (1M) - 94.0 mL Glycine - 0.50 gm Sodium chloride - 3.68 gm MilliQ water q.s 1000 mL	Sodium phosphate dibasic (anhydrous) - 16.35gm Potassium dihydrogen phosphate (Anhydrous) - 2.80 gm Sodium chloride - 0.15 gm MilliQ water q.s 1000 mL	1.0	100*	-
		2.0	70	30
		3.0	58	45
		4.0	56	48
		5.0	55	49
		6.0	50	50
		7.0	30	83
		8.0	-	100#
		9.0	-	100#

* pH to be adjusted with dilute hydrochloric acid solution
# pH to be adjusted with dilute sodium hydroxide solution

4.2.5. Stability Studies

4.2.5.1. Solution State Stability

Solution state stability was evaluated in various buffer solutions in the pH range of 1.2 to 8. A known concentration of TMZ standard (10 $\mu g.mL^{-1}$) was prepared in different pH buffers and the solutions were kept at 25.0 ± 2ºC in 5mL volumetric flasks in triplicate. At different time intervals (0, 12, 24, 48, 72, 96 and 120 h), samples were withdrawn and analyzed using the developed HPLC method as described in chapter 3. The % of drug remaining to be degraded was plotted against time and the degradation rate constant and order of degradation was determined.

4.2.5.2. Solid State Stability

In this study, TMZ was stored at various conditions i.e. room temperature (RT) condition (25 ± 2ºC, 60 ± 5% RH), accelerated condition (AC) (40 ± 2ºC, 75 ± 5% RH) and under refrigerated condition (5 ± 2ºC). Samples were withdrawn at different time intervals (0, 1, 2, 3 and 6 months) and analyzed using the HPLC method as described in chapter 3.

4.2.5.3. Drug-Excipient Compatibility Studies

In these studies, TMZ was admixed with various potential excipients (GMS, Compritol® 888ATO, Precirol® ATO5, PCL, poloxamer 188, and mannitol for the nanoformulation. The binary mixtures were prepared in 1:1 ratio by geometric mixing and stored at 60 ± 2ºC and 40 ± 2ºC, 75 ± 5% RH for 1 month. The samples were analyzed by DSC immediately after preparation of the mixture. After 1 month, the samples were analyzed by HPLC to determine TMZ content and also FTIR spectroscopy to assess any compatibility issues between the drug and the potential excipients. Further, the mixtures were assessed for any physical changes such as change in color, lump formation etc.

4.3. Results and Discussions

4.3.1. Bulk Characterization

Temozolomide appears as a light pink/tan colored crystalline powder with a characteristic odor. The pure drug displayed three absorption bands with maxima at λ of 212 nm, 252 nm and 329 nm in the UV spectrum for a concentration of 10 $\mu g.mL^{-1}$ in 100 mM hydrochloric acid medium (pH 1.2). Similar results have been reported in literature[5].

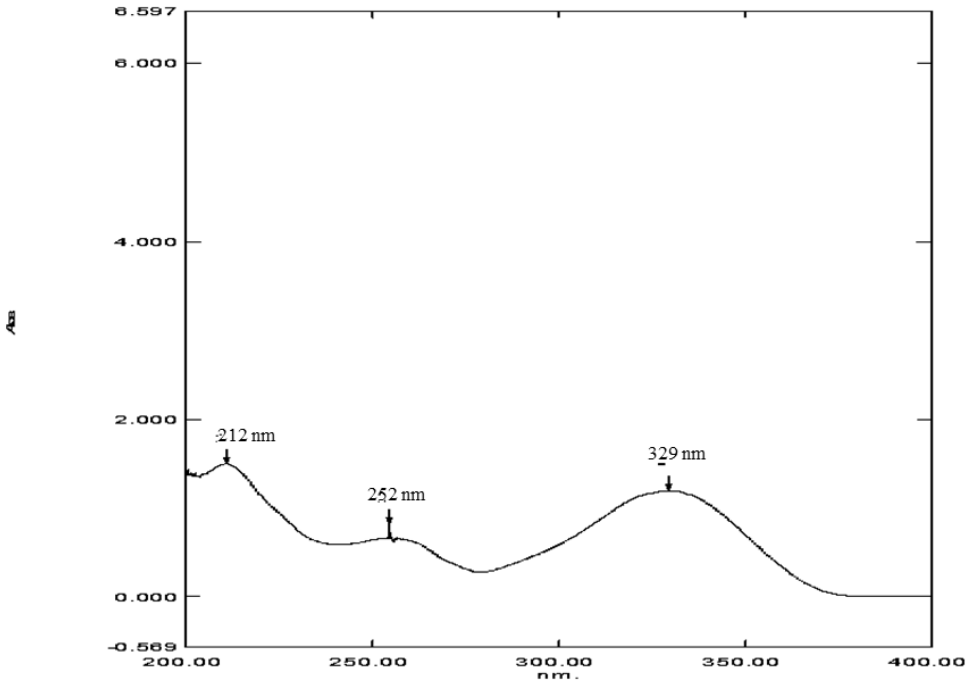

Fig. 4.1. UV absorption spectrum of temozolomide

The IR spectrum of the drug sample (Figure 4.2) was found to be similar to that of Temozolomide crystalline form III. The spectrum showed doublet at 3421 cm^{-1} and 3388 cm^{-1} presumed to have come from the primary amide N-H stretching vibrations (ɣ). The first amide band (C=O (ɣ)) from the primary and tertiary amide is present at 1758 cm^{-1} and 1732 cm^{-1}. A band at 1678 cm^{-1} is also observed which can come from the second amide band (N-H bending vibrations (δ)) as well as from C=N (γ) and C=C (γ) vibrations. Furthermore, characteristic IR bands at 3037 cm^{-1} (C-H stretching), 1452 cm^{-1} (C-H bending), 1577 cm^{-1} (N=N stretching) and 1402 cm^{-1} (C-N stretching) were observed confirming the identification of TMZ [6].

In DSC thermogram of TMZ (Figure 4.3), a sharp exothermic peak was observed at 209 ºC which is close to the reported value of 212ºC. The sharp peak indicates that drug is crystalline in nature. The drug was found to decompose upon heating as indicated by the charring instead of characteristic melting. Further, no peak was obtained on repeated measurement of the same sample indicating degradation. The results are in agreement with the reported literature [7,8].

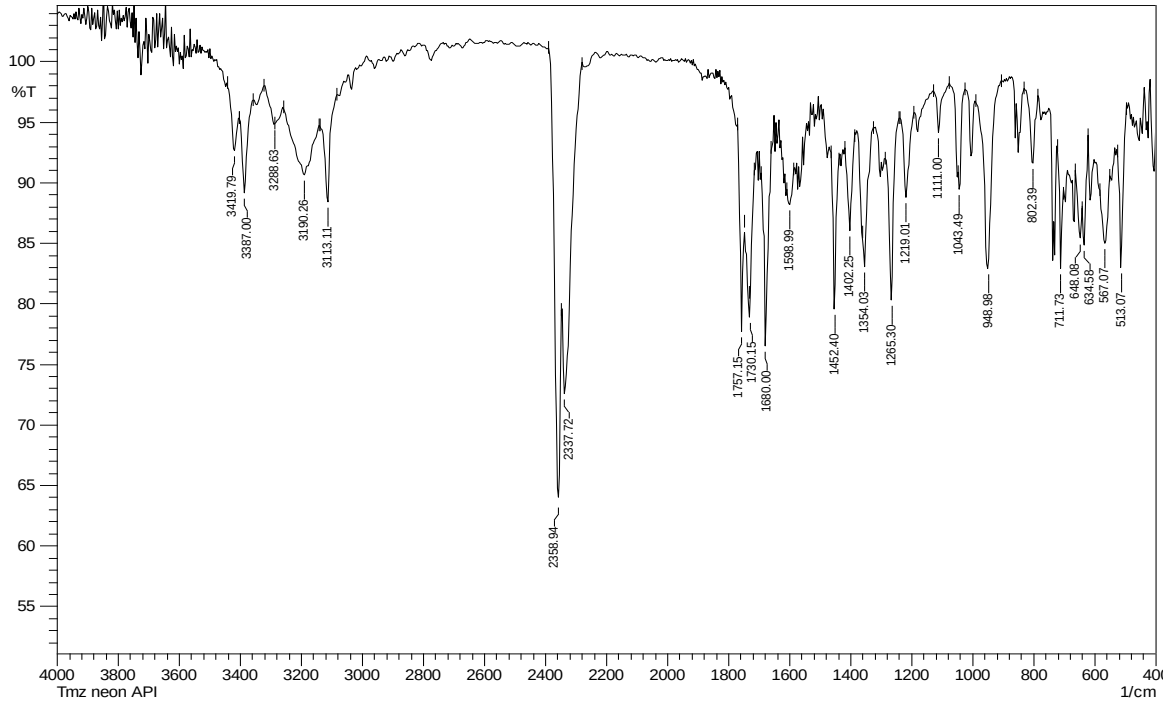

Fig. 4.2. FTIR spectrum of temozolomide

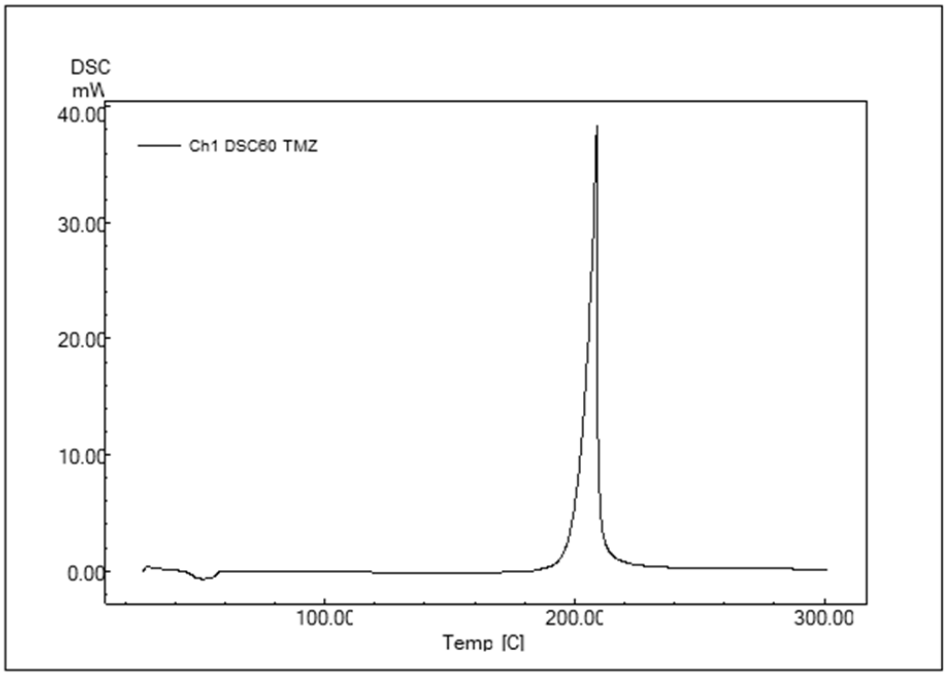

Fig. 4.3. DSC thermogram of temozolomide

4.3.2. Solubility Studies

TMZ showed pH independent solubility in aqueous buffers ranging from pH 1-6 and water owing to the fact that it exists in unionized state from pH 1-13 and therefore has no pKa [9]. The solubility profiles of TMZ in aqueous buffers are shown in Figure 4.4. The solubility of TMZ in aqueous buffers ranging from pH 1-6 and water was 4.604 ± 0.22 mg.mL^{-}1. A decrease in solubility was observed at pH 6 and above. This is probably due to the degradation of TMZ in media of pH >5 as already discussed in Chapter 3. In solvent stability studies, the highest solubility of TMZ was observed in DMSO and lowest in isopropyl alcohol. Although temozolomide is a hydrophilic drug with a reported log P of -1.153 [10], it exhibited solubility similar to water in most of the organic solvents such as acetone, methanol, acetonitrile and higher solubility in dichloromethane and DMSO. The solubility in various solvents is depicted in Figure 4.5.

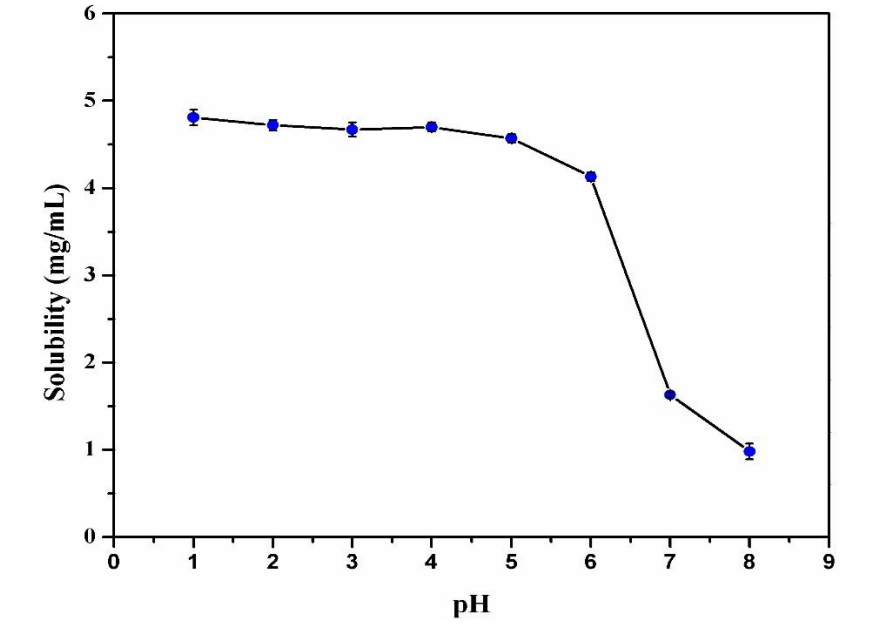

Fig.4.4. pH solubility profile of temozolomide in aqueous buffered media

4.3.5. Stability Studies

4.3.5.1. Solution State Stability

Solution stability of TMZ indicated that the degradation pathway followed first order kinetics. Further, the degradation was dependent on the pH, with the degradation rate

constant (K_{deg}) increasing as the pH shifts from acidic to neutral and basic. This is in accordance with the reported literature [11]. The log of % drug remaining to be degraded was plotted against time at all pH conditions and the corresponding K_{deg} was calculated. The $t_{90\%}$ values calculated ranged from 0.04 to 8.75 days (Table 4.2).

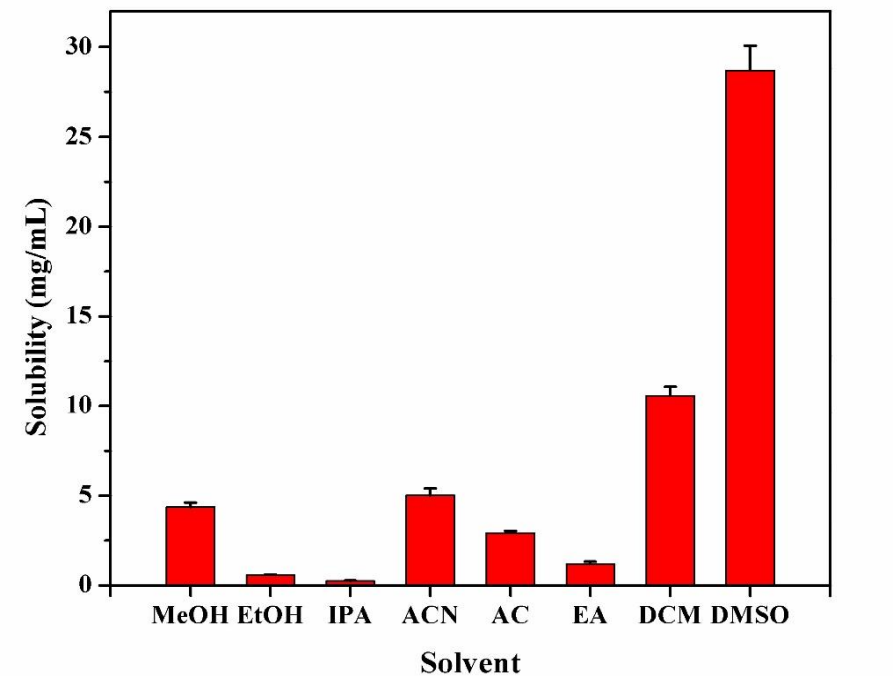

Fig. 4.5. Solubility of temozolomide in various non- aqueous solvents: MeOH - methanol; EtOH - ethanol; IPA - isopropyl alcohol; ACN - acetonitrile; AC - acetone; EA - ethyl acetate; DCM - dichloromethane; DMSO – dimethyl sulfoxide.

Table 4.2. Solution state stability data of temozolomide at different pH

pH	K_{deg}(days^{-1})	$t_{90\%}$ (days)	R^2
1.2	0.0116	9.09	0.9691
3.0	0.0116	9.09	0.9528
4.5	0.0230	4.59	0.9892
6.8	0.5286	0.20	0.9682
8.0	2.4984	0.04	0.9861

4.3.5.2. Solid State Stability

In solid state also, temozolomide followed first order rate kinetics, indicated by the high regression coefficient value. TMZ was stable at refrigerated condition with a $t_{90\%}$ value of about 52 months. At room temperature and accelerated conditions the $t_{90\%}$ value observed was 14.32 and 1.59 months respectively (Table 4.3). The decreased stability at room temperature and accelerated condition is because of higher % RH as TMZ is susceptible to degradation in presence of moisture. Further, under accelerated conditions, a darkening in color was observed which is indicative of moisture mediated degradation [12,13].

Table 4.3. Solid state stability data of temozolomide at different storage conditions

Storage condition	K_{deg}(months^{-1})	$t_{90\%}$ (months)	R^2
5 ± 2ºC	0.0020	52.50	0.9288
25 ± 2ºC, 60 ± 5% RH	0.0074	14.32	0.9443
40 ± 2ºC, 75 ± 5% RH	0.0665	1.59	0.9775

4.3.5.3. Drug-Excipient Compatibility Studies

DSC measures the transition in a system as a function of temperature and time thereby providing valuable information regarding physical and chemical changes such as melting point, glass transition temperature, thermal stability etc. The DSC study of the pure drug, excipients and the physical mixture of drug and excipients did not reveal any incompatibility between the drug and the excipients as shown in Figure 4.6 to 4.10. The exothermic peak of TMZ was well preserved in most of the cases with slight broadening and shifting of the peak to higher or lower temperature. The peak shape and enthalpy changes due to the presence of impurities in the sample. Hence, these minor changes in the drug exotherm might be attributed to the blend of drug and excipients which lowers the purity of each component in the mixture and doesn't necessarily indicate incompatibility [14].

In the isothermal stress testing, no significant changes were observed in the physical stability of the samples. At 60ºC, no changes in color was observed in all the blend samples compared to the pure drug and excipients at the same condition. However due to melting of lipids lump formation and stickiness was observed. At 40ºC/75% RH, a color change in the mixtures was observed with the samples turning tan colored. However, the color of pure drug under same condition also showed a change color from tan to brown. The color change was least in week 1 and most intense at 1 month. This is due to moisture mediated degradation of TMZ as already discussed earlier in this chapter and not due to any incompatibility with the excipients. Also, some of the lipid excipient blends were sticky in nature due to softening of the lipids.

The chemical stability study revealed that there was no significant change in TMZ content in the mixtures as compared to the pure drug under similar conditions. The assay (%) was in the range of 94.97 to 96.27 at 40ºC/75% RH and 96.19 to 97.13 at 60ºC.

The FTIR spectra of the drug-excipient mixtures (Figure 4.11) further confirmed the absence of any incompatibility between TMZ and the excipients as all the characteristic bands of TMZ, as discussed earlier in the chapter, were retained in all the drug-excipient mixtures investigated.

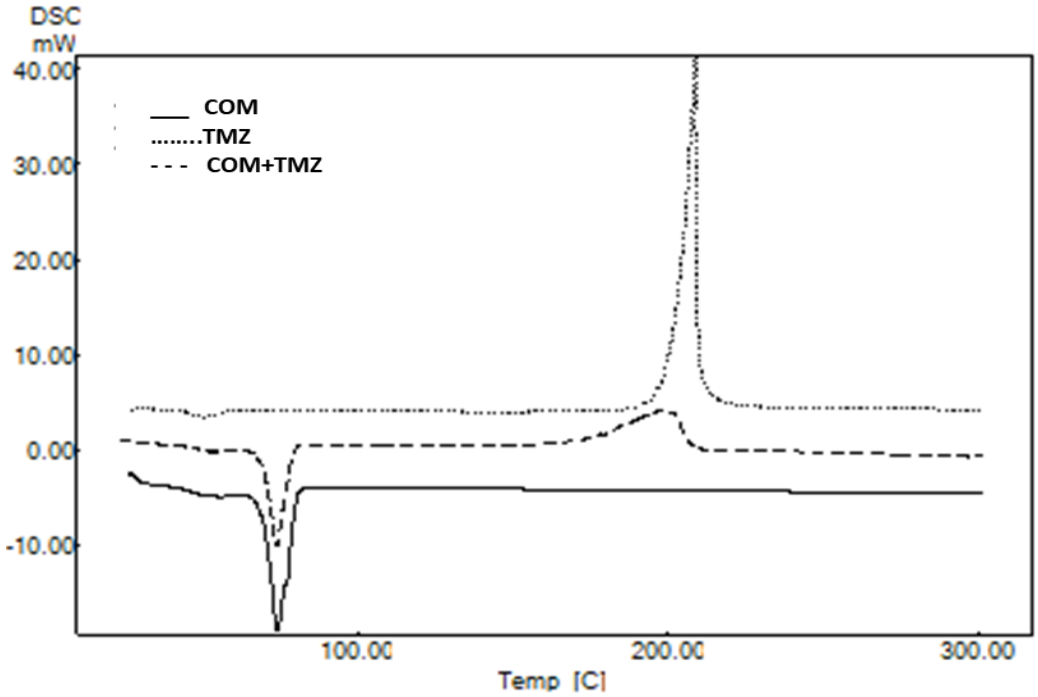

Fig. 4.6. DSC thermogram of TMZ, Compritol and their physical mixture

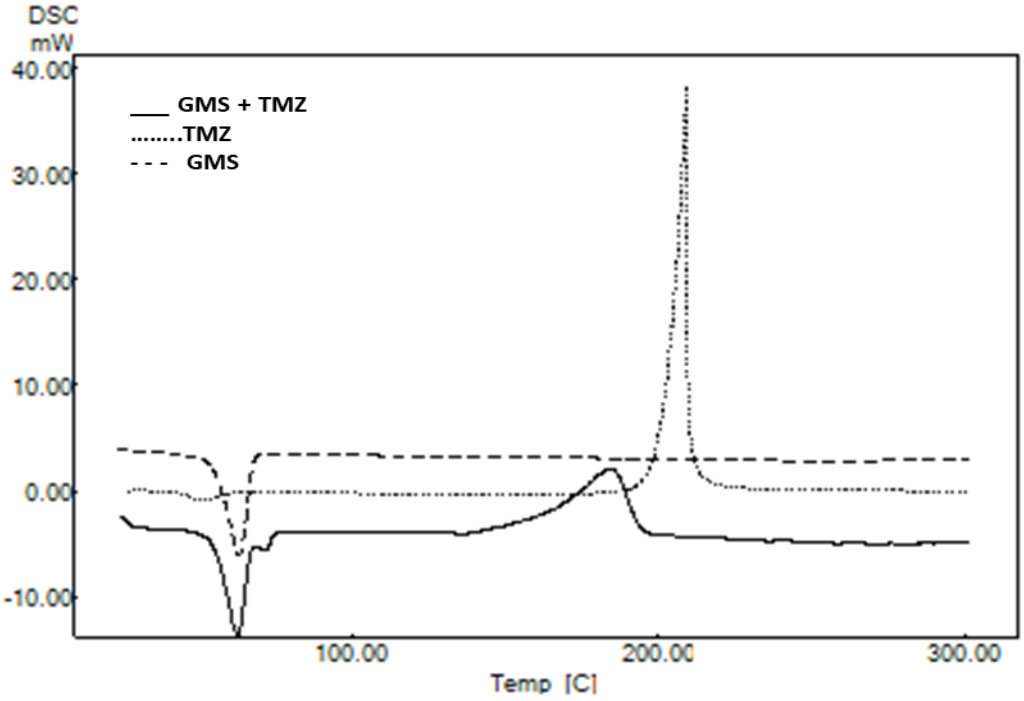

Fig. 4.7. DSC thermogram of TMZ, glyceryl monostearate and their physical mixture

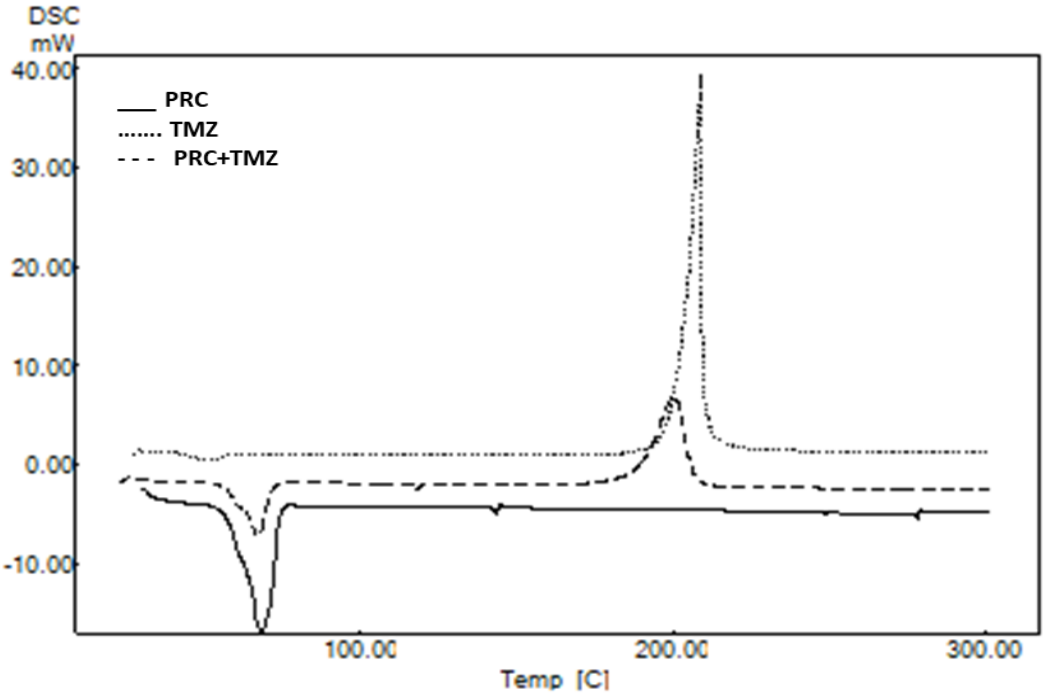

Fig. 4.8. DSC thermogram of TMZ, Precirol and their physical mixture

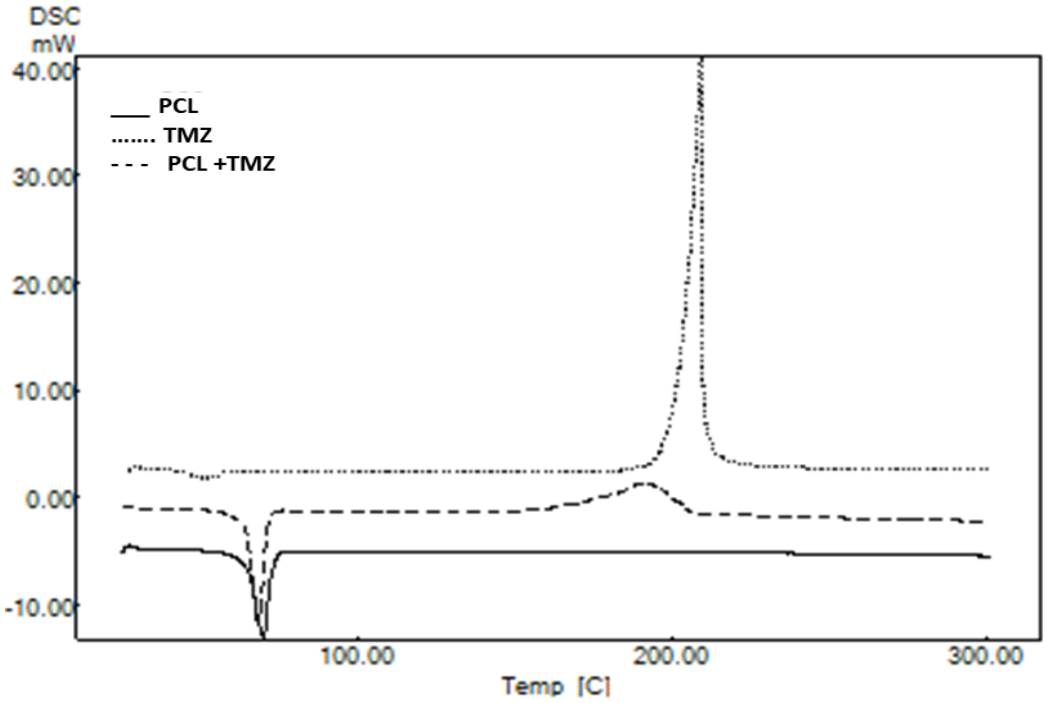

Fig. 4.9. DSC thermogram of TMZ, polycaprolactone and their physical mixture

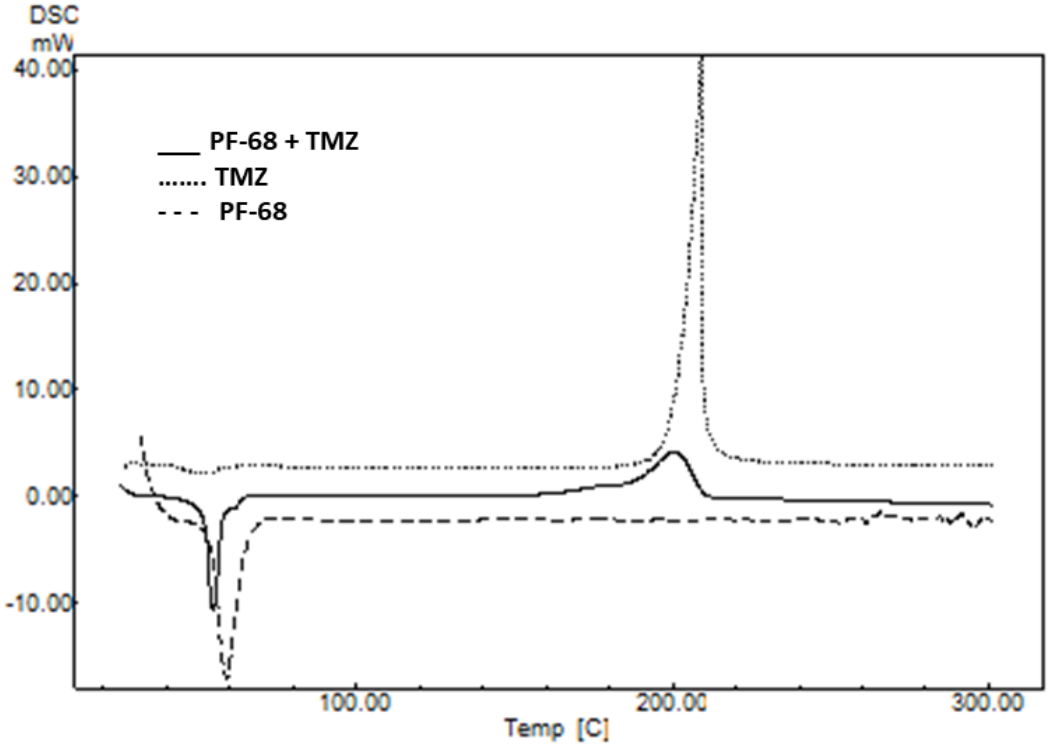

Fig. 4.10. DSC thermogram of TMZ, poloxamer 188 and their physical mixture

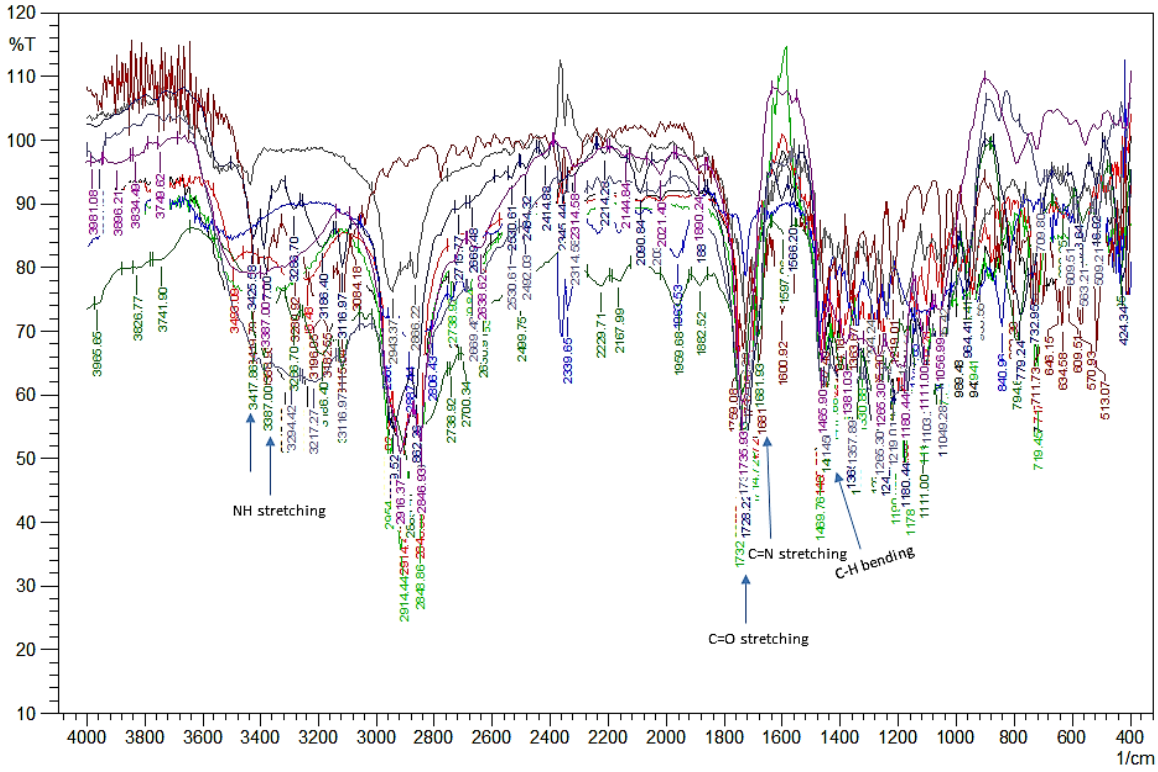

Fig. 4.11. FTIR spectra overlay of TMZ and its physical mixture with excipients

4.4. Conclusions

The temozolomide sample complied with all the identification tests. TMZ exhibited a pH independent solubility in various aqueous buffers (pH 1-6) and water. However, a lower concentration in solubility study was observed at higher pH (>6) due to the degradation of TMZ. Solubility studies with organic solvents revealed that although temozolomide is a hydrophilic drug, it exhibited solubility similar to water in most of the organic solvents such as acetone, methanol, acetonitrile and higher solubility in dichloromethane and DMSO. Solubility was highest in DMSO and lowest in isopropyl alcohol.

Solution state stability studies indicated that TMZ is more stable under acidic conditions and the degradation rate increases as the pH shifts from acidic to basic pH. The solid state stability indicated good stability of TMZ under refrigerated conditions but as TMZ is susceptible to moisture mediated degradation, the samples underwent degradation and change in color at accelerated conditions. Results of drug-excipient compatibility studies by

DSC, isothermal stress testing and FTIR demonstrated that TMZ had no significant interaction with the selected excipients.

The preformulation studies provided valuable information which has been helpful in selection of excipients and solvents for the fabrication of nanoparticles in addition to providing information regarding the optimum storage conditions to be maintained for the pure drug and the formulations.

References

1 Gibson, M. (2016) *Pharmaceutical Preformulation and Formulation: a Practical Guide from Candidate Drug Selection to Commercial Dosage Form*, CRC Press 1-15

2 Nyqvist, H. (1986) Preformulation Studies of Drug Substances for Solid Dosage Forms. *Drug Development and Industrial Pharmacy* 12 (7), 953-968

3 Monkhouse, D.C. (1984) Stability Aspects of Preformulation and Formulation of Solid Pharmaceuticals. *Drug Development and Industrial Pharmacy* 10 (8-9), 1373-1412

4 Herzfeldt, C.D. and Kümmel, R. (1983) Dissociation constants, solubilities and dissolution rates of some selected nonsteroidal antiinflammatories. *Drug Development and Industrial Pharmacy* 9 (5), 767-793

5 Lopes, I.C. et al. (2013) Temozolomide chemical degradation to 5-aminoimidazole -4-carboxamide–Electrochemical study. *Journal of Electroanalytical Chemistry* 704, 183-189

6 Łaszcz, M. et al. (2013) Identification and physicochemical characteristics of temozolomide process-related impurities. *Molecules* 18 (12), 15344-15356

7 Kozyr'kov, Y.Y. et al. (2014) Improved method for isolating temozolomide from its dimethylsulfoxide solvate. *Pharmaceutical Chemistry Journal* 48 (6), 398-401

8 Babu, N.J. et al. (2012) Crystal Engineering of Stable Temozolomide Cocrystals. *Chemistry – An Asian Journal* 7 (10), 2274-2285

9 SSchering Corporation, (2002) Clinical pharmacology and biopharmaceutics review : Temodar oral capsules; NDA supplement submitted to USFDA.

https://www.fda.gov/downloads/Drugs/DevelopmentApprovalProcess/DevelopmentResources/UCM447708.pdf. Content accessed in May 2018.

10 EMEA (2010) Assessment report for Temomedac Document Ref.:EMA/51724/2010 pp. 1-19, European Medicines Agency, London, United Kingdom.http://www.ema.europa.eu/docs/en_GB/document_library/EPAR__Public_assessment_report/human/001124/WC500073303.pdf. Accessed in May 2018.

11 Newlands, E.S. et al. (1997) Temozolomide: a review of its discovery, chemical properties, pre-clinical development and clinical trials. *Cancer Treatment Reviews* 23 (1), 35-61

12 Ambados, F. et al. (2015) Preparation Method and Stability of a Temozolomide Suspension: A Pilot Study. *Journal of Pharmacy Practice and Research* 42 (2), 111-114

13 EMEA (2004) Scientific discussion for the approval of Temodal. European Medicines Agency, London , United Kingdom. Accessed in May 2018. http://www.ema.europa.eu/docs/en_GB/document_library/EPAR__Scientific_Discussion/human/000229/WC500035617.pdf Content accessed in May 2018.

14 Pani, N.R. et al. (2011) Application of DSC, IST, and FTIR study in the compatibility testing of nateglinide with different pharmaceutical excipients. *Journal of Thermal Analysis and Calorimetry* 108 (1), 219-226

5. Formulation Design, Development and In Vitro Studies

5.1. Introduction

Drug delivery to the brain, especially for the treatment of brain tumors remains a challenge due to presence of the blood brain barrier (BBB) which due to its unique protective structural and functional features restricts the entry of molecules and therapeutics [1]. Nanoparticles have emerged as a potential delivery systems capable of enhancing the BBB permeability for efficient and safe delivery of therapeutics to the brain. Furthermore, nanoparticulate delivery systems have various other advantages such as protection of the encapsulated drug from degradation, providing controlled and prolonged release of the drug and selective biodistribution which can be utilized for targeted delivery of therapeutics to the tumor site and reduced side-effects [2]. This can lead to dose reduction which reduces the cost and ensures better patient compliance.

Although temozolomide (TMZ) is 100% bioavailable, it has a very short half-life and undergoes conversion to MTIC at physiological pH leading to only 20-30% of the plasma concentration achieved reaching the brain. Hence, to maintain therapeutic concentrations, TMZ is administered in high doses which leads to a number of dose limiting side-effects such as myelosuppression and cardiomyopathy [3,4]. Nanoparticulate delivery systems have been explored for delivery of anti-cancer drugs for targeted delivery besides potential reduction in dose and risk of side effects [5]. In the present study, efforts have been made to enhance the delivery of TMZ to the brain by designing nanoparticles using different biocompatible and biodegradable polymers/lipids. The nanoparticles were prepared by different techniques depending on the polymer/lipids used. The nanoparticles were further characterized and the selected optimized formulations were further taken up for in vitro cytotoxicity assay and in vivo pharmacokinetic and biodistribution studies.

5.2. Experimental

5.2.1. Materials

Temozolomide was received as a gift sample from Biophore India Pharmaceuticals Pvt. Ltd (Vishakhapatnam, India). Poly -ε-caprolactone (PCL; M.W 40,000), stearic acid, poloxamer 188 (Pluronic® F-68) and oleic acid was procured from Sigma Aldrich, USA. Glyceryl monostearate (GMS), Compritol® 888 ATO (glyceryl behenate), Precirol®ATO5 (glyceryl palmitostearate) was obtained as a gift sample from Gattefosse, India. Soy lecithin (Lipoid®

S75) was gifted by Lipoid GmbH, Germany. All solvents such as acetone, dichloromethane, ethanol, methanol, acetonitrile, ethyl acetate etc. were purchased from Merck, India. All buffer salts, sucrose, mannitol, sodium chloride were purchased from S.D Fine-Chem Ltd, India. Ultrapure water was prepared by filtering freshly collected MilliQ water (Millipore®, USA) through 0.22 µm membrane filter.

5.2.2. Instruments / Equipments

Magnetic stirrer hotplate with temperature control (Remi, India; Tarsons, India), microtip ultrasonic processor (500W; 20 kHz, Vibra-Cell™, SONICS®, USA) were used for nanoparticle preparation. Vacuum evaporator (Rotavapor R210, Büchi, Switzerland) was used for evaporation of organic solvents. Temperature controlled centrifuge (Centrifuge 5430R, Eppendorf, Germany) was used for separation of nanoparticles, -20^{0}C freezer (Vestfrost, India) was used for freezing the nanoparticle sample prior to lyophilization and lyophilizer (Freezone 2.5, Labconco, USA) was used for freeze drying of the nanoparticles. Ultrasonic bath (Toshiba, India) and laboratory centrifuge R8C (Remi, India) was used for sample preparation for determination of entrapment efficiency and drug loading. Zetasizer (Zetasizer nanoZS; Model: ZEN3600, Malvern, UK) was used for particle size and zeta potential characterization. Field emission scanning electron microscope (FESEM); (Apreo S, with Xt microscope control version 13.5.0, FEI limited, USA) was used for particle size and morphology characterization. Heat flux type differential scanning calorimeter (DSC-60, Shimadzu, Japan) was used for thermal analysis and for evaluating crystallinity powder X-ray diffraction (Rigaku Miniflex II diffractometer, Japan) was used.

For in vitro cell culture studies, CO_2 incubator (Thermo Scientific, USA) was used for culturing the cell lines and Multiskan microplate spectrophotometer (Thermo Scientific, USA) was used for cell analysis.

5.2.3. Preparation of PCL Nanoparticles

TMZ loaded nanoparticles using PCL were prepared by nanoprecipitation [6,7]. The fabrication technique was slightly modified with the aim to increase entrapment efficiency of the nanoparticles.

In the nanoprecipitation method, as tabulated in Table 5.5, TMZ and PCL were dissolved in acetone. The drug and polymer solution was injected into a mix of ultrapure water and

ethanol (3:1) containing poloxamer 188 under moderate stirring. Stirring was continued for 4h and then for another 50 minutes in the rotary evaporator at 30°C to allow evaporation of the organic solvent and solidification of the nanoparticles. The nanoparticles were centrifuged at 17,000 rpm for 20 minutes at 25°C to separate the nanoparticles. The pellet was resuspended in water containing 10% mannitol, frozen overnight at -20°C and then lyophilized.

To improve the entrapment efficiency, batches were also prepared by saturating the external aqueous phase by addition of sucrose /sodium chloride.

5.2.4. Preparation of Lipid Nanoparticles

5.2.4.1. Screening of Lipids

The selection criteria of lipids for preparation of lipid nanoparticles is based on the potential of the lipid to encapsulate TMZ. The partitioning behavior of TMZ in various lipids is a good indicator of the potential of the lipid to encapsulate TMZ. The partition behavior of TMZ in various solid lipids was evaluated by preparing a stock solution of TMZ (200 µg. mL^{-1}) in 0.25% acetic acid solution. 2mL of the TMZ solution was added to 5 mL glass vials containing 500 mg of the lipids (stearic acid, glyceryl monostearate, Precirol and Compritol) in molten state. The vials were shaken for 2h at 75 ± 5°C for allowing partitioning of TMZ in the lipids. TMZ solution of the same concentration was also kept under similar conditions as control. After the stipulated time of 2h, the samples were cooled and centrifuged at 10,000 rpm for 15 minutes. The aqueous phase was separated and analyzed by the HPLC method. Partition coefficient ($PC_{LIPID/WATER}$) was determined as

$$PC_{LIPID/WATER} = \frac{\text{TMZ input} - \text{Concentration of TMZ in aqueous phase}}{\text{Concentration of TMZ in aqueous phase}}$$

5.2.4.2. Preparation of Solid Lipid Nanoparticles

Solid lipid nanoparticles (SLN) were prepared by emulsification-solvent evaporation method [8,9] as tabulated in Table 5.6. Briefly, stearic acid (SA) and soy lecithin were dissolved in ethyl acetate and dichloromethane (10:1). The aqueous phase was prepared by dissolving TMZ in ultrapure water which was then emulsified with the organic phase to form

a primary emulsion using an ultrasonic processor for 90 sec at 25% amplitude. The primary emulsion was further emulsified with a 0.5% aqueous solution of PF-68 by ultrasonication for 120 sec at 25% amplitude to form a w/o/w emulsion. The emulsion was kept on stirring for 4h and then the organic solvent was removed by rotary evaporator at 30°C. Further, the nanoparticles were centrifuged at 17,000 rpm for 20 minutes at 25°C to separate the nanoparticles. The pellet was resuspended in ultrapure water containing 10%mannitol, frozen overnight at -20°C and then lyophilized.

5.2.4.3. Preparation of Nanostructured Lipid Carriers

Temozolomide loaded nanostructured lipid carriers (NLC) were prepared by emulsification-ultrasonication method [10,11] using oleic acid as the liquid lipid and glyceryl monostearate (GMS), Compritol® 888 ATO (COM) and Precirol®ATO5 (PRC) as the solid lipids. Briefly, the drug was dispersed in a molten mix of the solid and the liquid lipid at a temperature 10-15°C higher than the melting point of the respective solid lipid. An aqueous solution of the surfactant, PF-68 was prepared and heated to the same temperature. The hot surfactant solution was added to the molten lipid-TMZ mix under moderate stirring. The preemulsion formed was further subjected to ultrasonication for 6 minutes (500W; 25% amplitude) with 30 sec on and 10 sec off cycles maintaining the temperature at least 10°C above the melting point of the lipid. The emulsion was then kept in an ice bath under constant stirring for 4h after addition of chilled ultrapure water. The NLC were separated by centrifugation at 17,000 rpm for 15 minutes. The NLC were redispersed in a cryoprotectant solution of 15% w/w mannitol, kept overnight at -20°C and then lyophilized till a free flowing was obtained. The powder was transferred to a glass vial, sealed with parafilm and stored under refrigeration.

5.2.5. Experimental Design for Formulation Optimization

The preparation of nanoparticles is a multi-step process with a number of variables which can have an effect on the formulation characteristics. To optimize the manufacturing process and achieve reproducibility an understanding of critical formulation and process variables is important.

As nanoprecipitation process does not involve a large number of variables, for PCL nanoparticles traditional approach of formulation optimization involving varying a selected

parameter at a time and keeping all other parameters constant was used. Design of Experiments (DOE) was used for rest of the formulations.

For SLN, a 2^{5-1} fractional factorial design was applied to determine the effect of process parameters on nanoparticle characteristics. The independent parameters were chosen based on preliminary formulation designing studies. The parameters selected (Table 5.1) were the volume ratio between the inner water phase and the oil phase (V_{w1}/V_o) (X_1), SA concentration (X_2) with respect to solvent, the sonication time for the primary emulsification (X_3), TMZ concentration (X_4) and the soy lecithin (Lec) content in the inner water phase (X_5). Effect of independent variables were studied at three levels viz. high (+1), center (0) and low (-1) level.

Table 5.1. Process and formulation variables for SLN formulation addressed in the fractional factorial design

Parameter	Component	Units	Levels applied		
			Low (-1)	Center (0)	High (+1)
X_1	V_{w1}/V_o	ratio	0.1	0.25	0.4
X_2	C_{SA}	mg/mL	5	7.5	10
X_3	$t_{sonication}$	sec	90	150	210
X_4	M_{TMZ}	mg	5	7.5	10
X_5	M_{Lec}	mg	10	30	50

The levels were chosen to maximize the design space and at the same time enable feasible processing of the nanoparticles. Further, two additional center points were included to evaluate the non-linearity of the statistical model. The runs were randomized to eliminate variance due to bias. The response variables (dependent variables) analyzed were particle size (Y_1), entrapment efficiency (Y_2) and drug loading (Y_3). Each run was conducted in duplicate.

For NLC formulations, Box Behnken statistical design (BBD) was applied to study the effect of various variables on the nanoparticles. For NLC with Precirol as the solid lipid (PNLC), four independent parameters at three levels were chosen, whereas for NLC with GMS as the

solid lipid (GNLC) and NLC with Compritol (CNLC), based on the results of PNLC formulation, only three factors at three levels were selected for the optimization. The independent variables for PNLC, GNLC and CNLC is as given in Table 5.2 and 5.3 respectively. The response variables (dependent variables) analyzed were particle size (Y_1), entrapment efficiency (Y_2) and drug loading (Y_3) and each run was conducted in triplicate.

Table 5.2. Independent variables for PNLC formulation addressed in Box Behnken design.

Parameter	Component	Units	Levels applied		
			Low (-1)	Center (0)	High (+1)
X_1	$Drug/Lipid_T$	ratio	0.05	0.1	0.2
X_2	$Lipid_T$	mg	300	500	1000
X_3	$Lipid_S$ /Oil	ratio	0.5	1	2
X_4	C_{PF-68}	%	0.5	1.5	3.0

$Lipid_T$ – Total lipid; C_{PF-68} – Concentration of PF-68; $Lipid_S$ – Solid lipid

Table 5.3. Independent variables for GNLC and CNLC formulation addressed in Box Behnken design.

Parameter	Component	Units	Levels applied		
			Low (-1)	Center (0)	High (+1)
X_1	$Drug/Lipid_T$	ratio	0.1	0.2	0.3
X_2	$Lipid_s$/Oil	ratio	0.5	1	2
X_3	C_{PF-68}	%	0.5	1.5	3.0

$Lipid_T$ – Total lipid; C_{PF-68} – Concentration of PF-68; $Lipid_S$ – Solid lipid

Design-Expert® software (version 8.0.7.1, Stat-Ease Inc., MN) was used to design and study the experimental parameters and the obtained responses.

5.2.6. Characterization of Nanoparticles

5.2.6.1. Particle Size Distribution and Zeta Potential

The average particle size, size distribution and zeta potential of the prepared nanoparticle dispersions were measured by Zetasizer (nanoZS®, Malvern, UK) which uses Dynamic light scattering (DLS) technique for measurement of particle size and Laser-Doppler Micro-electrophoresis to measure zeta potential. The samples were appropriately diluted with ultrapure water, filled in disposable polystyrene cells and analyzed at 25°C. Backscattering was measured by a detector positioned at an angle of 175°.

The morphology of the optimized NLC formulation was visualized by FESEM (Apreo S, with Xt microscope control version 13.5.0, FEI limited, USA). Prior to analysis, 100 µL of the NLC dispersion was placed on a cover slip and dried overnight under vacuum. It was then gold sputter coated using a gold sputter module in a high vacuum evaporator (Quorum: ES; Quorum technologies, UK). These gold coated samples were then scanned and photomicrographs taken at acceleration voltage suitable for the sample.

5.2.6.2. Entrapment Efficiency and Drug Loading

To determine entrapment efficiency and drug loading, the nanoparticles were separated from the supernatant containing the free drug by centrifuging the nanoparticle suspension at 17,500 rpm for 1h. The separated nanoparticles were washed with ultrapure water to remove the adsorbed drug and the dispersion was centrifuged again and the supernatant added to the previously collected supernatant. Entrapment efficiency was determined by indirect method by analyzing the free drug in the supernatant collected.

For determination of drug loading, a known amount of nanoparticles was transferred to a 15 mL centrifuge tube and disrupted by addition of a suitable volume of acetonitrile and keeping the same in the ultrasonic bath for 30 minutes at 25°C for complete release of drug from the nanoparticulate system. This was followed by centrifugation at 5,000 rpm and the supernatant was analyzed by the in-house developed HPLC method after suitable dilution as reported in Chapter 3. Determinations were carried out in triplicates and reported as mean with standard deviation (SD).

Entrapment efficiency (EE) and drug loading (DL) was calculated using the following formula:

$$EE(\%) = \frac{\text{Total TMZ added} - \text{TMZ in supernatant}}{\text{Total TMZ added}} \text{ x } 100$$

$$DL\ (\%w/w) = \frac{\text{Amount of TMZ in nanoparticles (mg)}}{\text{Amount of nanoparticles (mg)}} \text{ x } 100$$

5.2.6.3. In Vitro Release Studies

In vitro release study of pure TMZ and TMZ loaded NLC was performed using the dialysis bag method [12]. In brief, dialysis membrane (Spectrapor, molecular weight cut off: 12,500 Da) was soaked in water 12h prior to the experiment. 2mL of the respective NLC dispersions, equivalent to 2.5 mg of TMZ, were filled in dialysis bags, tied at both the ends and immersed in a 50mL beaker containing 30mL of dissolution media (pH 5.0 acetate buffer). The temperature of the media was maintained at 37 ± 0.5°C and was continuously stirred at 100 rpm. At specified time intervals (0.08, 0.25, 0.5, 1, 2, 4, 6, 8, 12 and 24h) an aliquot of the sample was collected from the release medium and replaced with same volume of fresh medium. The collected samples were suitably diluted and analyzed by in –house developed HPLC method as described in Chapter 3. The cumulative % drug release was calculated and the data was fitted into various mathematical models, such as zero order, first order, Higuchi, Korsmeyer-Peppas, Hixson-Crowell, Makoid-Banaker and Baker-Lonsdale model for evaluation of release kinetics [13,14] using DDsolver software.

Zero order equation: $F = k_0.t$

First order equation: $F = 100.\ (1-e^{-k_1.t})$

Higuchi equation: $F = k_H.t^{0.5}$

Korsmeyer-Peppas equation: $F = k_{KP}.\ t^n$

Hixon-Crowell equation: $F = 100.\ [1-(1-k_{HC}.t)^3]$

Makoid-Banaker equation: $F = k_{MB}.t^n.e^{-k.t}$

Baker-Lonsdale equation: $k_{BL}.t = 3/2[1- (1 - F/100)^{2/3}] – F/100$

Weibull equation: $\ln [-\ln(1-F)]= - \beta \ln t_d + \beta \ln t$

In all models, F is the fraction (%) of drug released in time t; k_0 is the zero order release constant; k_1 is the first order release constant; k_H is the Higuchi release constant; k_{KP} is the release constant incorporating structural and geometric characteristics of the formulation; n is the diffusional exponent indicating the drug release mechanism. For spherical particles the value of n = 0.43 indicates Fickian diffusion; values between 0.43 and 0.85 ($0.43 < n < 0.85$) indicate non-Fickian release, the value of n is equal to 0.85 in case of zero order release (case II transport) and n >0.85 for Super Case II transport. k_{HC} is the release constant in Hixson-Crowell model; k_{BL} is the combined constant in Baker-Lonsdale model and is equal to $[3 \times D \times C_s /(r_0^2 \times C_0)]$, where D is the diffusion coefficient, C_s is the saturation solubility, r_0 is the initial radius for a sphere or cylinder or the half-thickness for a slab, and C_0 is the initial drug loading in the matrix. k_{MB}, n, and k are empirical parameters in Makoid–Banaker model (k_{MB}, n, $k > 0$), α is the scale parameter which defines the time scale of the process; β is the shape parameter which characterizes the curve as either exponential (β =1; case 1), sigmoid, S-shaped, with upward curvature followed by a turning point (β >1; case 2), or parabolic, with a higher initial slope and after that consistent with the exponential (β <1; case 3).

The most appropriate model was selected on the basis of regression coefficient (R^2), Akaike Information Criterion (AIC), and the Model Selection Criterion (MSC) and time taken for 50% drug release ($t_{50\%}$) and 90% drug release ($t_{90\%}$) were calculated for the best-fit model.

5.2.6.4. Thermal Studies

DSC analysis of optimized NLC formulations was carried out using DSC-60 (Shimadzu, Kyoto, Japan) instrument. The sample preparation was same as mentioned in section 4.2.3 of chapter 4. The thermograms of the formulations were compared with the thermograms of pure drug and excipients.

5.2.6.5. X-ray Diffraction (XRD) Study

Powder X-ray diffraction (PXRD) studies of temozolomide and NLC formulations were performed by Rigaku Miniflex II diffractometer (Rigaku, Japan) with CuK_α radiation wavelength

of 1.5405 Å used as X-ray source. For the measurements, samples were kept in glass sample holders followed by scanning from 10 to 60° with scan angular speed (2θ/min) of 2°/min.

5.2.7. Stability Studies

The stability of NLC in both dispersion and freeze dried state was evaluated at ambient (25 ± 2°C); refrigerated (5 ± 3°C); in hermetically sealed glass vials. The nanoparticles were evaluated for particle size, polydispersity index (PDI), zeta potential (ZP) and drug loading at 15 days, followed by 1, 3 and 6 months.

5.2.8. In Vitro Cytotoxicity Study

The cytotoxicity of pure TMZ and NLC formulations against U-87 MG glioma cells was evaluated by using MTT assay. U-87 MG glioma cell line procured from National Centre for Cell Science (NCCS), Pune, India were cultured in Dulbecco's modified Eagle's medium (DMEM) (Himedia), supplemented with 10% fetal bovine serum (Invitrogen) and antibiotic streptomycin (100 $mg.mL^{-1}$). The cultures were incubated at 37°C in 5% CO_2 humidified atmosphere. Briefly, the glioma cells were seeded in 96 well plates at a density of 8 x 10^3 cells and incubated for 12h to permit cell attachment. The cells were treated with pure TMZ, blank NLC with the composition similar to that of highest dose TMZ loaded NLC but without the drug and TMZ loaded NLC diluted with complete media to equivalent drug concentration ranging from 50, 100, 200 and 400 $\mu g.mL^{-1}$ and incubated for 72h. After the stipulated time MTT [3-(4,5-dimethylthiazol-2-yl)-2,5-diphenyltetrazolium bromide]; SRL, India) was added to each treated and control well and the cells were incubated for 4h. Formazan crystals were solubilized in dimethyl sulfoxide (DMSO), and readings were obtained at 570 nm with a differential filter of 630 nm using a Multiskan microplate spectrophotometer (Thermo Scientific, USA).

The percentage of viable cells was calculated using the following formula:

$$\text{Viability (\%w/w)} = \frac{\text{Mean absorbance of drug treated cells}}{\text{Mean absorbance of control}} \text{x} 100$$

5.3. Results and Discussion

5.3.1. PCL Nanoparticles

The PCL nanoparticles were prepared by nanoprecipitation method as it is a simple and easily reproducible method especially for polymeric nanoparticles. It is based on the interfacial deposition of polymers after displacement of a semi-polar solvent, miscible with water, from a lipophilic solution. Rapid diffusion of the solvent into the non-solvent phase decreases the interfacial tension between the two phases leading to an increase in surface area and subsequent formation of small droplets of organic solvent [15]. The key variables which have an impact on the nanoparticle characteristics are the selection of solvent and non-solvent, the volume of aqueous phase, concentration of the polymer, the nature and concentration of surfactant used and the aqueous phase agitation rate. Preliminary studies were carried without TMZ to optimize the preparation method. The variables evaluated for the optimization of the nanoparticle preparation were stirring speed, composition of the aqueous phase and its volume, volume of aqueous phase, polymer concentration and stabilizer type and concentration and the results are tabulated in Table 5.4. All the experiments were carried out in duplicate.

Acetone was selected as the solvent as it acts as a solvent for both PCL and TMZ, it is miscible with water and is easy to evaporate. TMZ being hydrophilic in nature has a tendency to diffuse out in the aqueous phase leading to poor entrapment efficiency. In order to improve entrapment efficiency, pure ethanol and a mix of ethanol and water in various proportions (1:3, 1:1, 3:1) was evaluated as a non-solvent for the nanoparticle preparation as TMZ is poorly soluble in ethanol. Other solvents such as ethyl acetate and isopropyl alcohol were also evaluated but they resulted in higher range of particle size. PF-68 was selected as the stabilizer as it showed desired particle characteristics in terms of size and PDI as compared to Pluronic F127 (PF-127) and Polyvinyl alcohol (PVA). An increase in PCL concentration resulted in an increase in particle size from 204 to 292 nm and an increase in PDI from 0.154 to 0.358. Use of surfactant in the range of 0.25 to 1% and stirring speed from 1200 to 600 rpm did not have a significant impact on the particle characteristics.

Loading TMZ into the nanoparticles did not significantly affect the particle size although a significant change in zeta potential was observed (Table 5.5). The entrapment efficiency

(EE) and drug loading (DL) of the TMZ loaded nanoparticles were found to be quite low. Efforts were made to enhance the drug entrapment by saturating the aqueous phase with sodium chloride/ sucrose so that less of TMZ will diffuse out in the aqueous phase. The strategy improved the drug loading but the entrapment efficiency was still very low. As the PCL nanoparticle formulation failed to achieve the desired drug entrapment, these formulations were not further taken up for in vitro release studies and also in vivo studies.

5.3.2. Solid Lipid Nanoparticles

Higher partitioning towards lipids indicates that the drug is more soluble in the lipid and less of it is available in the external aqueous phase, thereby increasing the potential to encapsulate the drug in the lipid nanoparticles. The partitioning of TMZ in various lipids is as shown in Figure 5.1.

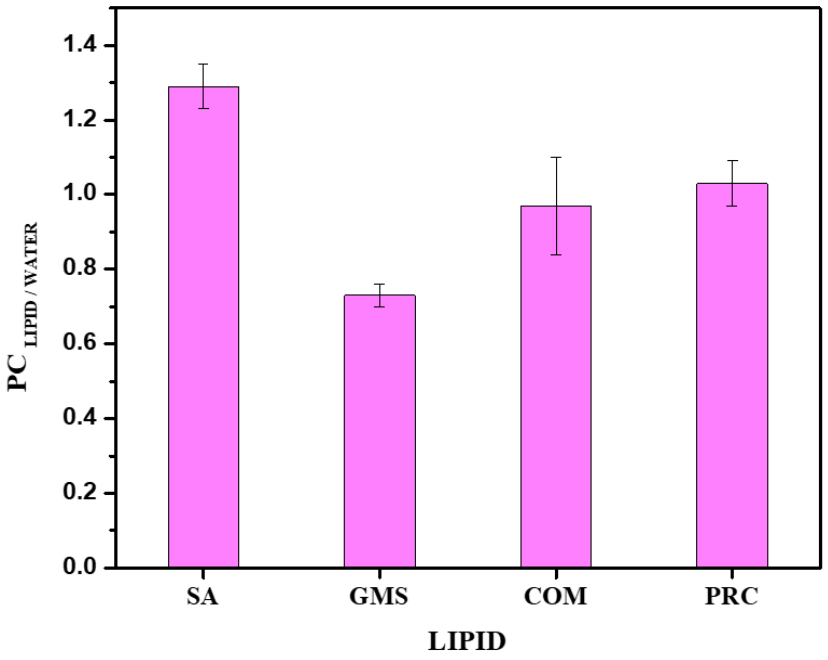

Fig. 5.1. Partitioning behavior of temozolomide in select lipids: SA - stearic acid; GMS - glyceryl monostearate; COM - Compritol® 888 ATO; PRC - Precirol ®ATO5.

The results indicate that partitioning of TMZ was greatest towards stearic acid (1.29) and lowest towards glyceryl monostearate (0.72). For COM and PRC, partitioning was close to 1.0. This is possibly because compared to GMS all other lipids are more hydrophobic in

Table 5.4. Optimization of various parameters for preparation of dummy PCL nanoparticles

Batch Code	PCL[a] (mg)	Stabilizer (%w/v)	Non-solvent Phase			Stirring speed (rpm)	Mean Particle size (nm) ± SD	PDI[e] ± SD	Zeta potential (mV)
			Water : Solvent ratio	Solvent	Volume (mL)				
PCL/1	25	0.50[b]	1:0	EtOH	40	1200	137.6 ± 5.2	0.302 ± 0.07	-29.2± 0.65
PCL/2	25	0.50[b]	3:1	EtOH	40	1200	239.1 ± 6.5	0.230 ± 0.04	-33.2 ± 1.64
PCL/3	25	0.50[b]	1:1	EtOH	40	1200	4587± 32.5	0.799 ± 0.09	-31.6± 1.25
PCL/4	25	0.50[b]	1:3	EtOH	40	1200	8706 ± 153.3	1.000 ± 0.00	-26.1 ± 0.98
PCL/5	25	0.50[b]	0:1	EtOH	40	1200	Agglomerates		-
PCL/6	25	0.50[b]	3:1	EtOH	40	600	213.0 ± 11.2	0.149 ± 0.07	-33.4 ± 1.21
PCL/7	25	0.50[b]	3:1	EtOH	40	900	204.3 ± 4.5	0.154 ± 0.04	-38.2 ± 0.55
PCL/8	25	0.50[b]	3:1	EtOH	40	1200	211.9 ± 4.6	0.202 ± 0.03	-38.1 ± 1.10
PCL/9	50	0.50[b]	3:1	EtOH	40	900	243.8 ± 6.2	0.180 ± 0.02	-39.5 ± 1.42
PCL/10	100	0.50[b]	3:1	EtOH	40	900	292.6 ± 10.3	0.358 ± 0.07	-40.1 ± 1.15
PCL/11	25	0.25[b]	3:1	EtOH	40	900	206.6 ± 9.7	0.157 ± 0.03	-39.9 ± 0.88
PCL/12	25	1.00[b]	3:1	EtOH	40	900	205.7 ± 5.4	0.113 ± 0.02	-39.7 ± 1.25
PCL/13	25	1.00[c]	3:1	EtOH	40	900	297.3 ± 6.2	0.203 ± 0.03	-9.78 ± 0.87
PCL/ 14	25	0.50[d]	3:1	EtOH	40	900	222.6 ± 3.4	0.278 ± 0.02	-32.9 ± 1.05
PCL/15	25	0.5[b]	3:1	EtOH	20	900	365.9 ± 13.0	0.400 ± 0.10	-40.8 ± 0.81
PCL/16	25	0.5[b]	3:1	EtOH	60	900	208.2 ± 4.8	0.150 ± 0.02	-39.3± 1.01
PCL/17	25	0.5[b]	3:1	IPA	40	900	272.2 ± 3.6	0.108 ± 0.03	-38.6 ± 0.98
PCL/18	25	0.5[b]	3:1	EA	40	900	339.0 ± 6.4	0.383 ± 0.03	-36.6 ± 1.12

[a] Polycaprolactone; ; [b] Pluronic F-68; [c] Polyvinyl Alcohol (PVA); [d] - Pluronic 127, [e] – Polydispersity index; EtOH – Ethanol ; IPA- Isopropyl Alcohol; EA- Ethyl acetate

Table 5.5. Composition and characterization of TMZ loaded PCL nanoparticles

Batch Code	PCL[a] (mg)	TMZ[b] (mg)	Non-solvent phase Ethanol : water (1:3)		Mean Particle size (nm) ± SD	PDI[e] ± SD	ZP[f] (mV)	EE[g] (%) ± SD	DL[h] (%) ± SD
			PF-68 [c] (%w/v)	Saturant					
TMZ/PCL/1	25	2	0.5	-	193.7 ± 6.22	0.138 ± 0.01	-13.9 ± 1.62	13.9 ± 2.01	0.64 ± 0.07
TMZ/PCL/2	25	2.5	0.5	-	175.6 ± 8.00	0.138 ± 0.01	-15.8± 0.84	4.60 ± 1.20	0.34 ± 0.05
TMZ/PCL/3	50	2	0.5	-	190.9 ± 4.50	0.175 ± 0.02	-10.8± 0.77	10.83 ± 1.64	0.11± 0.09
TMZ/PCL/4	50	5	0.5	-	219.6 ± 10.32	0.127 ± 0.04	-7.38± 1.22	18.55 ± 2.85	0.087 ± 0.02
TMZ/PCL/5	50	10	0.5	-	295.5 ± 10.10	0.456 ± 0.15	-6.26± 1.65	11.92 ± 2.85	1.41 ± 0.07
TMZ/PCL/4	100	2	0.5		234.4± 9.60	0.236 ± 0.05	-9.6± 0.90	12.86 ± 2.33	0.27 ± 0.04
TMZ/PCL/6	75	5	0.5	-	232.7 ± 8.11	0.198 ± 0.03	-5.47± 0.75	9.01 ± 1.61	0.05 ± 0.02
TMZ/PCL/7	100	10	0.5	-	220.7 ± 20.65	0.191 ± 0.05	-3.28± 1.35	12.65 ± 0.65	0.032 ± 0.01
TMZ/PCL/8	25	10	0.5	NaCl[d]	181.5 ± 10.66	0.194 ± 0.02	-1.32± 1.24	36.90 ± 1.85	0.36 ± 0.22
TMZ/PCL/9	25	25	0.5	Sucrose	236.7 ± 9.85	0.198 ± 0.01	-2.38± 0.85	9.56 ± 2.13	4.55 ± 1.75
TMZ/PCL/10	25	25	0.5	Mannitol	244.1± 7.62	0.231 ± 0.02	-4.34± 1.10	10.29 ± 3.05	4.79 ± 2.22

[a]Polycaprolactone; [b] Temozolomide ; [c] Pluronic F-68; [d] Sodium chloride; [e] Polydispersity index; [f] Zeta Potential; [g] Entrapment efficiency (%w/w); [h] Drug loading (%w/w)

nature. Generally, after cooling down of the lipid melt the solubility of drug in the lipids decreases. Lipids with mono- and diglycerides promotes drug solubilisation. Further, the entrapment of drug depends on the crystalline nature of the lipid. Precirol is a mixture of mono, di and tri glycerides of C_{16} and C_{18} fatty acids, whereas the crystalline lattice of Compritol is composed of very small amounts of unstable α polymorphic form which introduces imperfections in the crystal lattice therefore can accommodate more of the drug. GMS, on the other hand after recrystallization finally transforms into triclinic β form which because of its perfect crystal structure leads to expulsion of most of the dissolved drug [16-18] .

Based on the highest partitioning of TMZ in stearic acid, it was selected for the SLN formulation. Further, stearic acid is an endogenous long chain saturated fatty acid and a component of fats in animal and plant sources, thereby providing biocompatibility and low toxicity potential [19]. Preliminary batches of SLN were prepared with PRC and COM also besides stearic acid.

As discussed earlier, fractional factorial design was used for the stearic acid SLN formulations and batches were prepared accordingly (Table 5.6). Ethyl acetate was selected as the solvent for stearic acid. To improve the solubility of stearic acid a small proportion of dichloromethane was added. TMZ is poorly soluble in ethyl acetate therefore, using it in the organic phase will reduce the diffusion out to aqueous phase and enhance entrapment efficiency of TMZ. Further, researchers have reported the use of ethyl acetate for enhancing entrapment efficiency of hydrophilic drugs because the relatively high solubility of ethyl acetate in water results in fast diffusion of ethyl acetate from oil droplets into the outer aqueous phase during re-emulsification and solidification. This rapid solidification of double emulsion droplets minimizes the contact time between the drug and the aqueous phase increasing drug entrapment. Further, rapid solidification can significantly reduce the coalescence of the inner aqueous droplets forming a less interconnecting channel which may lead to low initial burst and constant drug release [20,21]. As can be seen from the results, although the entrapment and drug loading has improved but the particle size range obtained is from 323 to 4422 nm, which is quite high and not desirable for delivery to the brain. Trials taken with PRC, COM and GMS resulted in particle size in the range of 145.6 to 223.1 nm.

However, the drug loading and entrapment of the formulations was low. Therefore, this SLN formulation strategy was also not further evaluated.

5.3.3. Nanostructured Lipid Carriers

5.3.3.1. Formulation Considerations

Nanostructured lipid carriers (NLC) are second generation lipid nanoparticles composed of a blend of solid and liquid lipids. Replacing a portion of the solid lipid with an oil results in a less ordered matrix which increases the drug loading and prevents leaching out of the drug during storage. Emulsification-ultrasonication technique as described earlier in this chapter was used for the fabrication of NLC. The fabrication technique involves formation of a pre-emulsion of the molten lipid and the hot aqueous phase containing surfactant. Nanoparticles are formed by size reduction of the preemulsion by the cavitational forces generated by high energy sound waves using ultrasonic processor. Subsequent cooling of the emulsion causes solidification of the droplets leading to formation of nanoparticles [11,22]. Preliminary trials were taken with the selected solid lipids alone and with various liquid lipids such as oleic acid, Miglyol® 812, Labrafac™, isopropyl myristate and glyceryl monooleate. Based on the particle size and stability of the formulations, oleic acid was selected as the liquid lipid for the formulations.

5.3.3.2. Experimental Design

Design of experiments (DOE) is an optimization technique for products and/or processes developed to simultaneously evaluate all the potential factors speedily and in a systematic way. It involves use of statistical experimental designs which requires less experimentation and based on which mathematical equations and graphic outputs are generated which provide sufficient information on the effect of various factors (independent variables) on the response(s) (dependent variables). Box Behnken design was specifically selected because it requires fewer runs compared to central composite design and factorial design for three or four factors in addition to being more efficient with respect to the number of coefficients generated by the particular model divided by the number of experiments [23-25]. For BBD design for four factors at three levels, a total of 27 runs including three center points and for three factors at three level design 17 runs including five center points were required. The results obtained are tabulated in Table 5.7- 5.9.

Table 5.6. Composition and characterization of TMZ loaded stearic acid SLNs

Run	X_1[a] (V_{w1} /V_o[1])	X_2[b] SA (mg/ml)	X_3[c] Sonication time [1] (sec)	$X4$[d] TMZ (mg)	$X5$[e] Lecithin [1] (mg)	Mean Particle size (nm) ± SD	PDI[f] ± SD	Zeta potential (mV) ± SD	EE[g](%) ± SD	DL[h] (%) ± SD
1	-1	+1	-1	-1	-1	340.4 ± 8.10	0.165 ± 0.02	29.4± 1.18	14.23 ± 2.24	0.36 ± 0.06
2	-1	+1	+1	+1	-1	323.3 ± 9.45	0.172 ± 0.02	-3.56 ± 0.55	15.81 ± 1.22	0.77 ± 0.13
3	-1	-1	+1	+1	+1	760.6 ± 23.22	0.608 ± 0.10	2.21 ± 0.80	22.91 ± 2.55	2.27 ± 0.64
4	+1	-1	-1	+1	+1	2369 ± 125.50	1.00 ± 0.00	-0.366 ± 0.12	19.30 ± 0.93	7.00 ± 1.06
5	+1	+1	-1	+1	-1	1600 ± 84.34	1.00 ± 0.00	-5.16 ± 0.56	18.66 ± 1.57	3.64 ± 0.53
6	+1	+1	-1	-1	+1	4422 ± 156.80	0.946 ± 0.55	-0.980 ± 0.02	15.04 ± 0.85	1.62 ± 1.24
7	-1	-1	-1	-1	+1	2944 ± 114.23	0.417 ± 0.16	-1.16 ± 0.04	32.49 ± 2.73	1.95 ± 0.85
8	0	0	0	0	0	1773 ± 59.90	0.981 ± 0.15	-13.5 ± 0.02	13.74 ± 3.13	1.71 ± 0.68
9	+1	-1	-1	-1	-1	3050 ± 0.00	1.00 ± 0.00	-5.82 ± 0.05	15.05 ± 1.45	2.85 ± 1.66
10	-1	-1	-1	+1	-1	591.3 ± 55.78	0.536 ± 0.05	10.10 ± 0.03	15.84 ± 2.35	1.55 ± 0.79
11	-1	+1	+1	-1	+1	363.4 ± 44.65	0.307 ± 0.12	-10.4 ± 0.06	7.20 ± 1.13	0.15 ± 0.23
12	+1	-1	+1	+1	-1	2045 ± 98.05	1.00 ± 0.00	-7.05 ± 0.02	13.83 ± 1.25	5.42 ± 0.55
13	-1	+1	-1	+1	+1	3423 ± 123.44	0.488 ± 0.12	-7.75 ± 0.06	19.51 ± 1.46	0.98 ± 0.49
14	+1	+1	+1	+1	+1	582.9 ± 75.60	0.825 ± 0.09	-7.88 ± 0.04	35.21 ± 1.22	6.68 ± 0.38
15	-1	-1	+1	-1	-1	434.2 ± 23.10	0.326 ± 0.05	-9.87 ± 0.02	7.20 ± 1.16	0.41 ± 0.25
16	+1	+1	+1	-1	-1	1457 ± 45.25	0.980 ± 0.15	-10.5 ± 0.01	36.20 ± 0.75	3.88 ± 0.67
17	+1	-1	+1	-1	+1	2164 ± 100.23	1.00 ± 0.00	-6.50 ± 0.03	15.66 ± 2.56	2.47± 0.82
18	-1	-1	-1	-1	-1	498.0 ± 50.35	0.306 ± 0.08	-3.97 ± 0.01	22.91 ± 1.63	1.97 ± 0.60
19	+1	+1	+1	+1	-1	407.5 ± 10.22	0.485 ± 0.05	16.2 ± 0.85	16.93 ± 1.44	0.87 ± 0.43

a- ratio of volume of aqueous and organic phase in primary emulsion; (-1) 0.1, (0) 0.25, (+) 1:0.4; **b-** stearic acid; (-1) 5, (0) 7.5 (+) 10 mg/mL; **c-** (-1) 90, (0) 150 (+) 210 sec; **d-** (-1) 5, (0) 7.5 (+) 10 mg; **e-** (-1) 10, (0) 30, (+) 50mg; 1- primary emulsion; **f-** Polydispersity Index; **g** – Entrapment Efficiency (% w/w); **h** -Drug Loading (% w/w)

Design-Expert® software was used to generate polynomial equations which include the main effects and interaction effects based on various parameters like predicted residual sum of squares, multiple correlation coefficients and adjusted multiple correlation coefficient. Statistical validation of the polynomial equations obtained was confirmed by ANOVA. Response surface plots were obtained from the software which illustrate the effect of critical variables on the responses i.e. as particle size, entrapment efficiency and drug loading. The careful study of the polynomial equations and surface plots would be helpful in understanding the effects of each factor independently and in combination with other factors on each response parameter.

I. Effects on Particle Size

The particle size obtained by executing the runs of the respective designs (Table 5.8-5.10) ranged from 108.85 to 264.45 nm, 143.35 to 449.45 nm and 122.85 to 333.50 nm for PNLC, CNLC and GNLC formulations respectively indicating the sensitivity of the independent variables selected for the study. The effect of independent variables on particle size can be explained by the following polynomial equations generated by the Design Expert software:

For PNLC: Particle size = +181.35 – 6.70A – 28.57B + 9.42C +26.87D …….. (Eq. 1)

For CNLC: Particle size = + 228.12 + 24.85A + 34.97B +71.73C – 73.30 AB + 3.73 AC + 36.27BC + 48.87A^2 + 74.29B^2 - 61.06C^2 ……..(Eq. 2)

For GNLC: Particle size = +201.48 + 11.07A + 19.40B +60.26C ……...(Eq. 3)

Where in case of PNLC, A is the drug-to-lipid ratio, B is amount of lipid, C is lipid-to-oil ratio and D is surfactant concentration. For CNLC and GNLC, A is the drug-to-lipid ratio, B is the lipid-to-oil ratio and c is the surfactant concentration.

The sign and value of the coefficients represent the tendency and magnitude of the effect of the independent variable on the dependent variable, respectively. In the polynomial equation, a positive value represents an effect that favors the response due to synergistic effect, while a negative value indicates an antagonistic effect between the factor and the response [26].

The models selection and ANOVA analysis is given in Table 5.7. The F values and p-value (Prob > F) less than 0.1000 imply that the models are significant. Further, for adequate precision, which measures the signal to noise ratio, a ratio greater than 4 is desirable.

The adjusted R-squared is in reasonable agreement with the predicted R-squared. For all the formulations, adequate precision was greater than 4.0 as represented in Table 5.10 and hence the model was suitable for navigating the design space.

Table 5.7. Statistical parameters for model selection for particle size.

Formulation	Model	F value	p-value (Prob >F)	Adj. R-Squared	Pred. R-Squared	Adeq. Precision
PNLC	Linear	9.68	0.0001	0.5719	0.4565	11.322
CNLC	Quadratic	10.06	0.0102	0.8535	0.7433	10.142
GNLC	Linear	12.66	0.0007	0.7141	0.5823	10.459

The response surface plots for particle size obtained by the software are as shown in Figure 5.2. A 3D response surface plot is a graphical representation of a regression equation indicating changes in response against two independent variables at a time, keeping rest of the variables constant at their middle levels [27].

From the analysis of coefficient of equations (1-3) and surface plots in Fig 5.2 (a-e), it is evident that the particle size is affected by the independent variables. The positive and negative value of a factor in the polynomial equation indicates that the effect of the factor is to increase or decrease the response respectively. For PNLC formulation, an increase in total lipid concentration leads to decrease in mean particle size. However, the formulations with high lipid content had poor physical stability probably because at higher concentrations, lipids have a higher tendency to coalesce leading to instability. In PNLC and CNLC formulations an increase in the solid lipid-to-oil ratio increases the particle size and vice versa. The presence of oil enhances the emulsification of the solid lipid, thereby reducing the particle size. Therefore, reduced oil proportion will result in comparatively larger particles.

Further, an increase in drug-to-lipid ratio and surfactant concentration also lead to an increase in particle size. This can be attributed to an increase in viscosity in the system due to the increased concentration of drug and/or surfactant leading to increase in particle size [28,29].

Table 5.8. Composition and characterization of NLC with Precirol® ATO5 and oleic acid (PNLC)

Run	X_1[a] (TMZ/Lipid$_T$)	X_2[b] Lipid$_T$ (mg)	X_3[c] (Lipid$_S$/Oil)	$X4$[d] PF-68 (mg)	Mean Particle size (nm) ± SD	PDI[f] ± SD	Zeta potential (mV) ± SD	EE[g](%) ± SD	DL[h] (%) ± SD
1	0	0	0	0	192.15 ± 6.91	0.250 ± 0.05	-19.95 ± 3.27	30.04 ± 6.24	3.16 ± 0.85
2	0	+1	+1	0	180.1 ± 6.65	0.304 ± 0.02	-18.65 ± 5.20	24.54 ± 7.17	2.53 ± 0.76
3	0	0	0	0	208.65 ± 7.42	0.318 ± 0.01	-22.85 ± 4.17	34.64 ± 1.83	3.54 ± 0.37
4	0	+1	0	-1	133.95 ± 7.00	0.207 ± 0.02	22.40 ± 3.96	34.24 ± 2.50	3.59 ± 0.23
5	0	-1	0	+1	210.25 ± 5.87	0.379 ± 0.01	-30.25 ± 1.32	30.31 ± 1.78	3.21 ± 0.31
6	0	0	+1	+1	206.75 ± 4.75	0.349 ± 0.01	21.35 ± 1.64	31.66 ± 0.97	3.16 ± 0.26
7	+1	0	0	+1	184.90 ± 1.70	0.307 ± 0.03	-23.3 ± 0.07	22.85 ± 0.23	4.55 ± 0.18
8	0	0	-1	+1	196.7 ± 1.56	0.259 ± 0.01	-16.05 ± 4.53	33.68 ± 1.06	3.40 ± 0.27
9	0	0	+1	-1	164.3 ± 5.73	0.432 ± 0.02	-14.55 ± 3.66	28.19 ± 2.11	2.78 ± 0.26
10	0	0	0	0	197.45 ± 5.20	0.425 ± 0.05	-17.00 ± 3.45	28.02 ± 3.37	3.09 ± 0.45
11	0	-1	-1	0	215.25 ± 4.69	0.366 ± 0.02	-23.4 ± 2.64	25.17 ± 3.32	2.51 ± 0.39
12	-1	-1	0	0	264.45 ± 5.99	0.327 ± 0.02	-24.00 ± 2.83	34.58 ± 4.58	1.84 ± 0.38
13	-1	0	0	+1	192.10 ± 4.47	0.317 ± 0.03	-30.55 ± 3.04	38.46 ± 2.37	1.90 ± 0.10
14	-1	0	+1	0	233.35 ± 5.70	0.351 ± 0.01	-24.75 ± 2.33	32.47 ± 0.70	1.63 ± 0.07

Cont...

Run	X_1[a] (TMZ/Lipid$_T$)	X_2[b] Lipid$_T$(mg)	X_3[c] (Lipid$_S$/Oil)	$X4$[d] PF-68 (mg)	Mean Particle size (nm) ± SD	PDI[e] ± SD	Zeta potential (mV) ± SD	EE[f] (%) ± SD	DL[g] (%) ± SD
15	+1	0	0	-1	133.65 ± 4.10	0.315 ± 0.01	39.20 ± 2.40	21.84 ± 0.93	4.36 ± 0.18
16	+1	-1	0	0	221.90 ± 7.25	0.322 ± 0.03	36.35 ± 3.69	27.38 ± 1.63	5.37 ± 0.36
17	0	+1	0	+1	177.10 ± 3.41	0.328 ± 0.04	-25.70 ± 3.76	34.06 ± 3.73	3.66 ± 0.50
18	-1	0	-1	0	176.50 ± 5.12	0.343 ± 0.03	-33.00 ± 0.71	35.59 ± 5.00	1.90 ± 0.15
19	+1	0	-1	0	171.90 ± 3.47	0.332 ± 0.01	-30.55 ± 3.32	31.42 ± 3.96	6.33 ± 0.93
20	-1	+1	0	0	144.30 ± 4.07	0.315 ± 0.01	39.70 ± 5.48	44.50 ± 5.16	2.23 ± 0.37
21	0	0	-1	-1	144.54 ± 3.14	0.325 ± 0.02	27.60 ± 3.11	26.64 ± 1.16	2.72 ± 0.09
22	-1	0	0	-1	108.85 ± 0.21	0.267 ± 0.01	-35.85 ± 4.00	33.19 ± 5.20	1.66 ± 0.30
23	0	-1	0	-1	159.95 ± 0.07	0.309 ± 0.02	-11.65 ± 0.78	25.92 ± 1.05	2.61 ± 0.18
24	0	-1	+1	0	201.35 ± 4.23	0.315 ± 0.02	-48.05 ± 3.46	29.25 ± 1.38	2.91 ± 0.20
25	0	+1	-1	0	149.25 ± 2.72	0.275 ± 0.01	-32.00 ± 0.71	38.63 ± 8.67	3.90 ± 0.98
26	+1	0	+1	0	181.25 ± 4.66	0.342 ± 0.03	-33.40 ± 1.70	29.92 ± 1.20	6.04 ± 0.15
27	+1	+1	0	0	145.60 ± 1.13	0.280 ± 0.01	-34.85 ± 3.74	14.07 ± 3.45	2.84 ± 0.71

a – Temozolomide /Total Lipid ratio; (-1) 0.05, (0) 0.1, (+1) 0.2; **b** – Amount of total lipid (-1) 300, (0) 500, (+1) 1000mg; **c** - Solid lipid / Oil ratio; (-1) 0.05, (0) 0.1, (+1) 0.2;

d – Pf-68 concentration (-1) 0.5, (0) 1.5, (+1) 3.0 %w/v ; **e-** Polydispersity Index ; **f-** Entrapment efficiency (%w/w); **g** – Drug Loading (%w/w).

Table 5.9. Composition and characterization of NLC with Compritol® ATO 888 and oleic acid (CNLC)

Run	X_1[a] (TMZ/Lipid$_T$)	X_2[b] (Lipid$_S$/Oil)	$X3$[c] PF-68 (mg)	Mean Particle size (nm) ± SD	PDI [d] ± SD	Zeta potential (mV) ± SD	EE [e](%) ± SD	DL [f] (%) ± SD
1	0	-1	+1	242.9 ± 5.09	0.257 ± 0.01	-23.05 ± 0.07	35.27 ± 1.41	7.09 ± 0.28
2	-1	-1	0	209.65 ± 0.92	0.268 ± 0.01	-25.35 ± 1.20	24.92 ± 2.69	2.55 ± 0.29
3	+1	-1	0	449.45 ± 10.54	0.507 ± 0.01	-31.9 ± 5.80	27.34 ± 4.86	8.01 ± 1.51
4	0	+1	-1	167.25 ± 6.83	0.328 ± 0.05	-32.85 ± 3.32	35.14 ± 3.43	6.91 ± 0.70
5	+1	0	-1	157.9 ± 3.39	0.309 ± 0.02	-27.3 ± 1.13	25.32 ± 2.02	7.51 ± 0.47
6	0	-1	-1	143.35 ± 0.21	0.243 ± 0.02	-24.25 ± 0.78	44.16 ± 6.93	8.82 ± 1.73
7	-1	0	-1	159.15 ± 3.04	0.342 ± 0.01	-29.3 ± 0.42	41.10 ± 3.05	4.33 ± 0.06
8	0	+1	+1	411.9 ± 32.34	0.430 ± 0.04	-32.85 ± 2.76	30.84 ± 1.10	6.13 ± 0.76
9	0	0	0	238.1 ± 13.32	0.268 ± 0.05	-25.3 ± 1.13	32.98 ± 0.55	6.03 ± 1.05
10	+1	+1	0	346.3 ± 20.08	0.649 ± 0.01	-26.05 ± 0.64	24.19 ± 0.44	7.12 ± 0.33
11	-1	0	+1	266.5 ± 13.72	0.350 ± 0.03	-27.3 ± 0.02	43.70 ± 0.68	4.35 ± 0.84
12	0	0	0	230.2 ± 6.93	0.449 ± 0.08	-23.7 ± 1.13	31.99 ± 2.45	6.05 ± 0.47
13	0	0	0	216.05 ± 5.27	0.411± 0.03	-24.7 ± 2.55	31.60 ± 0.91	5.56 ± 0.26
14	+1	0	+1	280.15 ± 2.19	0.372 ± 0.03	-24.00 ± 2.26	48.31 ± 2.18	13.83 ± 1.31
15	-1	+1	0	399.7 ± 1.98	0.454 ± 0.08	-24.6 ± 1.70	34.35 ± 2.15	3.53 ± 0.12

a – Temozolomide /Total Lipid ratio; (-1) 0.05, (0) 0.1, (+1) 0.2; **b**-Solid lipid / Oil ratio; (-1) 0.05, (0) 0.1, (+1) 0.2; **c** – Pf-68 concentration (-1) 0.5, (0) 1.5, (+1) 3.0 %w/v; **d**- Polydispersity Index; **e**- Entrapment efficiency (%w/w); **f** – Drug Loading (%w/w).

Table 5.10. Composition and characterization of NLC with glyceryl monostearate and oleic acid (GNLC)

Run	X_1 [a] (TMZ/Lipid$_T$)	X_2 [b] (Lipid$_S$/Oil)	$X3$ [c] PF-68 (mg)	Mean Particle size (nm) ± SD	PDI [d] ± SD	Zeta potential (mV) ± SD	EE [e] (%) ± SD	DL [f] (%) ± SD
1	0	-1	+1	208.05 ± 9.12	0.165 ± 0.01	-39.50 ± 1.56	31.51 ± 1.75	6.42 ± 0.22
2	-1	-1	0	210.55 ± 5.30	0.218 ± 0.01	-46.45 ± 0.59	34.02 ± 1.26	3.46 ± 0.05
3	+1	-1	0	210.85 ± 4.17	0.217 ± 0.02	-46.60 ± 1.41	33.45 ± 0.51	9.72 ± 0.40
4	0	+1	-1	159.95 ± 9.21	0.311 ± 0.06	-48.30 ± 2.40	19.02 ± 2.11	3.87 ± 0.49
5	+1	0	-1	122.85 ± 3.18	0.224 ± 0.01	-49.85 ± 2.47	18.89 ± 0.87	5.55 ± 0.25
6	0	-1	-1	126.50 ± 0.71	0.214 ± 0.01	-47.65 ± 3.04	27.32 ± 1.37	5.49 ± 0.32
7	-1	0	-1	133.00 ± 0.42	0.223 ± 0.01	-50.20 ± 0.99	18.64 ± 0.96	1.86 ± 0.09
8	0	+1	+1	333.50 ± 2.26	0.337 ± 0.04	-36.60 ± 1.56	27.52 ± 3.44	5.56 ± 0.52
9	0	0	0	212.90 ± 0.14	0.264 ± 0.02	-44.90 ± 0.20	32.21 ± 0.87	6.58 ± 0.24
10	+1	+1	0	248.35 ± 0.07	0.379 ± 0.02	-46.10 ± 0.85	19.31 ± 1.38	5.73 ± 0.54
11	-1	0	+1	231.70 ± 3.94	0.250 ± 0.01	-38.15 ± 0.21	28.85 ± 2.35	2.94 ± 0.30
12	0	0	0	204.15 ± 10.21	0.267 ± 0.01	-44.05 ± 1.20	32.21 ± 0.77	6.58 ± 0.24
13	0	0	0	199.45 ± 5.87	0.296 ± 0.03	-41.95 ± 1.77	28.90 ± 1.06	5.04 ± 0.45
14	+1	0	+1	251.10 ± 6.29	0.268 ± 0.05	-39.30 ± 0.71	28.28 ± 0.82	8.48 ± 0.25
15	-1	+1	0	169.35 ± 4.03	0.339 ± 0.01	-49.40 ± 0.57	19.46 ± 1.22	1.93 ± 0.11

a – Temozolomide /Total Lipid ratio; (-1) 0.05, (0) 0.1, (+1) 0.2; **b**-Solid lipid / Oil ratio; (-1) 0.05, (0) 0.1, (+1) 0.2; **c** – PF-68 concentration (-1) 0.5, (0) 1.5, (+1) 3.0 %w/v; **d**- Polydispersity Index; **e**- Entrapment efficiency (%w/w); f – Drug Loading (%w/w).

The high value of coefficients in polynomial equation for PNLC (–28.57B and +26.87D), CNLC (+71.73 C) and GNLC (+60.26 C) compared to other coefficients indicate that these factors have a major negative and positive effect respectively on the particle size. The interaction between drug-to-lipid ratio (A) and lipid to oil ratio (B) having a negative impact on the studied response i.e. particle size in CNLC was evident from the high value (-73.30) of coefficient for AB. These interaction effects were not observed for PNLC and GNLC as is evident from the absence of interaction coefficients.

II. Effects on Entrapment Efficiency

The entrapment efficiency (EE) varied from 14.07 to 44.5% for PNLC, 17.08 to 48.35 for CNLC and 18.64 to 34.02 for GNLC formulations. The polynomial equation generated to explain the effect of the evaluated independent variables on the EE is as follows (Eq. 4-6) and the response surface plots as generated by the Design Expert software are as represented in Figure 5.3-5.5.

For PNLC: $EE\ (\%) = +30.42 - 5.94A + 1.45B - 1.26C + 1.75D - 1.07AD - 4.54BC - 1.14BD - 0.90CD$ ..... (Eq. 4)

For CNLC: $EE\ (\%) = +47.08 + 3.45A - 2.75B + 0.84C + 6.08\ AB + 2.42AC - 6.84\ BC - 13.43B^2$ ..... (Eq. 5)

For GNLC: $EE\ (\%) = + 26.86 - 0.13A - 5.12B + 4.04C$ ..... (Eq. 6)

Where in case of PNLC, A is the drug-to-lipid ratio, B is amount of lipid, C is lipid-to-oil ratio and D is surfactant concentration. For CNLC and GNLC, A is the drug-to-lipid ratio, B is the lipid-to-oil ratio and C is the surfactant concentration.

The statistical parameters for model selection are as tabulated in Table 5.11. The adjusted R-squared is in reasonable agreement with the predicted R-squared value. The results indicate that the model is significant and the model was suitable for navigating the design space. The equations (Eq.4-6) and surface plots (Fig. 5.3-5.5) suggest that entrapment efficiency is significantly affected by lipid-to-oil ratio, drug-to-lipid ratio and surfactant concentration.

Increase in proportion of oil in the NLC may help in increasing entrapment of the drug possibly by enhancing the solubility of the drug in the lipid matrix. Further, in the NLCs, the presence of liquid lipids increases imperfections in the crystal structure increasing the capacity to accommodate more drug further increasing the EE [11]. Drug-to-lipid ratio also

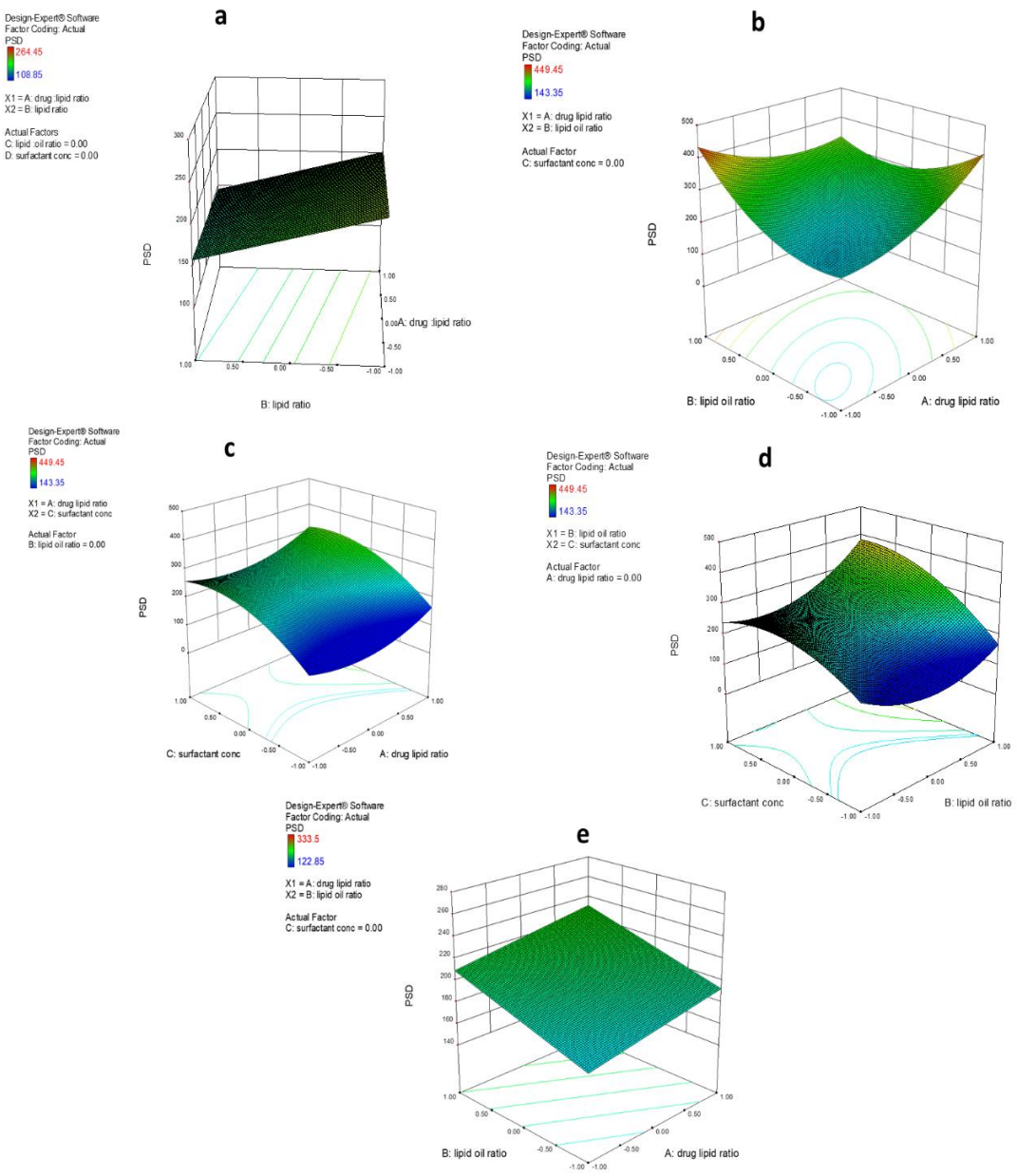

Fig. 5.2. Response surface graphs showing effects of a) PNLC: drug-to-lipid ratio (A) and lipid concentration (B); b) CNLC: drug-to-lipid ratio (A) and lipid-to-oil ratio (B); c) CNLC: drug-lipid ratio (A) and surfactant concentration (C); d) CNLC: lipid-to-oil ratio (B) and surfactant concentration (C) e) GNLC: drug-to-lipid ratio (A) and lipid-to-oil ratio (B) on particle size

Table 5.11. Statistical parameters for model selection for entrapment efficiency (EE, %)

Formulation	Model	F value	p-value (Prob >F)	Adj. R-Squared	Pred. R-Squared	Adeq. Precision
PNLC	Reduced 2FI	3.74	0.0096	0.4573	0.3568	6.244
CNLC	Quadratic	3.62	0.0850	0.6227	0.5086	6.926
GNLC	Linear	7.23	0.0060	0.5718	0.4458	10.459

increases the entrapment of the drug as more drug is available for entrapment. However, at higher ratios the entrapment efficiency does not increase due to limiting factors such as partitioning capability of the drug into the lipid. Increase in surfactant concentration also increases the entrapment efficiency, but at higher levels it has a negative impact on the EE. This may be due to increase in the solubility of the drug in the lipid matrix. However, at higher extreme levels, the surfactant solubilizes the drug and increases partitioning into the external aqueous phase resulting in decreased drug entrapment [25,30,31].

The interaction of factors was also found to have a significant effect on the entrapment efficiency. The coefficients for BC for PNLC and CNLC generated were - 4.54 and - 6.84 respectively. The negative sign indicates an antagonistic effect on the response. Positive effect of interaction AB (6.08) was observed in CNLC.

III. Effect on Drug Loading

The drug loading (DL) ranged from 1.63 to 6.33 % for PNLC, 1.76 to 13.40 for CNLC and 1.86 to 9.72 for GNLC formulations.

The polynomial equation generated by the software to examine the effect of selected factors on drug loading (DL %) is given as follows (Eq. 7-9) and the response surface plots generated are as shown in Figure 5.6.

For PNLC: DL % = +3.24 +1.53A +0.025B – 0.14C + 0.18D……. (Eq.7)

For CNLC: DL % = +6.93 + 3.89A - 0.28B + 0.29C ……... (Eq.8)

For GNLC: DL % = +5.38 + 2.41A -1.00B + 0.83C ……... (Eq.9)

Where for PNLC, A is the drug-to-lipid ratio, B is amount of lipid, C is lipid-to-oil ratio and

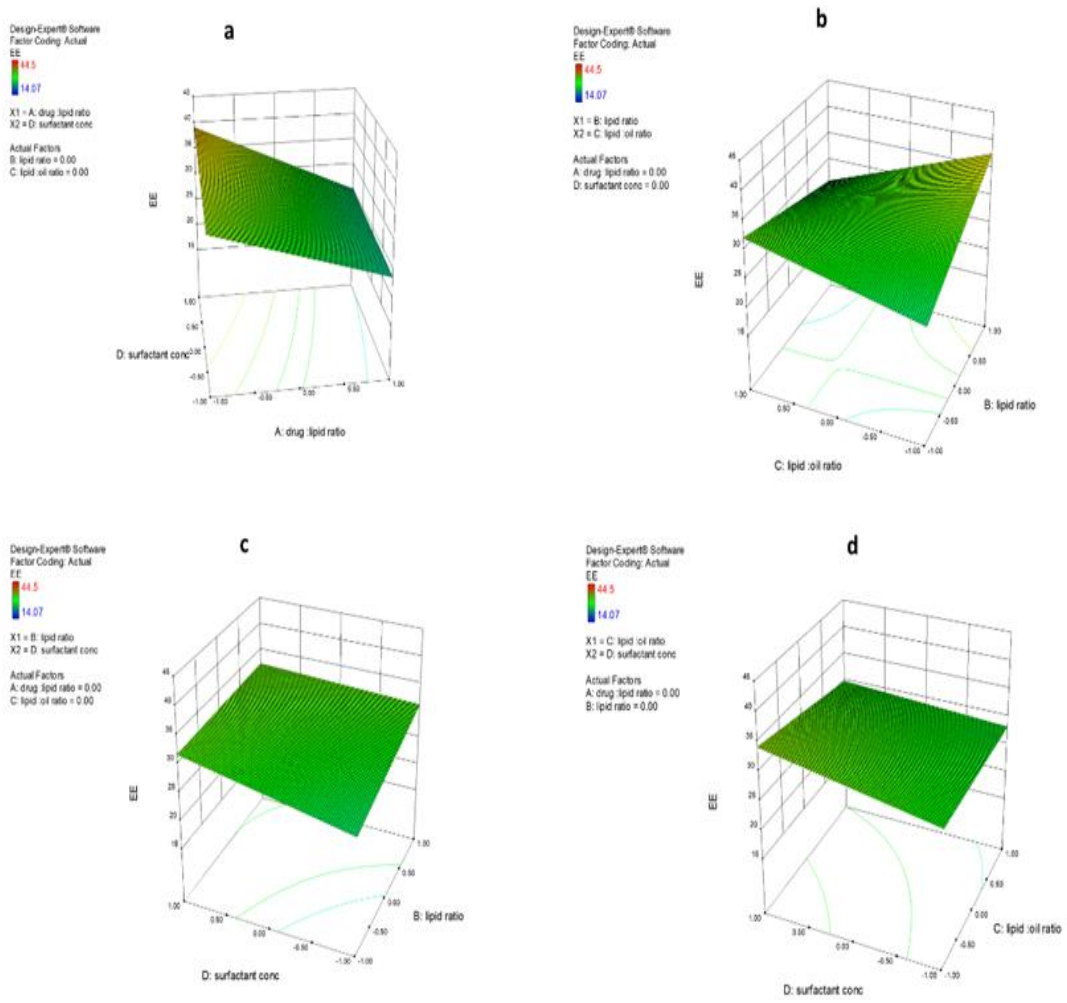

Fig. 5.3. Response surface graphs showing effects of a) drug-to-lipid ratio (A) and surfactant concentration (D); b) lipid amount (B) and lipid-to-oil ratio (C); and c) lipid amount (B) and surfactant concentration (D) d) lipid-to-oil ratio (C) and surfactant concentration (D) on entrapment efficiency in PNLC formulations

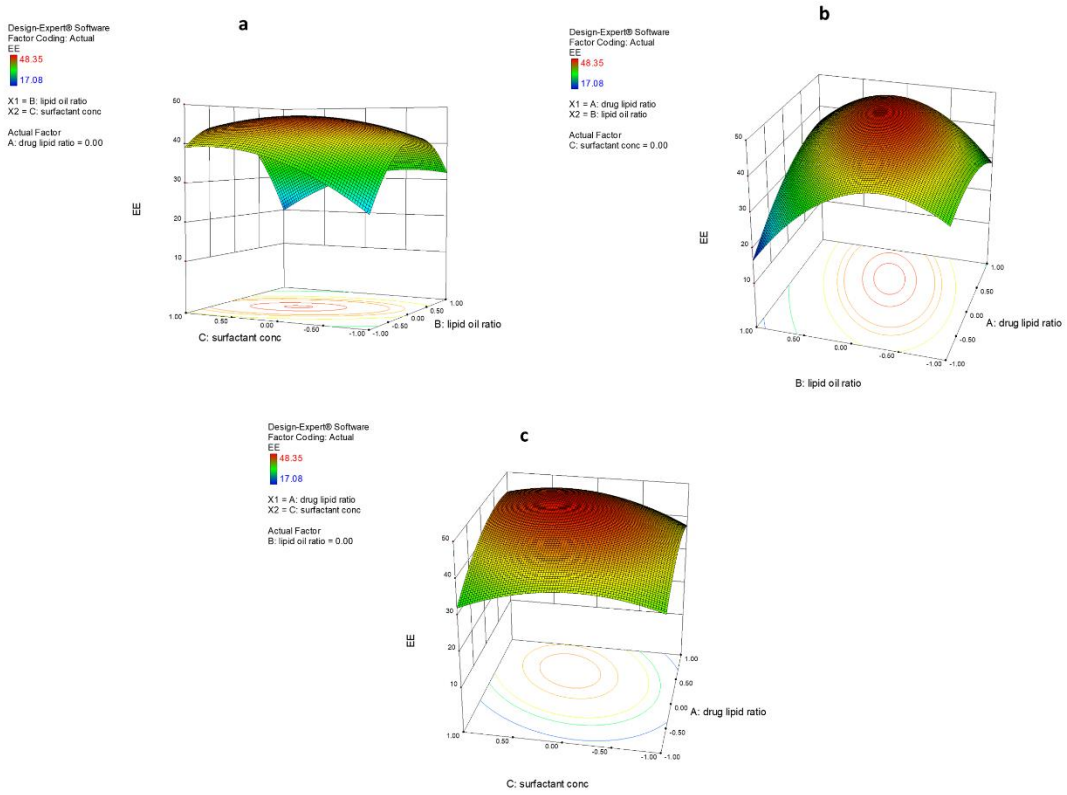

Fig. 5.4. Response surface graphs showing effects of a) lipid-to-oil ratio (B) and surfactant concentration (C); b) drug-to-lipid ratio (A) and lipid-to-oil ratio (B); and c) drug-to-lipid ratio (A) and surfactant concentration (C) on entrapment efficiency in CNLC formulations

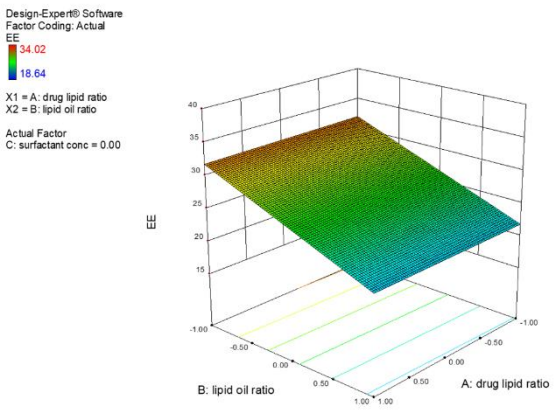

Fig. 5.5. Response surface graphs showing effects of drug-to-lipid ratio (A) and lipid-to-oil ratio on entrapment efficiency in GNLC formulations

D is surfactant concentration. For CNLC and GNLC, A is the drug-to-lipid ratio, B is the lipid-to-oil ratio and c is the surfactant concentration.

The statistical parameters for model selection are as tabulated in Table 5.12. The results indicate that the model is significant and the model was suitable for navigating the design space.

Table 5.12. Statistical parameters for model selection for drug loading (DL, %).

Formulation	Model	F value	p-value (Prob >F)	Adj. R-Squared	Pred. R-Squared	Adeq. Precision
PNLC	Linear	14.34	< 0.0001	0.6723	0.5642	11.229
CNLC	Linear	9.71	0.0020	0.6511	0.4806	7.900
GNLC	Linear	21.47	< 0.0001	0.8143	0.7484	13.688

From the regression equations (Eq. 7-9) and the response surface graphs (Fig. 5.6), it can be inferred that the drug loading is affected by the drug-to-lipid ratio significantly. Increase in the amount of drug leads to an increase in the concentration of drug per emulsion droplet leading to an increase in the drug loading. Drug loading is also dependent on drug-lipid interaction and higher drug -lipid interaction and partitioning in lipid results in increased drug loading [32]. The coefficients of factor A for PNLC (+1.53), CNLC (3.89) and GNLC (2.41) are the highest and bear a positive sign which indicates the synergistic effect of the factor on drug loading. All other factors had low coefficients indicative of a comparatively lesser effect on the drug loading.

IV. Other Findings

In addition to the discussed factors, sonication time also had an influence on the particle size and distribution. The effect of sonication time was also studied during preliminary studies. As the sonication time was increased from 3 to 6 min, a reduction in particle size was observed. However, at 6 and 10 minutes, no significant change in particle size and PDI was observed. As exposing the drug to sonication at higher temperature for longer period of time might result in degradation of the drug. Therefore, a sonication time of 6 minutes was selected for the fabrication of NLC.

As already discussed, an increase in lipid content as investigated in PNLC formulations resulted in satisfactory particle size although it did not have a significant effect on drug entrapment. However, the formulations were observed to be unstable during storage due to coalescence of the lipid particles. Therefore, the total amount of lipid selected for fabrication and optimization of CNLC and GNLC formulations was 500 mg.

The effect of freeze drying and redispersibility on the formulations was also studied. It was observed that the formulations with higher surfactant concentration resulted in easy dispersion of the NLC. Formulations with higher proportion of oil i.e $\leq$ 0.5 solid lipid-oil ratio upon lyophilization were not readily dispersible and were slightly sticky in nature. This observation was an important consideration during selection of optimized formulations. Studies with and without cryoprotectants was also carried out. A number of cryoprotectants such as mannitol, sucrose, trehalose and dextrose were evaluated at different concentrations. Mannitol was found to improve significantly the stability of the NLC during freezing and lyophilization procedure at 15% w/w concentration. The freeze-dried formulation was free flowing and easily redispersible and no significant change in particle size was observed as shown in Figure 5.7.

5.3.4. Optimization and Validation

The Design expert software was used to get the optimized formulations. The desirability criteria set was minimum particle size and maximum entrapment efficiency and drug loading. Further, the criteria for the lipid amount and the lipid-to-oil ratio to be used was restricted to around 500 mg and > 0.5 respectively considering their effect on stability and characteristics of freeze dried particles as discussed earlier in the chapter.

Batches of NLC with the predicted parameters were prepared (n=3) to validate the optimization procedure being evaluated. The predicted levels of factors and responses are given below along with the practically obtained values in brackets.

a) PNLC: Drug-to-lipid ratio – 0.220; lipid amount – 540 mg; $lipid_s$-to-oil ratio – 1.07 and surfactant concentration 2.1% w/v with predicted responses: Size -158.6 nm (167.30 ± 4.15 nm); EE – 38.2 % (37.22 ± 1.23 %); DL – 8.97 % (8.15 ± 0.54).

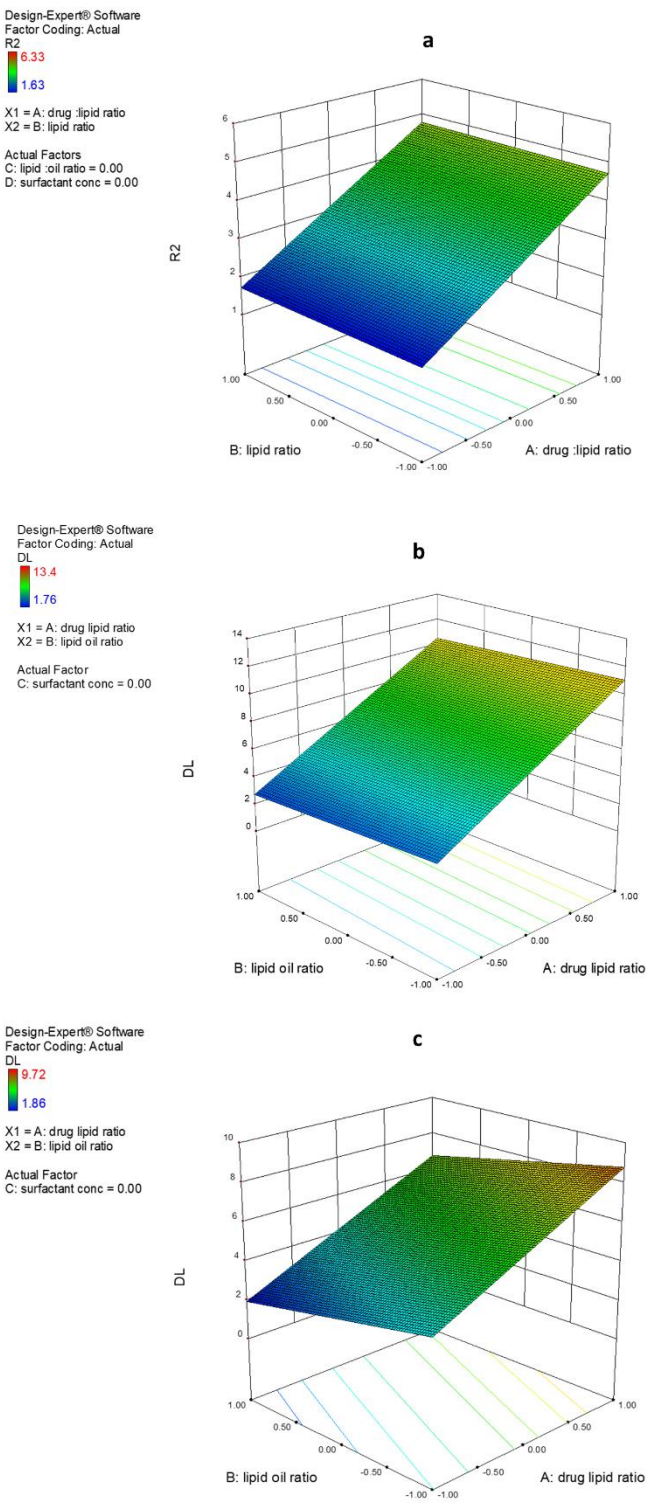

Fig. 5.6. Response surface graphs showing effects of a) drug-to-lipid ratio (A) and lipid concentration (B); b and c) drug-to-lipid ratio (A) and lipid-to-oil ratio (B); lipid ratio (A) on drug loading in PNLC, CNLC and GNLC formulations respectively

b) GNLC: Drug-to-lipid ratio – 0.22; $lipid_s$-to-oil ratio – 0.88 and surfactant concentration 1.75 % w/v with predicted responses: Size -180.9 nm (174.15 ± 4.76 nm); EE – 37.33 % (35.12 ± 2.45 %); DL – 8.36 % (7.75 ± 0.65).

c) CNLC: Drug-to-lipid ratio – 0.20; $lipid_s$-to-oil ratio – 1.0 and surfactant concentration 1.54 % w/v with predicted responses: Size -219.2 nm (229.24 ± 8.76 nm); EE - 33.64 % (30.75 ± 1.54 %); DL – 5.42 % (5.01 ± 0.46).

The practical values were in reasonable agreement with the predicted values confirming the validity of the optimization method. These optimized formulations were taken for further characterization, in vitro and in vivo studies.

5.3.5. Particle Size, Zeta Potential and Morphology

Particle size and its distribution is an important characteristic which has an influence on the stability, solubility, release rate and biological performance of the NLC. For site-specific delivery, a 50–300 nm range is preferred especially for central nervous system disorders and chemotherapeutic agents [11]. Particle size distribution by intensity profile, SEM images and zeta potential of the optimized formulations are given in Figure 5.7-5.9. The polydispersity index (PDI) observed was 0.325 ± 0.071, which although being satisfactory, is towards the higher side. This is possibly because NLC are not spherical particles and the formulations may contain other colloidal forms such as micelles and this may lead to higher PDI [33,34]. Particle morphology significantly influences drug loading, encapsulation efficiency, drug release characteristics, pharmacokinetics, biodistribution and targeted delivery of NLC. It also plays an important role in cellular uptake, receptor binding and interaction with cells. The SEM images showed that most of the particles were anisometric and the surface of the particles was irregular. Particle size of the NLC was also confirmed by SEM and it was observed that the size of the particles was significantly lesser than the size indicated by the DLS. Anisometric particles have high surface area, in addition to short diffusion pathways as compared to spherical particles. Due to the higher surface area, non-spherical particles require higher amounts of surfactants for stabilization [35-37]

Zeta potential (ZP) is the electric potential of a particle not on its surface but away from it in a diffuse layer, which related to particle movement in the liquid is known as the slipping or shear plane. It is closely related to surface morphology and stability of the suspension. ZP gives important information on the long-term stability of nanoparticles and their tendency to

agglomerate. The zeta potential of PNLC, CNLC and GNLC formulations were observed to be 37.7 ± 2.24, 26 ± 2.36 and -43.34 ± 3.42 mV respectively. The results of zeta potential indicate good stability of the NLC as for good stability a minimum of ± 30 mV is desired. When steric stabilizers such as poloxamers are used, they get adsorbed on the particles leading to reduction in the zeta potential, and for such systems, a minimum ZP of ± 20 mV is desirable [35].

5.3.6. In Vitro Release Studies

The in vitro release curves obtained by the dialysis bag method, as described in section 5.2.6.3, from the NLC formulations and pure TMZ investigated over 24h are shown in Figure 5.10 to 5.12. Cumulative drug release of pure TMZ showed 77.53 ± 1.25% in 2h. After 2h a decrease in concentration was observed possibly because of conversion of TMZ in the media. For PNLC, CNLC and GNLC the cumulative drug release was 81.44 ± 5.23, 85.26 ± 0.81 and 76.83 ± 1.99 % respectively after 24h. Each point represents mean ± SD of three observations. An initial burst release was observed in all the formulations (50-60%) within 1h followed by sustained release. The initial burst release maybe due to the presence of drug particles at the surface of the nanoparticle which get precipitated and entrapped on the nanoparticle when sudden cooling of the hot emulsion is carried out. Further, during the cooling phase a solid core starts forming at the recrystallization temperature and the crystallized core is no longer available for repartitioning of the drug, hence it concentrates in the shell or on the surface of the particle. As the nanoparticles are anisometric in shape, as revealed by SEM, it considerably increases the surface area in addition to shorter diffusion pathways as compared to spherical particles which also may be responsible for the burst release of the drug. Furthermore, a number of other factors such as the type of solid lipid, proportion of oil, fabrication temperature, type and concentration of stabilizer used besides the particle size of the NLC also has an effect on the release pattern [38,39].

The drug release from nanoparticles determines its biological effect and hence is of paramount importance. For elucidation of the release kinetics, the dissolution data was fitted into various mathematical models. The best fit model for in vitro release was selected on the basis of three commonly used criteria i.e. R^2, AIC and MSC. For the most suitable model, the R^2 value should be close to 1, the AIC value should be low and the MSC value should be

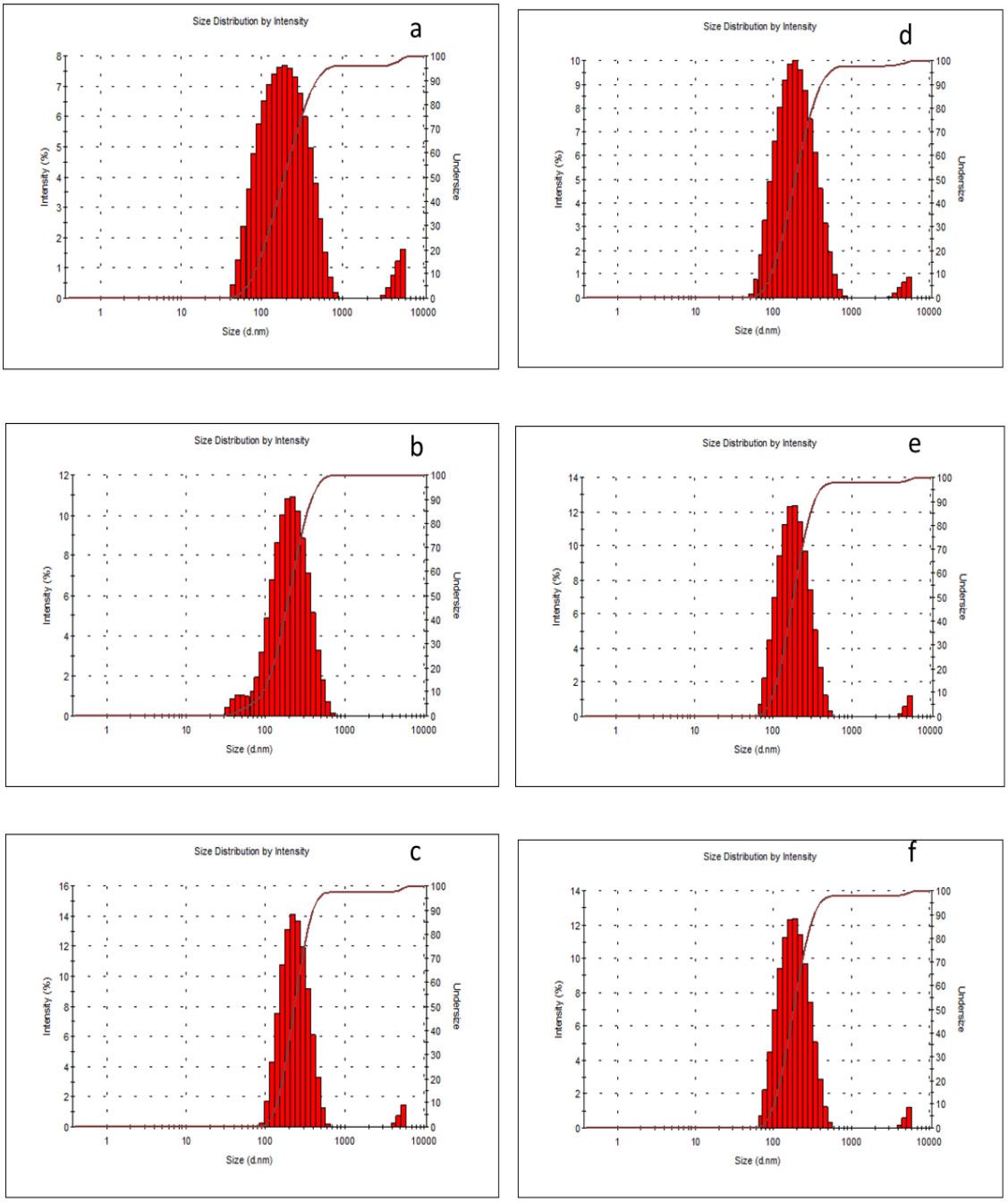

Fig. 5.7. Particle size distribution before (a,b,c) and after freeze drying (d,e,f) of PNLC, GNLC and CNLC formulations respectively

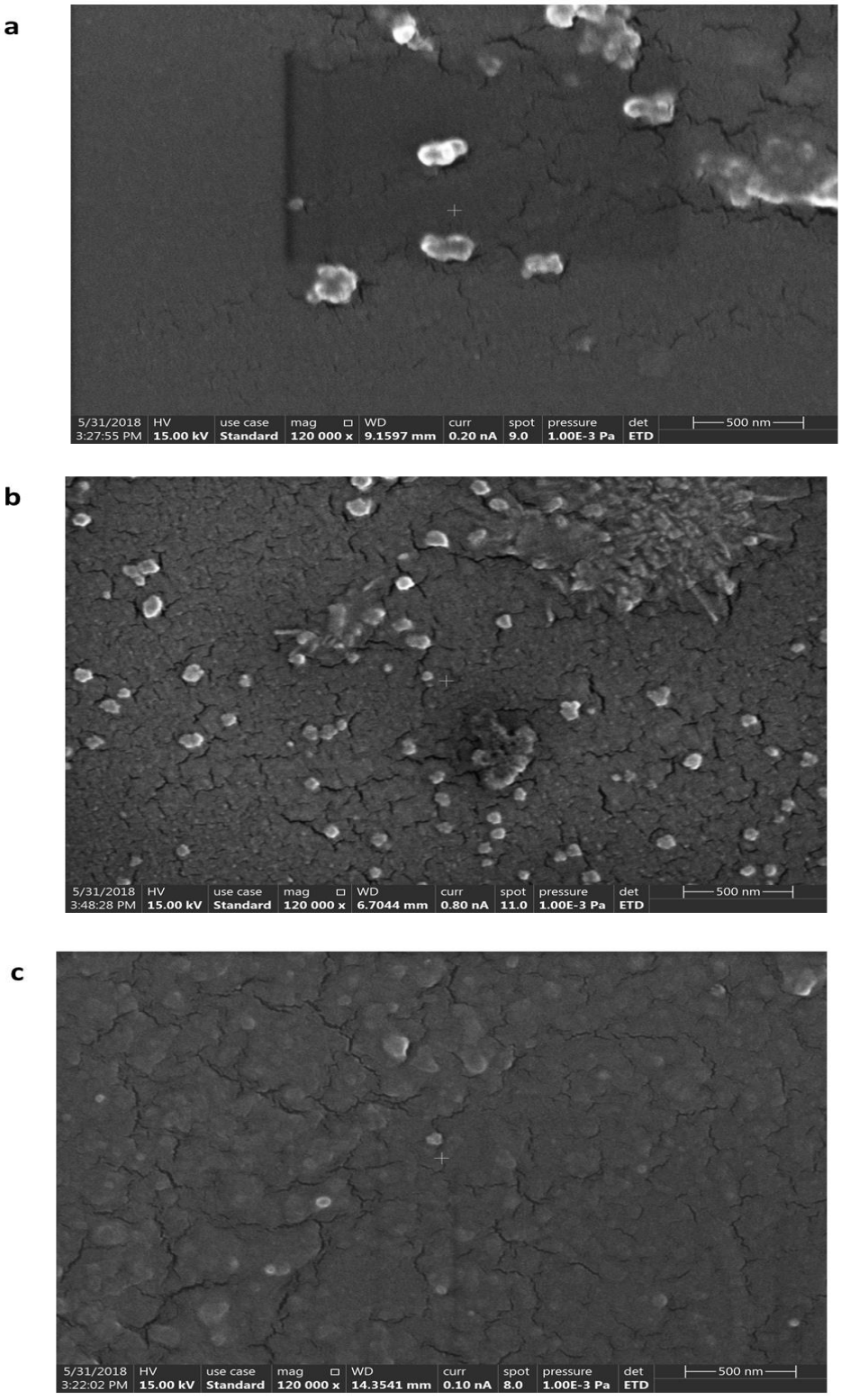

Fig. 5.8. FESEM images of a) PNLC**;** b) CNLC and c) GNLC formulations

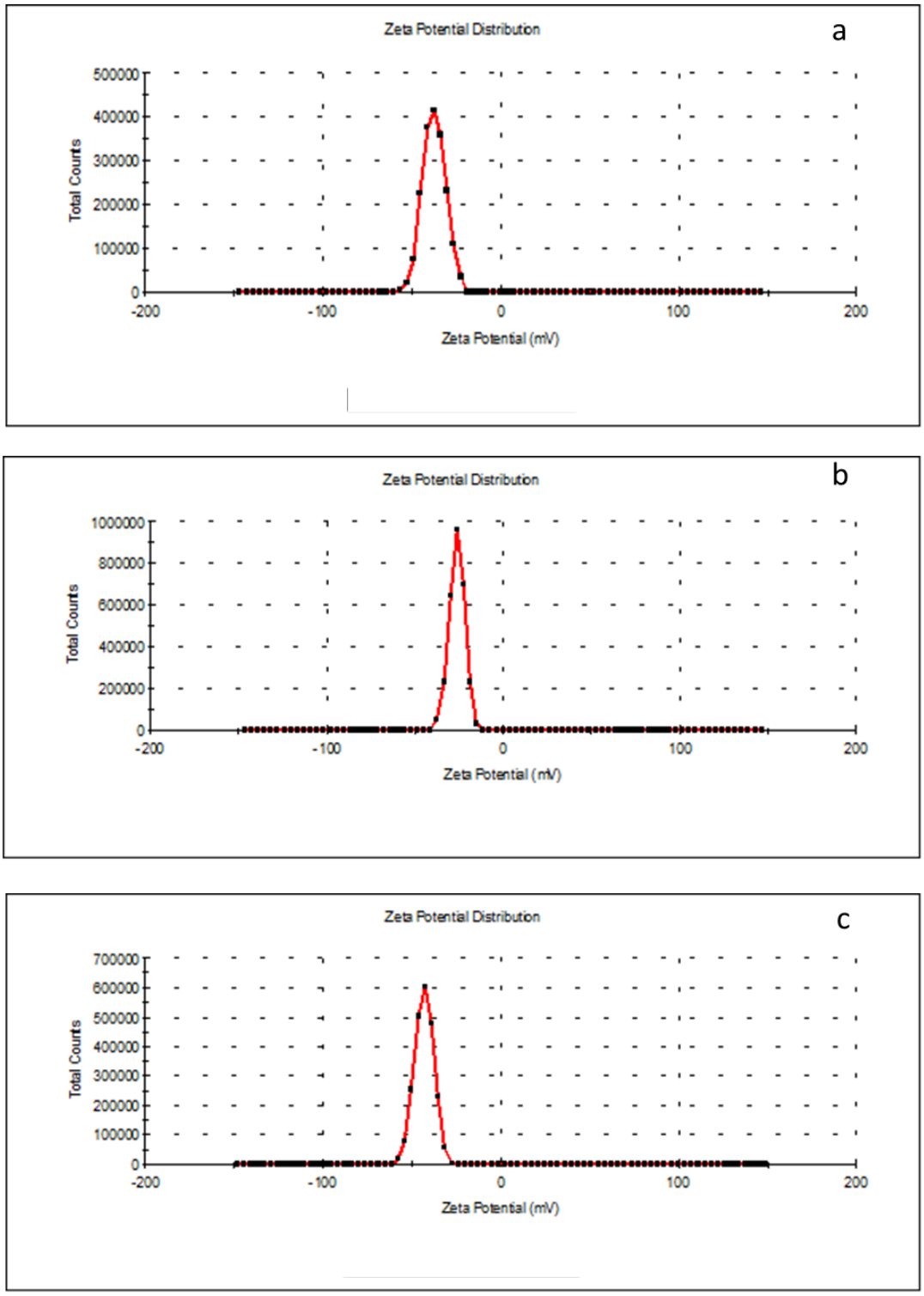

Fig. 5.9. Representative zeta potential distribution of a) PNLC; b) CNLC and c) GNLC formulations

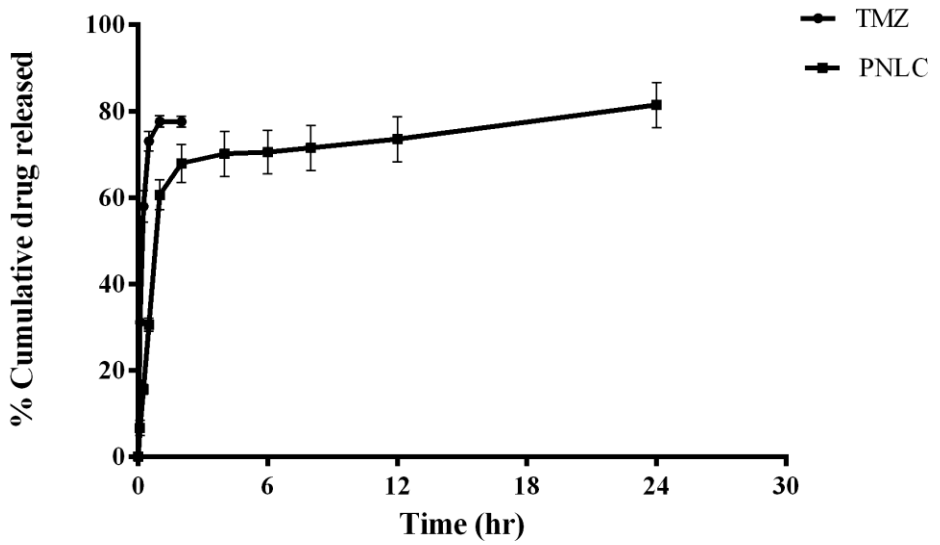

Fig. 5.10. In vitro drug release profile of pure temozolomide and optimized PNLC formulation in pH 5.0 acetate buffer. Each point represents mean ± SD of three observations

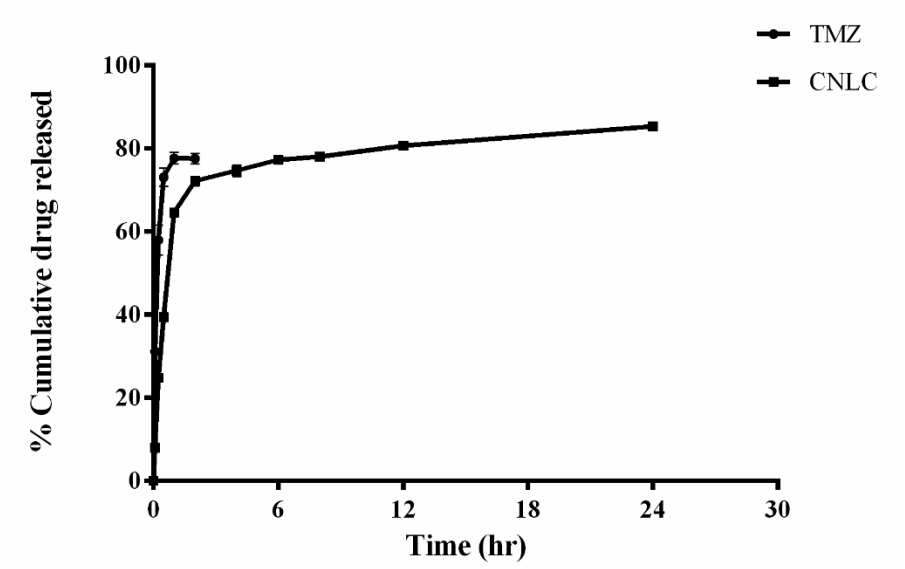

Fig. 5.11 In vitro drug release profile of pure temozolomide and optimized CNLC formulation in pH 5.0 acetate buffer. Each point represents mean ± SD of three observations

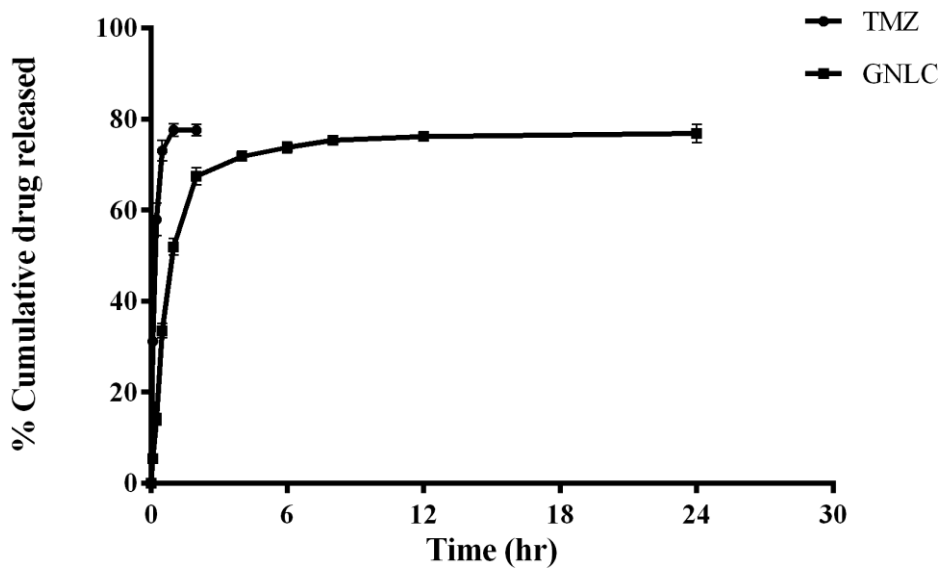

Fig. 5.12 In vitro drug release profile of pure temozolomide and optimized GNLC formulation in pH 5.0 acetate buffer. Each point represents mean ± SD of three observations

high. Generally, MSC value of more than two to three indicates a good fit. The various models and their results for R^2, AIC and MSC are presented in table 5.13. From regression analysis, drug release from the NLC was most appropriately described by Korsmeyer-Peppas model. Also, known as power law, this model has been frequently used to describe the release kinetics of modified release formulations. The value of n as discussed earlier is used to differentiate between the various drug release mechanisms and is influenced by the nature and geometry of the drug delivery system. This model considers only the early portion of a release profile (F<60%). The values of n, release rate constant, k, and T_{50} values based on this model are presented in Table 5.14. The value of n<0.5 indicate that the release from the nanoparticles follows Fickian diffusion [40].

5.3.7. Thermal Studies

DSC thermograms of the NLC formulations are as shown in Figure 5.13. As represented in chapter 4, the DSC thermogram of TMZ shows an exothermic peak at around 210°C, which corresponds to its melting point. The exothermic peak was also observed in physical mixtures of the drug with the lipids. It is observed that the exothermic peak of TMZ no longer exists or is reduced to a great extent in the thermograms of NLC formulations indicating that TMZ

in the formulation might be in an amorphous form or dispersed within the lipid at a molecular level. Similar reports of loss of crystallinity have been reported in literature for lipid nanoparticles. In DSC thermograms of NLC, additional peak observed at 169.5°C was of mannitol (used as cryoprotectant).

5.3.8. XRD Studies

The XRD study was carried out to support the DSC data to verify the reduction in crystalline nature of TMZ in the NLC formulations. The XRD spectrum of pure temozolomide in Fig. 5.13a showed distinct and intense peaks at 2θ scale indicating the crystalline nature of the drug. In contrast, there was a considerable reduction in the intensity of all peaks in the NLC formulations (Fig. 5.13 b-d). Therefore, it can be concluded that TMZ is present in amorphous state in the optimized NLC formulations.

5.3.9. Stability Studies

The results of 1 and 6 months stability studies are shown in Table 5.15. It was observed that nanoparticle batches in dispersion state showed minimal aggregation at both ambient and refrigerated storage conditions. However, after 1 month, a significant decrease in drug content was observed along with microbial growth in the samples stored at ambient temperature. In refrigerated samples, although the drug content did not undergo a significant change, microbial growth was observed at around 2 months.

In freeze dried state, there was no significant change in the characteristics of the nanoparticles at refrigerated conditions, whereas increase in particle size and decrease in drug content was observed in the samples kept at ambient temperature. Based on the stability data it is recommended to store the formulations at refrigerated conditions. Further, if the NLC formulation needs to be stored in the dispersed state, a suitable preservative should be added to the formulations to prevent any microbial growth during storage [11].

5.4.1. In Vitro Cytotoxicity Study

MTT assay is one of the widely used methods to assess the potency of cytotoxic drugs. It is an in vitro colorimetric test that is used to measure cell proliferation rate and conversely the reduced cell viability as a result of metabolic changes due to apoptosis or cell death. The MTT assay is based on the reduction of MTT (yellow colored), which depends on cellular

Table 5.13. Results of release model selection criteria for NLC formulations

Model	PNLC			CNLC			GNLC		
	R^2	AIC	MSC	R^2	AIC	MSC	R^2	AIC	MSC
Zero Order	-0.5505	107.2247	-0.9350	-0.7901	109.4402	-1.1349	-0.5466	107.4874	-0.9202
First order	0.6543	90.7167	0.5657	0.7695	86.8908	0.9150	0.7264	88.4340	0.8119
Higuchi	0.4881	95.0344	0.1732	0.3977	97.4583	-0.0457	0.5004	95.0582	0.2097
Hixon-Crowell	0.3978	96.8214	0.0107	0.3300	98.6300	-0.1522	0.4698	95.7103	0.1504
Baker-Lonsdale	0.7730	86.0901	0.9863	0.7260	88.7965	0.7418	0.8013	84.9142	1.1319
Makoid-Banakar	0.9060	80.3962	1.5039	0.9305	77.7105	1.7496	0.9431	75.1564	2.0190
Korsmeyer-Peppas	0.9519	73.0119	2.1752	0.9672	69.4654	2.5033	0.9612	70.9340	2.4028

Table 5.14. Mathematical parameters of the selected model for the in vitro release data of NLC formulations

Model	PNLC				CNLC				GNLC			
	n	k_{KP}	$T_{50\%}$	$T_{90\%}$	n	k_{KP}	$T_{50\%}$	$T_{90\%}$	n	k_{KP}	$T_{50\%}$	$T_{90\%}$
Korsmeyer-Peppas	0.136	54.939	0.750	38.154	0.121	60.954	0.445	25.098	0.148	53.796	0.860	32.491

Table 5.15. Stability study results for freeze dried optimized temozolomide loaded NLC formulations stored at various conditions

Formulation	Initial		1 month				6 month			
			25 ± 2°C		5 ± 3°C		25 ± 2°C		5 ± 3°C	
	Size ± SD (nm)	DL ± SD (%w/w)	Size ± SD (nm)	DL ± SD (%w/w)	Size ± SD (nm)	DL ± SD (%w/w)	Size ± SD (nm)	DL ± SD (%w/w)	Size ± SD (nm)	DL ± SD (%w/w)
PNLC	167.30 ± 4.15	8.15 ± 0.54	165.61± 2.20	7.95 ± 0.42	172.16 ± 3.56	8.18 ± 0.35	188.65 ± 4.76	6.79 ± 0.31	175.10 ± 3.21	7.83 ± 0.66
GNLC	174.15 ± 4.76	7.75 ± 0.65	186.26 ± 3.54	7.59 ± 0.19	178.35 ± 5.05	7.78 ± 0.23	191.15 ± 3.25	6.61 ± 0.46	180.54 ± 3.80	7.50 ± 0.33
CNLC	229.24 ± 8.76	5.01 ± 0.46	238.37 ± 4.36	4.69 ± 0.27	232.57 ± 5.90	5.07 ± 0.25	256.11 ± 4.76	4.25 ± 0.25	237. 63 ± 3.25	4.77 ± 0.25

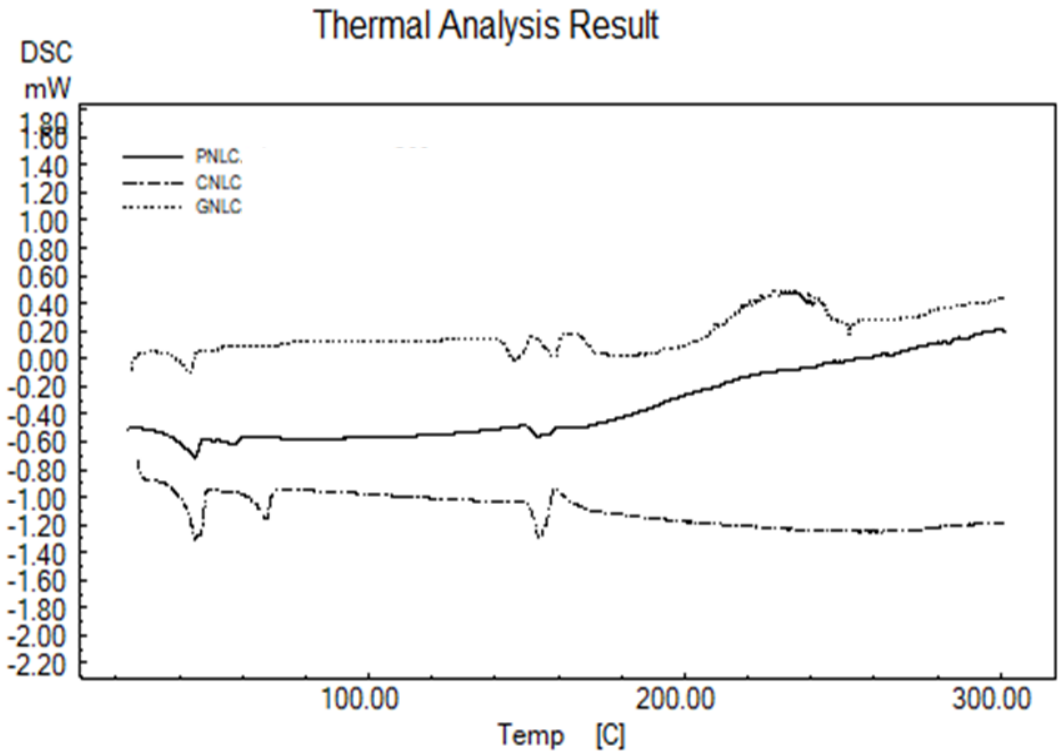

Fig. 5.13. DSC thermogram of NLC formulations

metabolic activities due to NAD(P)H-dependent cellular oxidoreductase enzymes to insoluble formazan. The rapidly growing and metabolically active cells exhibit high rates of MTT reduction to formazan while the dead or inactive cells fail to do so. Formazan formed is a purple colored compound that is dissolved by using DMSO with characteristic absorption at 570 nm. The intensity of purple color is directly proportional to the enzymatic activity of cells and therefore the cell viability. Reduced intensity of purple color of formazan indicates reduced cell number and therefore the cytotoxic potential of the substance under study [41].

The results of the MTT study are presented in Figure 5.15. The IC_{50} values determined for TMZ and the NLC formulations are presented in Table 5.16. Significantly less reduction in cell viability was observed for blank NLCs, with lipid and surfactant composition equivalent to the highest dose of the respective TMZ formulations, depicting the safety of the lipids and other excipients used in formulating nanoparticles. The effect on cell viability was observed to be dose dependent. Significant and consistent reduction in cell viability was observed as the dose of pure TMZ increased from 50 to 400 $\mu g.mL^{-1}$. However, for NLC formulations

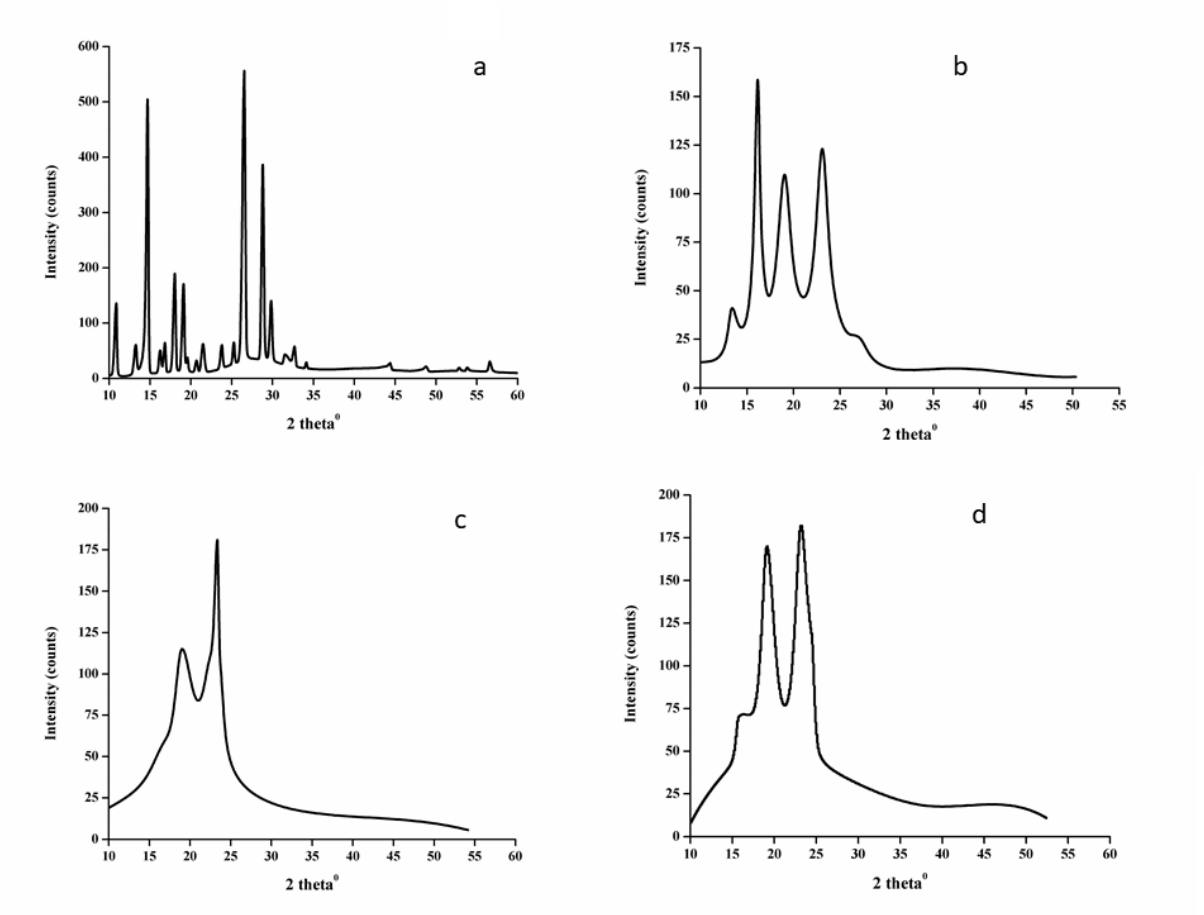

Fig. 5.14. X-ray diffraction patterns of a) Temozolomide, b) PNLC, c) CNLC, and d) GNLC formulations

there was a massive reduction in cell viability as the dose increased from 50 to 100 µg.mL^{-1} and no significant change was observed at 200 and 400 µg.mL^{-1} concentrations because only a small population of viable cells was remaining. The nanoparticulate TMZ showed increased cytotoxicity and significantly reduced IC_{50} values compared to pure TMZ. This is probably because of the sustained release properties of nanoparticles and also due to the "nano size" effect the cell uptake and internalization is increased which increases the cytotoxicity. [42,43]. The cell uptake of nanoparticles is dependent on various factors such as size, shape, charge and hydrophobicity. The hydrophobicity plays an important role as it determines the interaction of the nanoparticles with the cell membranes with more hydrophobic particles having greater interaction with the cell membranes. As PNLC and CNLC are more hydrophobic as compared to GNLC, their cell uptake may be more leading

to increased cytotoxicity and reduced IC_{50}. The enhanced efficacy may also be due to enhanced permeability across the endothelial cells by overcoming P-gp efflux [44-46].

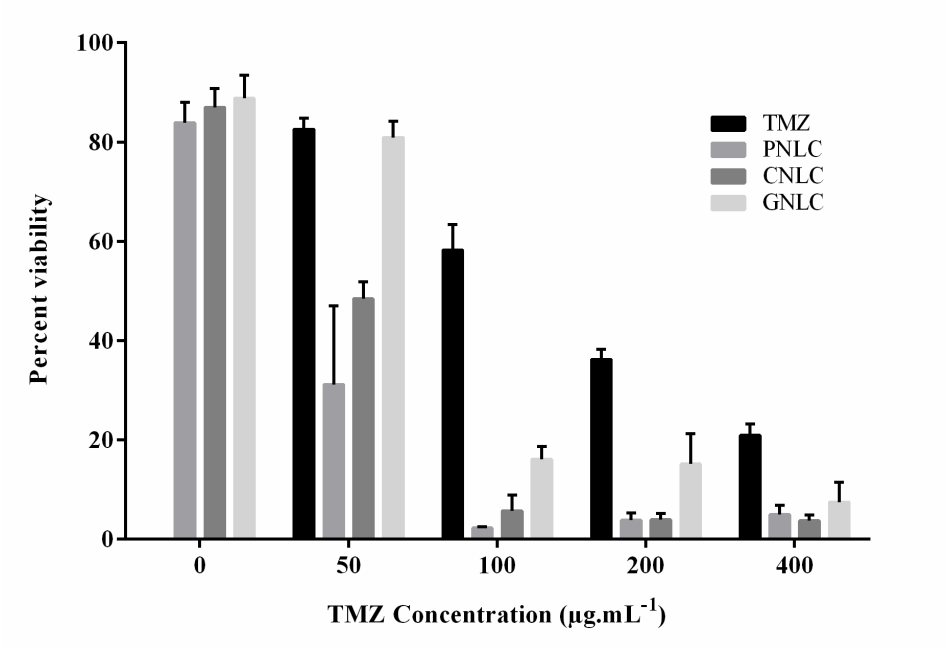

Fig. 5.15. In vitro assessment of cytotoxicity of blank NLC, pure TMZ and TMZ loaded NLC in U-87 MG glioma cells by MTT assay

Table 5.16. IC_{50} values of pure TMZ and NLC formulations in U-87 MG glioma cell line

Formulation	**IC50 (µg. mL^{-1}) ± SEM**
Pure TMZ	108.60 ± 2.65
PNLC	45.92 ± 3.89
CNLC	50.12 ± 1.30
GNLC	71.30 ± 1.69

Conclusions

Temozolomide nanoparticles were successfully fabricated as polymeric nanoparticles using PCL as the polymer, as SLN using stearic acid as the lipid and as nanostructured lipid carriers using glyceryl monostearate, Precirol and Compritol as the solid lipid and oleic acid as the liquid lipid. However, the polymeric nanoparticles and SLN formulation were not further investigated because of poor entrapment of TMZ in the fabricated nanoparticles. The NLC

formulations produced nanoparticles below < 250 nm and had narrow size distribution with good encapsulation efficiency and extended release. The influence of various formulation variables such as drug-to-lipid ratio, solid lipid-to-oil ratio and surfactant concentration on nanoparticle characteristics i.e. particle size, entrapment efficiency and drug loading were studied in detail using DoE. SEM images revealed that the particles were anisometric in shape and with irregular surface. The NLC formulations extended the release of TMZ for 24 hours as observed in the in vitro release studies. Further, as the particles are anisometric, as revealed by SEM, it considerably increases the surface area in addition to shorter diffusion pathways as compared to spherical particles. The freeze dried particles showed good redispersibility and stability during storage under refrigerated conditions. The NLC formulations had enhanced cytotoxicity and low IC_{50} values as compared to the pure TMZ which further enhances the efficiency of the formulations for treatment of brain tumors. To establish the suitability of the NLC formulations as a potential carrier system for better delivery of TMZ, the optimized formulations were taken further for pharmacokinetic and biodistribution studies.

References

1 Chen, Y. et al. (2004) Drug delivery across the blood-brain barrier. *Current Drug Delivery* 1(4) 361-376

2 Joseph, E. and Saha, R.N. (2013) Advances in brain targeted drug delivery: nanoparticulate systems. *Journal of PharmaSciTech* 3 (1), 1-8

3 Huang, G. et al. (2008) Solid lipid nanoparticles of temozolomide: Potential reduction of cardial and nephric toxicity. *International Journal of Pharmaceutics* 355 (1), 314-320

4 Payne, M.J. et al. (2005) Temozolomide in the treatment of solid tumours: current results and rationale for dosing/scheduling. *Critical Reviews in Oncology/Hematology* 53 (3), 241-252

5 Lee, C.Y. and Ooi, I.H. (2016) Preparation of temozolomide-loaded nanoparticles for glioblastoma multiforme targeting—ideal versus reality. *Pharmaceuticals* 9 (3), pii: E54

6 Galindo-Rodriguez, S. et al. (2004) Physicochemical parameters associated with nanoparticle formation in the salting-out, emulsification-diffusion, and nanoprecipitation methods. *Pharmaceutical Research* 21 (8), 1428-1439

7 Zili, Z. et al. (2005) Preparation and characterization of poly-ε-caprolactone nanoparticles containing griseofulvin. *International Journal of Pharmaceutics* 294 (1), 261-267

8 Gallarate, M. et al. (2009) Preparation of solid lipid nanoparticles from W/O/W emulsions: Preliminary studies on insulin encapsulation. *Journal of Microencapsulation* 26 (5), 394-402

9 Rosca, I.D. et al. (2004) Microparticle formation and its mechanism in single and double emulsion solvent evaporation. *Journal of Controlled Release* 99 (2), 271-280

10 Naseri, N. et al. (2015) Solid lipid nanoparticles and nanostructured lipid carriers: structure, preparation and application. *Advanced Pharmaceutical Bulletin* 5 (3), 305-313

11 Khosa, A. et al. (2018) Nanostructured lipid carriers for site-specific drug delivery. *Biomedicine & Pharmacotherapy* 103, 598-613

12 Shen, J. and Burgess, D.J. (2013) In vitro dissolution testing strategies for nanoparticulate drug delivery systems: recent developments and challenges. *Drug Delivery and Translational Research* 3 (5), 409-415

13 Costa, P. and Sousa Lobo, J.M. (2001) Modeling and comparison of dissolution profiles. *European Journal of Pharmaceutical Sciences* 13 (2), 123-133

14 Zhang, Y. et al. (2010) DDSolver: an add-in program for modeling and comparison of drug dissolution profiles. *The AAPS Journal* 12 (3), 263-271

15 Rao, J.P. and Geckeler, K.E. (2011) Polymer nanoparticles: Preparation techniques and size-control parameters. *Progress in Polymer Science* 36 (7), 887-913

16 Vivek, K. et al. (2007) Investigations of the effect of the lipid matrix on drug entrapment, in vitro release, and physical stability of olanzapine-loaded solid lipid nanoparticles. *AAPS PharmSciTech* 8 (4), 16-24

17 Souto, E.B. et al. (2006) Polymorphic behaviour of Compritol®888 ATO as bulk lipid and as SLN and NLC. *Journal of Microencapsulation* 23 (4), 417-433

18 Wang, F.C. et al. (2016) Phase diagram of glycerol monostearate and sodium stearoyl lactylate. *Crystal Growth & Design* 16 (1), 297-306

19 Severino, P. et al. (2011) Polymorphism, crystallinity and hydrophilic–lipophilic balance of stearic acid and stearic acid–capric/caprylic triglyceride matrices for production of stable nanoparticles. *Colloids and Surfaces B: Biointerfaces* 86 (1), 125-130

20 Meng, F.T. et al. (2003) W/O/W double emulsion technique using ethyl acetate as organic solvent: effects of its diffusion rate on the characteristics of microparticles. *Journal of Controlled Release* 91 (3), 407-416

21 Cohen-Sela, E. et al. (2009) A new double emulsion solvent diffusion technique for encapsulating hydrophilic molecules in PLGA nanoparticles. *Journal of Controlled Release* 133 (2), 90-95

22 Üner, M. (2016) Characterization and Imaging of Solid Lipid Nanoparticles and Nanostructured Lipid Carriers. In *Handbook of Nanoparticles* (Aliofkhazraei, M., ed.), pp. 117-141, Springer International Publishing

23 Singh, B. et al. (2011) Developing oral drug delivery systems using formulation by design: vital precepts, retrospect and prospects. *Expert Opinion on Drug Delivery* 8 (10), 1341-1360

24 Ferreira, S.L.C. et al. (2007) Box-Behnken design: an alternative for the optimization of analytical methods. *Analytica Chimica Acta* 597 (2), 179-186

25 Ferreira, M. et al. (2015) Optimization of nanostructured lipid carriers loaded with methotrexate: A tool for inflammatory and cancer therapy. *International Journal of Pharmaceutics* 492 (1), 65-72

26 Dudhipala, N. and Janga, K.Y. (2017) Lipid nanoparticles of zaleplon for improved oral delivery by Box–Behnken design: optimization, in vitro and in vivo evaluation. *Drug development and industrial pharmacy* 43 (7), 1205-1214

27 Gupta, B. et al. (2016) Effects of formulation variables on the particle size and drug encapsulation of imatinib-loaded solid lipid nanoparticles. *AAPS PharmSciTech* 17 (3), 652-662

28 Azhar Shekoufeh Bahari, L. and Hamishehkar, H. (2016) The impact of variables on particle size of solid lipid nanoparticles and nanostructured lipid carriers; A Comparative Literature Review. *Advanced Pharmaceutical Bulletin* 6 (2), 143-151

29 Sharma, N. et al. (2016) Effect of process and formulation variables on the preparation of parenteral paclitaxel-loaded biodegradable polymeric nanoparticles: A co-surfactant study. *Asian Journal of Pharmaceutical Sciences* 11 (3), 404-416

30 Cooper, D.L. and Harirforoosh, S. (2014) Effect of formulation variables on preparation of celecoxib loaded polylactide-co-glycolide nanoparticles. *PLoS ONE* 9 (12), e113558

31 Gulec, M. et al. (2012) Nephrotoxic effects of chronically administered olanzapine and risperidone in male rats. *Klinik Psikofarmakoloji Bülteni-Bulletin of Clinical Psychopharmacology* 22 (2), 139-147

32 Simeon, K.A.a.U.E.a.E.O.A. (2015) The effect of formulation variables on drug loading of antitubercular drugs in nanoparticle formulations. *Materials Research Express* 2 (9), 095403

33 Selvamuthukumar, S. and Velmurugan, R. (2012) Nanostructured Lipid Carriers: A potential drug carrier for cancer chemotherapy. *Lipids in Health and Disease* 11, 159-159

34 Jores, K. et al. (2004) Investigations on the structure of solid lipid nanoparticles (SLN) and oil-loaded solid lipid nanoparticles by photon correlation spectroscopy, field-flow fractionation and transmission electron microscopy. *Journal of Controlled Release* 95 (2), 217-227

35 Tamjidi, F. et al. (2013) Nanostructured lipid carriers (NLC): A potential delivery system for bioactive food molecules. *Innovative Food Science & Emerging Technologies* 19 (Supplement C), 29-43

36 Moghimi, S.M. et al. (2012) Factors Controlling Nanoparticle Pharmacokinetics: An Integrated Analysis and Perspective. *Annual Review of Pharmacology and Toxicology* 52 (1), 481-503

37 Truong, N.P. et al. (2015) The importance of nanoparticle shape in cancer drug delivery. *Expert Opinion on Drug Delivery* 12 (1), 129-142

38 zur Mühlen, A. et al. (1998) Solid lipid nanoparticles (SLN) for controlled drug delivery – Drug release and release mechanism. *European Journal of Pharmaceutics and Biopharmaceutics* 45 (2), 149-155

39 Müller, R.H. et al. (2000) Solid lipid nanoparticles (SLN) for controlled drug delivery – a review of the state of the art. *European Journal of Pharmaceutics and Biopharmaceutics* 50 (1), 161-177

40 Zuo, J. et al. (2014) Evaluation of the DDSolver Software Applications. *BioMed Research International* 2014, 204925

41 Bahuguna, A. et al. (2017) MTT assay to evaluate the cytotoxic potential of a drug. *Bangladesh Journal of Pharmacology* 12 (2), 115-118

42 Ling, Y. et al. (2012) Temozolomide loaded PLGA-based superparamagnetic nanoparticles for magnetic resonance imaging and treatment of malignant glioma. *International Journal of Pharmaceutics* 430 (1–2), 266-275

43 Lewinski, N. et al. (2008) Cytotoxicity of Nanoparticles. *Small* 4 (1), 26-49

44 Tosi, G. et al. (2016) The "fate" of polymeric and lipid nanoparticles for brain delivery and targeting: Strategies and mechanism of blood–brain barrier crossing and trafficking into the central nervous system. *Journal of Drug Delivery Science and Technology* 32 (Part B), 66-76

45 Samadi Moghaddam, M. et al. (2015) Enhanced cellular uptake of nanoparticles by increasing the hydrophobicity of poly(lactic acid) through copolymerization with cell-membrane-lipid components. *Chemical Communications* 51 (78), 14605-14608

46 Fröhlich, E. (2012) The role of surface charge in cellular uptake and cytotoxicity of medical nanoparticles. *International Journal of Nanomedicine* 7, 5577-5591

6. Pharmacokinetics and Biodistribution Studies

6.1. Introduction

The most important aspect to be considered after development of a delivery system is to evaluate its therapeutic efficacy, safety, its potential to deliver the therapeutic agent preferentially to the target site and to establish the dosage regimen. Pharmacokinetics plays a critical role in the drug development process as it provides information on the absorption, distribution, metabolism and elimination of the drugs in man and animals which have an influence on the efficacy, safety and targeting potential of the drug. Preclinical studies on animals can help in identifying a lead compound, selection of the best formulation, determination of the route, frequency and duration of exposure in addition to determining the starting dose for phase I clinical trials in humans [1-3]. The better therapeutic efficacy of nanoparticulate delivery systems for anticancer therapeutics and other drugs is because of the altered pharmacokinetics in blood as well as the target site such as a solid tumor or a target organ. Pharmacokinetic profile of novel delivery systems can indicate possibility of achieving better therapeutic efficacy. Thus pharmacokinetics and biodistribution studies of designed novel delivery systems is essential. The biological performance of a nanocarrier is dependent on a number particle characteristics such as the particle size and its distribution, its morphology, shape, surface potential and surface chemistry [4]. To estimate the alteration in the in vivo behavior of nanoparticulate systems and to evaluate their safety and efficacy, pharmacokinetic studies are performed in animal models. The pharmacokinetic and biodistribution studies have been performed for various nanocarriers and a significant change in the pharmacokinetic parameters and distribution to various organs has been reported [5-7]. In the present study nanostructured lipid carrier (NLC) delivery systems of temozolomide (TMZ) have been developed with the objective to enhance its delivery to the brain. The concentration of TMZ in plasma and organs was determined after intraperitoneal administration of pure TMZ and NLC formulations in a rat model. The pharmacokinetic parameters and biodistribution of the NLC formulations were determined and compared to that of the drug so as to evaluate the effect of the nanoformulation on the pharmacokinetics and distribution to the target organ i.e. brain besides other organs.

6.2. Experimental

6.2.1. Materials and Equipment

Drug, formulation excipients and chemicals were obtained from same sources as mentioned in Chapter 3. Ketamine and xylazine used as anesthetic agents were procured from Sigma Aldrich Corporation, India. All surgical instruments like scissors, forceps and syringes used sterilized before use. A high speed homogenizer (Kinematica Polytron® PT1600E, USA) was used for the preparation of tissue homogenates. Selective optimized formulations (PNLC, CNLC and GNLC) as discussed in chapter 5 were used for these studies and compared with pure TMZ solution by intravenous (i.v) and intraperitoneal (i.p) route.

6.2.2. Animals

Healthy male Wistar rats were selected for pharmacokinetic and biodistribution studies of pure TMZ and TMZ loaded NLC formulations. Rats with average weight of 275 ± 25 g (12-15 weeks old) were issued from Central Animal Facility (CAF), BITS, Pilani (Reg. No. 417/01/a/CPCSEA) after procurement from Chaudhary Charan Singh Agricultural University, Hisar, India. Animals were kept in standard plastic cages maintained under controlled conditions (23 ± 2°C, 60 ± 5% RH and 12h dark-light cycle) and provided standard laboratory pellet food with water ad libitum. Rats were acclimatized to the study environment for at least five days before commencing the study. All experimental protocols were approved by the Institutional Animal Ethics Committee (IAEC) prior to the commencement of work (Protocol No. IAEC/RES/23/07). All experimental procedures including euthanasia and disposal of carcass were in accordance with the guidelines set by the Institute, IAEC and the Committee for the Purpose of Control and Supervision of Experiments on Animals (CPCSEA), India. All animals were kept under observation during the entire study for any unusual signs, general conditions, potential clinical signs, toxicity or mortality.

6.2.3. In Vivo Pharmacokinetics and Biodistribution Studies

Pharmacokinetic studies were carried out after single dose administration of pure TMZ by intravenous (i.v) and intraperitoneal (i.p) route and the NLC formulations by i.p route. The concentration of TMZ was determined in plasma and specific organs namely brain, spleen,

heart, lungs, kidneys and liver for determination of pharmacokinetic parameters and biodistribution profile of TMZ and the NLC formulations. All the procedures were followed according to the standard protocol.

The animals were randomly selected in groups of three and each time point for pharmacokinetics studies n=6 and for biodistribution studies n=4 was taken. Prior to the commencement of the study the animals were fasted overnight (12-15h) with water given ad libitum. The animals were marked, weighed and dosed as per their body weight. The pure drug was first dissolved in 100 µL DMSO and then diluted and dissolved in sterile water for injection. The NLC formulations were dispersed in sterile water for injection. A dose equivalent to 10 $mg.kg^{-1}$ was administered in the tail vein for i.v administration of pure TMZ and in the lower right quadrant of the abdomen for i.p administration of pure TMZ and NLC formulations. All the solutions and dispersions were prepared fresh and used immediately without any additional treatments.

Blood samples (0.5mL) at each sampling point were withdrawn from the retro orbital sinus at 0.25, 0.5, 1, 2, 4, 8, 10, 12 and 18h for i.v route group and 0.08, 0.25, 0.5, 1, 2, 4, 8, 10, 12 and 18h for the i.p groups. Blood samples were collected in pre-chilled 2mL microcentrifuge tubes containing 10% EDTA as anticoagulant and mixed well. The samples were centrifuged at 8000 rpm for 30 minutes at 4°C. The supernatant was collected, immediately acidified with 1M formic acid, labeled and stored in -20°C till further analysis. In i.p dosing, after collection of blood at 0.5, 1, 2, 4 and 8h, the animals were sacrificed and their tissues (brain, spleen, heart, lungs, kidneys and liver) were collected and processed for tissue homogenates as described in section 3.6.2. The sample analysis by HPLC was carried out within 7 days of sample collection using the extraction procedure and the validated bioanalytical method described in chapter 3.

6.2.4. Pharmacokinetic and Biodistribution Data Analysis

The data of drug concentration in plasma and various tissues such as brain, liver, lungs, kidney, spleen and heart at different time intervals were analyzed by the non-compartmental analysis method using WinNonlin® ver. 2.1 (Pharsight Corporation, USA) software. Data was expressed as mean ± SD. Pharmacokinetic parameters such as C_{max}, AUC $_{0\text{-}inf}$, MRT, V_d, and Cl were determined. Finally the results were compared by one way

ANOVA using GraphPad Prism® software ver. 6.01 taking $p < 0.05$ as the level of significance.

6.3. Results and Discussion

The i.p route of administration was selected for the comparative study of pharmacokinetics and biodistribution of TMZ formulations mainly as i.p route of administration is the very commonly used route for animal studies because of the challenges in intravenous administration and also larger volumes can be administered if required [8]. Specifically, in case of TMZ, the route of administration is not of significant consideration because the drug is 100% bioavailable by i.p route [9] and studies have shown that intraperitoneal delivery had the largest effect on tumor volume as compared to other routes [10] and in mice with intracranial xenografts, it increased median survival times 1.7 to 13.9 fold [11].

6.3.1. Plasma Pharmacokinetics

The plasma concentrations-time profiles of TMZ after single dose i.v and i.p administration of pure temozolomide and that of three selected NLC formulations (PNLC, CNLC and GNLC) after i.p administration are presented in Figure 6.1. The pharmacokinetic parameters calculated are presented in Table 6.1. The pharmacokinetic profile of i.v route TMZ solution showed a rapid distribution into the tissues resulting in a decrease in the concentration of TMZ in plasma with detectable concentration of TMZ up to 8h only. The profile for i.p route showed rapid but low absorption with attainment of t_{max} at 1h followed by decline with detectable concentration of TMZ up to 10h.

The $AUC_{0\text{-}inf}$ of TMZ solution by i.v and i.p route was 17.58 ± 4.23 and 18.37 ± 2.30 respectively indicating that bioavailability by i.p route is equivalent to that of i.v route. The MRT of TMZ (i.p) is significantly higher than TMZ (i.v) (2.77h against 1.66 h) indicating that the residence time of molecule is more in the body. This may be due to the fact that unlike i.v route, the drug is not instantly available in the vasculature by i.p route but is dependent on the absorption rate from the site of injection resulting in higher MRT value and the extension of detectable plasma concentration from 8h to 10h, as observed in the pharmacokinetic profile of TMZ administered by i.v and i.p route respectively. Further, in i.v route full amount of drug is immediately exposed to metabolism and elimination process thus reducing concentration and MRT.

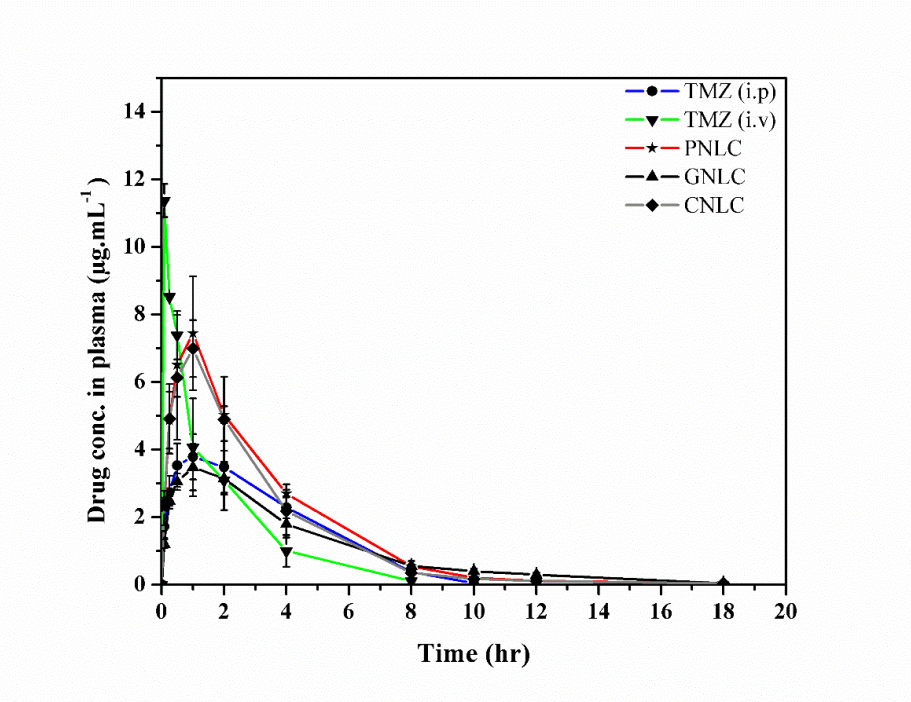

Fig. 6.1. Plasma concentration vs time profile of temozolomide after i.v administration and i.p administration of temozolomide and NLC formulations.

Table 6.1. Summary of pharmacokinetic parameters of TMZ after i.v administration and i.p administration of pure drug and NLC formulations

Parameters	TMZ (i.v)	TMZ (i.p)	PNLC	GNLC	CNLC
t_{max} (h)	-	1.0	1.0	1.0	1.0
C_{max} (µg.mL^{-1})	-	3.79 ± 0.67	7.44 ± 1.69	3.48 ± 0.69	6.99 ± 0.84
AUC $_{0\text{-inf}}$ (µg.h.mL^{-1})	17.58 ± 4.23	18.37 ± 2.30	27.68 ± 3.07	18.49 ± 2.95	24.81 ± 6.91
V_d (L.kg^{-1})	0.98 ± 0.28	1.09 ± 0.47	1.29 ± 0.31	2.14 ± 0.31	1.62 ± 0.77
Cl (L.h^{-1}.kg^{-1})	0.586 ± 0.14	0.55± 0.07	0.36 ± 0.04	0.55 ± 0.08	0.42 ± 0.12
AUMC (µg.h^2.mL^{-1})	29.623 ± 9.99	52.464 ± 1.71	81.864 ± 9.67	76.150 ± 12.46	69.070 ± 15.30
MRT (h)	1.66 ± 0.17	2 .77** ± 0.17	2.96 ± 0.02	4.11* ± 0.35	2.75 ± 0.25

All values are expressed as mean ± SD (n=3). *P<0.05 as compared to pure TMZ (i.p) using one way ANOVA followed by Tukey's multiple comparisons test. ** P<0.05 Comparison of TMZ (i.v) and TMZ (i.p) by t-test.

As compared to the TMZ solution, the pharmacokinetic parameters of NLC formulations showed an increase in the $AUC_{0\text{-inf}}$ of 27.68 ± 3.07 and 24.81 ± 6.91 µg.h.mL^{-1} for PNLC

and CNLC formulations respectively whereas for GNLC the $AUC_{0\text{-}inf}$ (18.49 ± 2.95) was comparable to that of pure TMZ solution. This may be because the V_d of GNLC (2.14 ± 0.31 $L.kg^{-1}$) is much higher than that of PNLC (1.29 ± 0.31 $L.kg^{-1}$) and CNLC (1.62 ± 0.77 $L.kg^{-1}$) formulations indicating higher distribution into the extravascular tissues, thereby lesser concentration in the plasma. The MRT of the NLC formulations especially of GNLC was higher than the TMZ solution which probably confirms more distribution to other tissues/ organs with higher V_d and MRT. MRT is the average time a molecule spends in the body after absorption. In case of the PNLC and CNLC formulation absorption is faster compared to GNLC as is indicated by the C_{max} of 7.44 ± 1.69, 6.99 ± 0.84 and 3.48 ± 0.69 respectively though t_{max} remained the same. Thus, their elimination rate will be faster as most drugs follow first order kinetics according to which the rate of elimination is dependent on the concentration, explaining their lesser MRT compared to GNLC. Also, MRT might be affected by the release rate from the NLC carrier, the degradation rate of TMZ at physiological pH in addition to presence of poloxamer 188 on surface of the nanoparticles which help it to evade the RES. Similar observations have been reported earlier [12,13]

6.3.2. Tissue Distribution Studies

The biodistribution was studied in various organs such as brain, spleen, heart, lungs, kidneys and liver in rats after administration of single dose of 10 $mg.kg^{-1}$ TMZ solution and NLC formulations by i.p route. The $AUC_{0\text{-}inf}$ and C_{max} of TMZ in various organs studied has been depicted in Fig. 6.2.

6.3.2.1. Brain Biodistribution Studies

The concentration of TMZ in rat brain after administration of TMZ solution and PNLC, CNLC and GNLC formulations was determined at 0.5, 1, 2, 4 and 8h and presented as a function of time in Figure 6.3. The various pharmacokinetic parameters calculated are presented in Table 6.2.

The biodistribution studies of TMZ solution showed relatively slow and low permeability of TMZ into the brain with C_{max} of 14.14 ± 1.36 $\mu g.g^{-1}$ at 0.88 ± 0.22h (t_{max}) post dosing and an $AUC_{0\text{-}inf}$ of 47.11 ± 1.33 $\mu g.h.g^{-1}$. Compared to this all the NLC formulations showed a significantly high C_{max} of 19.09 ± 0.51, 25.26 ± 1.62 and 25.72 ± 0.70 $\mu g.g^{-1}$ and $AUC_{0\text{-}inf}$

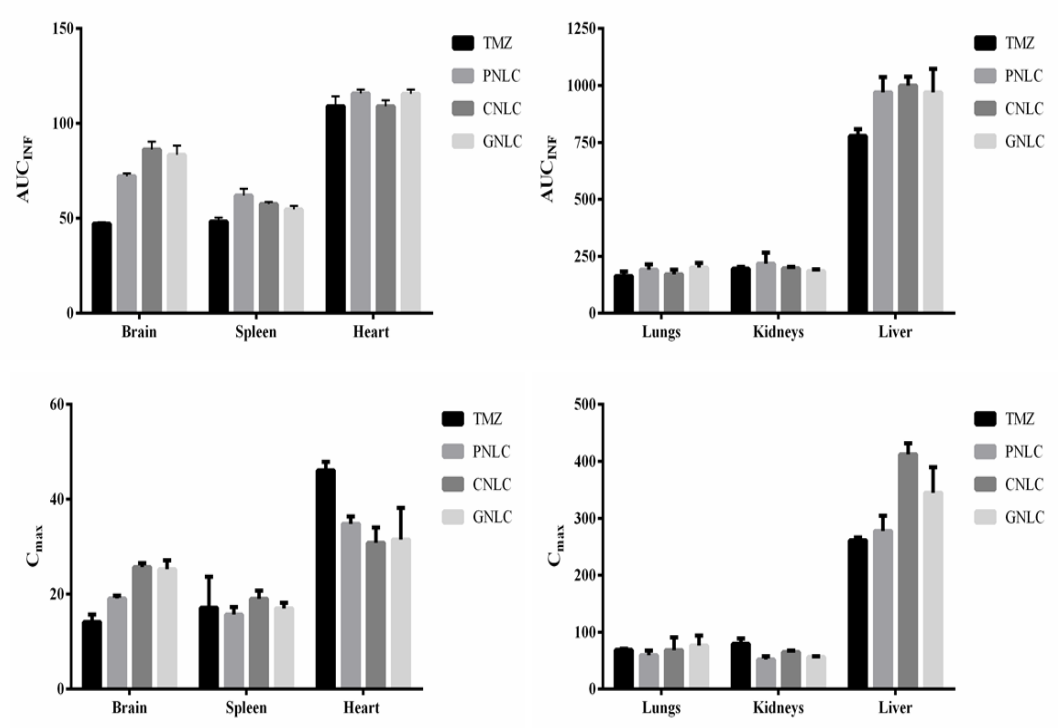

Fig. 6.2. $AUC_{0\text{-}inf}$ and C_{max} of TMZ in various organs after single dose i.p administration of TMZ solution and NLC formulations.

of 72.25 ± 2.45, 83.42 ± 8.38 and 86.36 ± 6.88 μg.h.g^{-1} for PNLC, GNLC and CNLC formulations respectively at 0.75 and 1h respectively. An increase in MRT was also observed for all the formulations. The increase in C_{max}, $AUC_{0\text{-}inf}$ along with high MRT indicates enhanced permeation and residence time of TMZ in the brain. This may be because of the particle size of the formulations at around 200 nm and steric hindrance due to surfactants such as poloxamer 188 increases the circulation time by escaping the reticuloendothelial system and thereby increases the contact time between the blood brain barrier (BBB) capillaries and the nanoparticles resulting in enhanced permeability [14,15].

Further, the TMZ is capable of crossing the BBB but at physiological pH it gets undergoes conversion to MTIC, which due to hydrophilic nature cannot permeate the BBB. TMZ loaded in nanoparticles protects the drug from conversion thereby making more of the drug available for permeation through the BBB [9]. Various other mechanisms have been suggested for enhanced delivery of nanocarriers across the BBB, which include increased

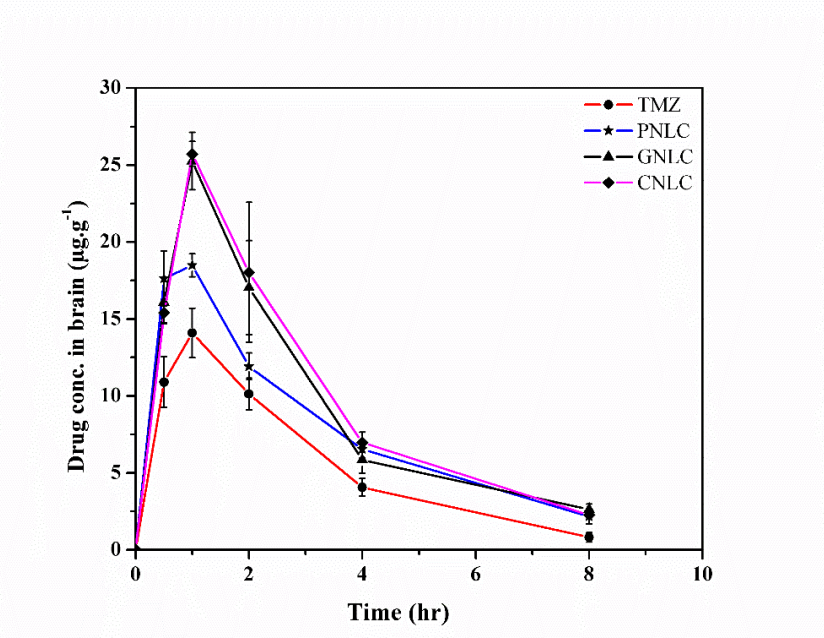

Fig. 6.3. Biodistribution profile of TMZ in the brain following administration of a single dose of TMZ solution and NLC formulations by i.p route

retention of the nanoformulations due to adsorption on the capillary walls of the blood brain barrier, opening of the tight junctions of the BBB endothelial cells, membrane fluidization of the endothelial cell membrane lipids due to surfactant effect of nanoparticulate systems, inhibition of the efflux transporters and transcytosis of nanoparticles through the endothelium [16-18]. The results indicated that all the NLC formulations have successfully enhanced the permeability of temozolomide to the brain. The formulations showed an increase of 35-82% in C_{max} and 53.3-83.3% in AUC on an average indicating that the objective of the work i.e. enhancing delivery of TMZ to the brain was successfully achieved.

6.3.2.2. Spleen Biodistribution Studies

The biodistribution profile of TMZ in spleen after administration of single oral dose of TMZ solution and NLC formulations by i.p route is given in Figure 6.4 and the calculated pharmacokinetic parameters are tabulated in Table 6.3. For TMZ solution a C_{max} of 17.15 ± 1.69 µg.g^{-1} was achieved in 0.88 ± 0.22h post dose and resulting in an $AUC_{0\text{-}inf}$ of 48.36 ± 3.54 µg.h.g^{-1} and MRT of 2.57 ± 0.19h. The C_{max} of all the three NLC formulations achieved was more or less similar to that of the TMZ solution. However, the $AUC_{0\text{-}inf}$ of PNLC (62.01± 6.26 µg.h.g^{-1}) and CNLC (57.53 ±1.98 µg.h.g^{-1}) were significantly higher than that

of TMZ solution whereas, although GNLC showed an increase in AUC $_{0\text{-inf}}$ (54.65 ± 3.35 µg.h.g^{-1}) it was not significantly high. The MRT was also comparatively higher for PNLC, CNLC and GNLC to the TMZ solution with the values of 4.65 ± 0.97, 3.38 ± 0.20 and 3.19 ± 0.28h respectively. The increase in AUC and MRT may be because of slow elimination of nanoparticles from the spleen. This may be due to splenic capture of nanoparticles in which particles larger than 200nm incapable of crossing the endothelial slit of splenic sinuses are filtered off and retained in the red pulp of the spleen where they are internalized by the red macrophages and destroyed slowly [19].

Table 6.2. Summary of pharmacokinetic parameters of TMZ in the brain following single dose i.p administration of TMZ solution and NLC formulations

Parameters	TMZ	PNLC	GNLC	CNLC
t_{max} (h)	0.88 ± 0.22	0.75± 0.25	1.0 ± 0.00	1.0 ± 0.00
C_{max} (µg.g^{-1})	14.14 ± 1.36	19.09 ± 0.51*	25.26 ± 1.62*	25.72 ± 0.70*
AUC $_{0\text{-inf}}$ (µg.h.g^{-1})	47.11 ± 1.33	72.25 ± 2.45*	83.42 ± 8.38*	86.36 ± 6.88*
MRT (h)	2.71 ± 0.24	3.55 ± 0.40*	3.30 ± 0.07*	3.17 ± 0.08

All values are expressed as mean ± SD (n=3). *P<0.05 as compared to pure TMZ (i.p) using one way ANOVA followed by Tukey's multiple comparisons test.

6.3.2.3. Heart Biodistribution Studies

The biodistribution profile of TMZ in the heart after administration of single oral dose of TMZ solution and NLC formulations by i.p route is given in Figure 6.5 and the pharmacokinetic parameters calculated by the software are tabulated in Table 6.4. TMZ solution showed a C_{max} of 46.06 ± 1.60 µg.g^{-1} at 1h post dose with an AUC $_{0\text{-inf}}$ of 109.08 ± 9.02 µg.h.g^{-1} and MRT value of 2.72 ± 0.13h. The C_{max} values of PNLC, GNLC and CNLC were 34.83 ± 1.33, 31.51± 5.79 and 30.84 ± 2.77 µg.g^{-1} at 1h post dosing with an $AUC_{0\text{-inf}}$ of 115.77 ± 3.69, 115.59 ± 3.88 and 108.98 ± 5.51 µg.h.g^{-1} respectively. The data shows that although there is a significant decrease in C_{max} of all the three formulations compared to TMZ solution, the change in $AUC_{0\text{-inf}}$ is not significant. This may be because of lesser elimination of TMZ in formulation as compared to the TMZ solution from heart due to the sustained release of the TMZ from the NLC which also increases the MRT. The MRT for PNLC, GNLC and CNLC is 3.15 ± 0.11, 3.77 ± 0.23 and 3.47 ± 0.10h respectively. The

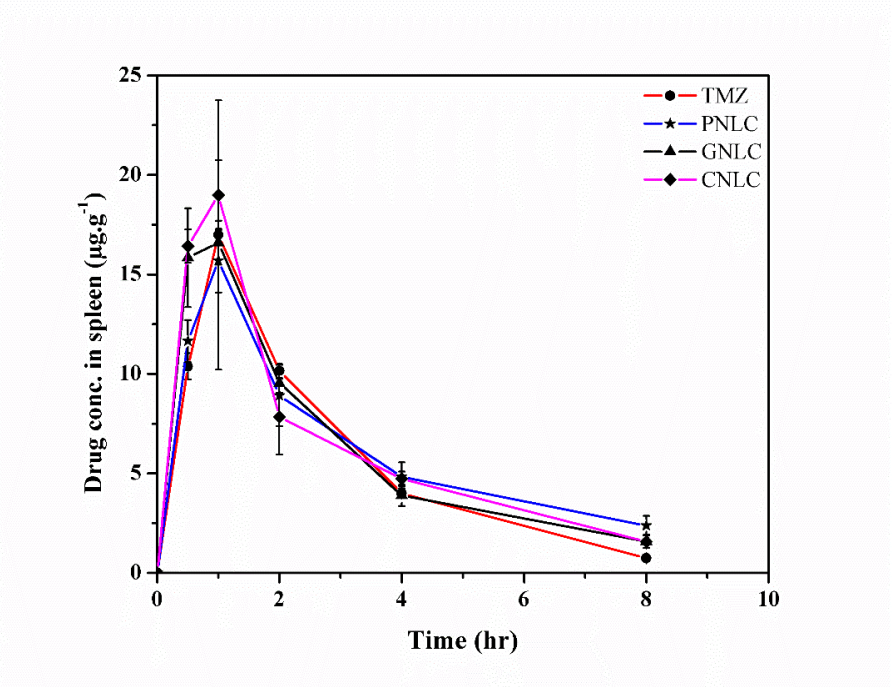

Fig. 6.4. Biodistribution profile of TMZ in the spleen following administration of a single dose of TMZ solution and NLC formulations by i.p route

Table 6.3. Summary of pharmacokinetic parameters of TMZ in the spleen following single dose i.p administration of TMZ solution and NLC formulations

Parameters	TMZ	PNLC	GNLC	CNLC
t_{max} (h)	0.88 ± 0.22	1.0± 0.00	0.88 ± 0.22	1.0± 0.00
C_{max} (µg.g^{-1})	17.15 ± 1.69	15.69 ± 1.39	17.01 ± 1.02	18.99 ± 1.53
AUC $_{0\text{-inf}}$ (µg.h.g^{-1})	48.36 ± 3.54	62.01 ± 6.26*	54.65 ± 3.35	57.53 ± 1.98*
MRT (h)	2.57 ± 0.19	4.65 ± 0.97*	3.19 ± 0.28	3.38 ± 0.20

All values are expressed as mean ± SD (n=3). *P<0.05 as compared to pure TMZ (i.p) using one way ANOVA followed by Tukey's multiple comparisons test.

significantly less concentration of TMZ in the heart for all the three NLC formulations indicate that as compared to the pure drug less of TMZ is distributed in the heart. This is of importance because cardiotoxicity is a known side effect of temozolomide [12] and these formulations might help in decreasing toxicity in the heart.

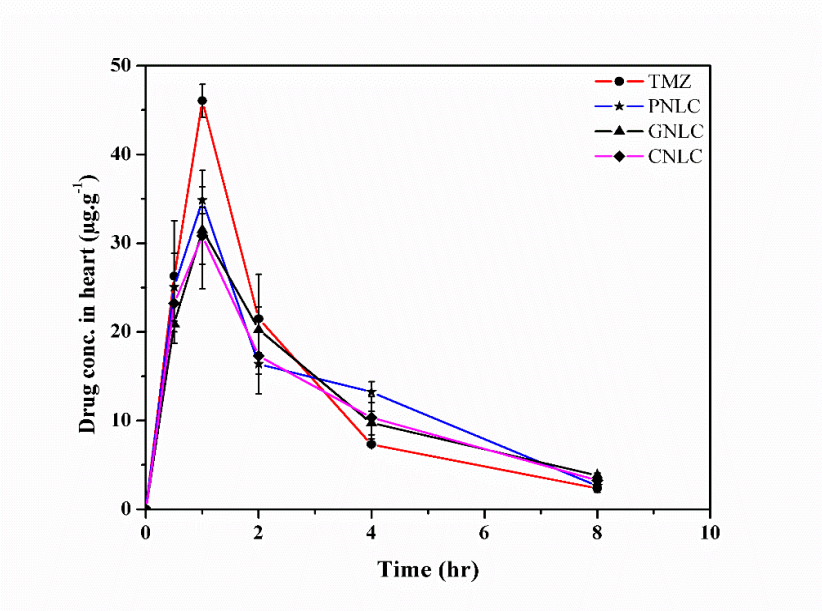

Fig. 6.5. Biodistribution profile of TMZ in the heart following administration of a single dose of TMZ solution and NLC formulations by i.p route

Table 6.4. Summary of pharmacokinetic parameters of TMZ in the heart following single dose i.p administration of TMZ solution and NLC formulations

Parameters	TMZ	PNLC	GNLC	CNLC
t_{max} (h)	1.0± 0.00	1.0± 0.00	1.0± 0.00	1.0± 0.00
C_{max} (µg g^{-1})	46.06 ± 1.60	34.83 ± 1.33**	31.51± 5.79*	30.84 ± 2.77*
AUC $_{0\text{-inf}}$ (µg.h.g^{-1})	109.08 ± 9.02	115.77 ± 3.69	115.59 ± 3.88	108.98 ± 5.51
MRT (h)	2.72 ± 0.13	3.15 ± 0.11*	3.77 ± 0.23*	3.47 ± 0.10*

All values are expressed as mean ± SD (n=3). *P<0.05; **P< 0.1 as compared to pure TMZ (i.p) using one way ANOVA followed by Tukey's multiple comparisons test.

6.3.2.4. Lungs Biodistribution Studies

The biodistribution profile of TMZ in the lungs after administration of single oral dose of TMZ solution and NLC formulations by i.p route is given in Figure 6.6 and the pharmacokinetic parameters calculated by the software are tabulated in Table 6.5. As is evident from the data, there is no significant change in the C_{max} and $AUC_{0\text{-inf}}$ of the TMZ

solution (68.76 ± 1.76 µg.g^{-1} ; 163.50 ± 16.64 µg.h.g^{-1}) and PNLC (59.44 ± 6.90 µg.g^{-1}; 190.94 ± 20.05 µg.h.g^{-1}), GNLC (76.46 ± 15.29 µg.g^{-1}; 200.34 ± 17.14 µg.h.g^{-1}) and CNLC (68.36 ± 19.60 µg.g^{-1}; 171.05 ± 17.34 µg.h.g^{-1}) respectively. An increase in MRT was observed in case of PNLC (3.06 ± 0.33h) and CNLC (3.24 ± 0.23h) compared to GNLC (2.72 ± 0.06 h) and TMZ solution (2.48 ± 0.16 h).This may be due to the slower and sustained release of TMZ from the nanoparticles in the system. The increased AUC and MRT indicates the potential of the formulations especially PNLC and CNLC to be explored for the treatment of non-small cell lung cancer, Lewis lung cancer for which TMZ has demonstrated activity in salvage therapy during Phase II clinical trials [20].

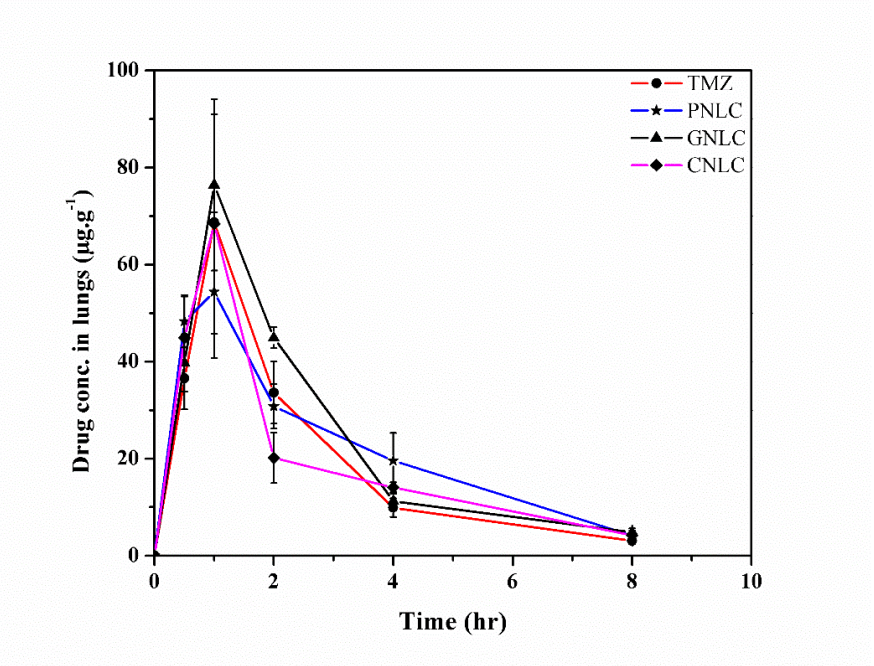

Fig. 6.6. Biodistribution profile of TMZ in the lungs following administration of a single of TMZ solution and NLC formulations by i.p route

6.3.2.5. Kidneys Biodistribution Studies

The biodistribution profile of TMZ in kidneys after administration of single oral dose of TMZ solution and NLC formulations by i.p route is given in Figure 6.7 and the calculated pharmacokinetic parameters are tabulated in table 6.6. The biodistribution of TMZ solution resulted in a C_{max} of 79.47 ± 8.15 µg.g^{-1} at 1h post dose. The $AUC_{0\text{-}inf}$ calculated was 195.60

Table 6.5. Summary of pharmacokinetic parameters of TMZ in the lungs following single dose i.p administration of TMZ solution and NLC formulations

Parameters	TMZ	PNLC	GNLC	CNLC
t_{max} (h)	1.0± 0.00	0.75± 0.25	1.0 ± 0.00	1.0 ± 0.00
C_{max} (µg.g^{-1})	68.76 ± 1.76	59.44 ± 6.90	76.46 ± 15.29	68.36 ± 19.60
AUC $_{0\text{-inf}}$ (µg.h.g^{-1})	163.50 ± 16.64	190.94 ± 20.05	200.34 ± 17.14	171.05 ± 17.34
MRT (h)	2.48 ± 0.16	3.06 ± 0.33*	2.72 ± 0.06	3.24 ± 0.23*

All values are expressed as mean ± SD (n=3). *P<0.05 as compared to pure TMZ (i.p) using one way ANOVA followed by Tukey's multiple comparisons test.

± 7.14 µg.h.g^{-1} with MRT of 2.64 ± 0.38h. The C_{max} of PNLC (51.96 ± 4.96 µg g^{-1}), GNLC (56.18 ± 1.03 µg g^{-1}) and CNLC (65.04 ± 2.49 µg g^{-1}) were significantly lesser than that of TMZ solution. However, the $AUC_{0\text{-inf}}$ calculated for PNLC (217.94 ± 41.55 µg.h.g^{-1}), GNLC (184.88 ± 6.85 µg.h.g^{-1}) and CNLC (196.75 ± 5.78µg.h.g^{-1}) were similar to that of the TMZ solution. The MRT calculated was 4.56 ± 1.17, 3.18 ± 0.12 and 3.25 ± 0.13h for PNLC, GNLC and CNLC respectively indicating higher residence time compared to TMZ solution. As discussed earlier, the increase in MRT is because of the slow and prolonged release of the drug from the nanoparticles and possible decreased renal clearance. The cutoff size for renal excretion is approximately 5.5nm according to recent research using quantum dots, and nanoparticles being much larger result in reduced renal clearance and prolonged circulation [21]. The NLC formulations can be used to reduce the side-effects and toxicity of TMZ.

6.3.2.6. Liver Biodistribution Studies

The biodistribution profile of TMZ in the liver after administration of single oral dose of TMZ solution and selected NLC formulations by i.p route is given in Figure 6.8 and the pharmacokinetic parameters calculated by the software are tabulated in Table 6.7. TMZ solution showed a C_{max} of 261.26 ± 4.46 µg.g^{-1} at 1 h post dose with an AUC $_{0\text{-inf}}$ of 777.87 ± 7.14 µg.h.g^{-1} and MRT value of 2.56 ± 0.09 h. The C_{max} values of PNLC, GNLC and CNLC were 277.72 ± 23.12, 344.62 ± 38.92 and 412.15 ± 16.67 µg.g^{-1} at 1h post dosing with an $AUC_{0\text{-inf}}$ of 969.91 ± 58.18, 968.91 ± 90.31 and 998.76 ± 34.29 µg.h.g^{-1} respectively.

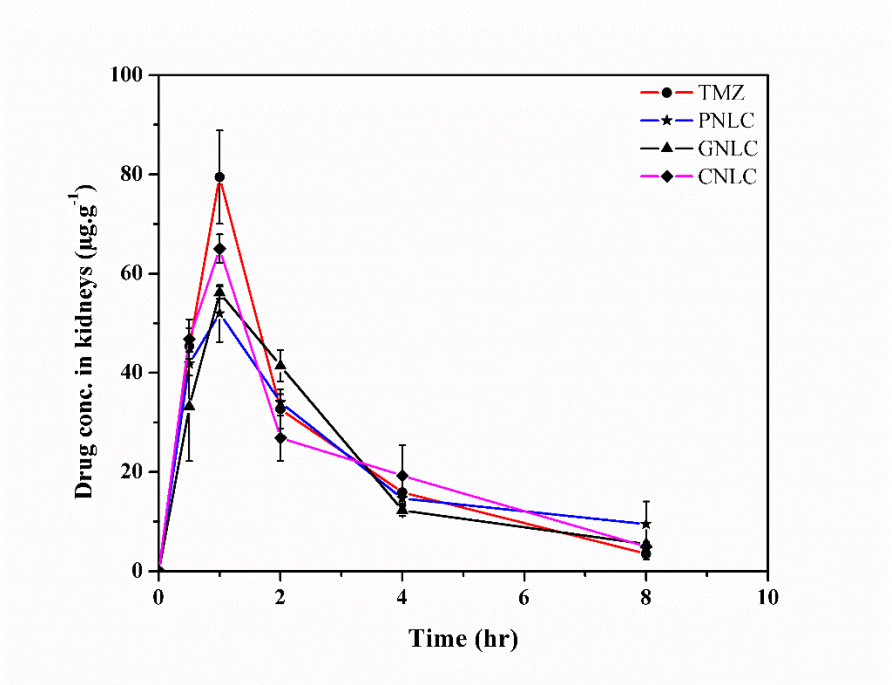

Fig. 6.7. Biodistribution profile of TMZ in the kidneys following administration of a single of TMZ solution and NLC formulations by i.p route

Table 6.6. Summary of pharmacokinetic parameters of TMZ in the kidneys following single dose i.p administration of TMZ solution and NLC formulations

Parameters	TMZ	PNLC	GNLC	CNLC
t_{max} (h)	1.0± 0.00	1.0± 0.00	1.0± 0.00	1.0± 0.00
C_{max} (µg.g^{-1})	79.47 ± 8.15	51.96 ± 4.96*	56.18 ± 1.03*	65.04 ± 2.49*
AUC $_{0\text{-inf}}$ (µg.h.g^{-1})	195.60 ± 7.14	217.94 ± 41.55	184.88 ± 6.85	196.75 ± 5.78
MRT (h)	2.64 ± 0.38	4.56 ± 1.17*	3.18 ± 0.12	3.25 ± 0.13

All values are expressed as mean ± SD (n=3). *P<0.05 as compared to pure TMZ (i.p) using one way ANOVA followed by Tukey's multiple comparisons test

The MRT calculated was 3.72 ± 0.51, 3.59 ± 0.65 and 3.14 ± 0.14 h for PNLC, GNLC and CNLC respectively. The data indicates a significant increase in the C_{max}, $AUC_{0\text{-inf}}$ and MRT possibly because tissues like liver, spleen, bone marrow and also tumors have a leaky

endothelial wall which enhances uptake of nanoparticles. In liver, the enhanced uptake is because of the presence of macrophages in the tissue [21].

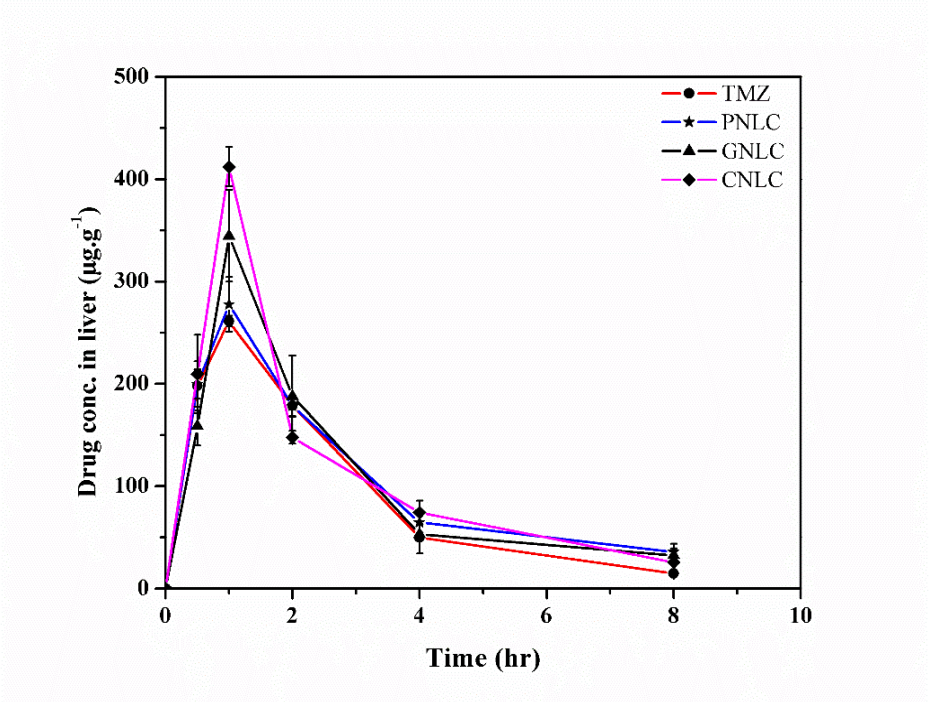

Fig. 6.8. Biodistribution profile of TMZ in the liver following single dose i.p administration of TMZ solution and NLC formulations

Table 6.7. Summary of pharmacokinetic parameters of TMZ in the liver following single dose i.p administration of TMZ solution and NLC formulations

Parameters	TMZ	PNLC	GNLC	CNLC
t_{max} (h)	1.0± 0.00	1.0± 0.00	1.0± 0.00	1.0± 0.00
C_{max} (µg.g^{-1})	261.26 ± 4.46	277.72 ± 23.12	344.62 ± 38.92*	412.15 ± 16.67*
AUC $_{0\text{-inf}}$ (µg.h.g^{-1})	777.87 ± 7.14	969.91 ± 58.18*	968.91 ± 90.31*	998.76 ± 34.29*
MRT (h)	2.56 ± 0.09	3.72 ± 0.51*	3.59 ± 0.65*	3.14 ± 0.14

All values are expressed as mean ± SD (n=3). *P<0.05 as compared to pure TMZ (i.p) using one way ANOVA followed by Tukey's multiple comparisons test

Conclusions

The pharmacokinetic and biodistribution studies of TMZ and the optimized NLC formulations were carried out in rats by administering a single oral dose of the pure drug by

both i.v and i.p administration and formulations by i.p route at a dose of 10 $mg.kg^{-1}$. The designed NLC formulations showed a significant increase in the $AUC_{0\text{-}inf}$ with increased residence time as is inferred from the detectable TMZ levels in plasma till 18h compared to 10h for the pure drug. Most importantly, the objective of our study which was to enhance availability of TMZ in the brain was successfully achieved as the formulations showed significant increase in C_{max}, $AUC_{0\text{-}inf}$ and MRT compared to the pure TMZ. Biodistribution studies showed enhanced permeation and residence time of TMZ in the brain possibly due to the nanosized of the formulation and reduction in conversion of TMZ into MTIC which has poor permeability in the brain. Higher uptake of TMZ as compared to the pure drug by RES organs was also observed i.e. spleen and liver in addition to brain whereas uptake by kidneys and heart reduced. The lower uptake by kidneys and heart is of significance as it can result in potential reduction in the adverse effects of TMZ i.e. cardiotoxicity and nephrotoxicity. The increased uptake and residence time in the lungs of the formulations can be explored as a potential carrier for treatment of non-small cell lung cancer, for which TMZ has shown activity during phase-II clinical trials.

The pharmacokinetic and biodistribution studies confirmed the nanoparticulate delivery systems designed i.e. the NLC formulations altered the pharmacokinetic parameters and biodistribution of TMZ thereby effectively enhancing permeability of TMZ in the brain. Further, the formulations enhance permeation by to protecting the drug from degradation at physiological pH in addition to prolonging the levels of TMZ by sustained release from the NLC. Thus, NLCs are suitable carriers for enhancing delivery to the brain and reducing the side effects associated with temozolomide.

References

1 Tozer, T.N. and Rowland, M. (2010) *Clinical pharmacokinetics and pharmacodynamics concepts and applications*, 4th Ed. Wolters Kluwer Health and Lippincott Williams & Wilkins, Philadelphia PA 1-15

2 Steinmetz, K.L. and Spack, E.G. (2009) The basics of preclinical drug development for neurodegenerative disease indications. *BMC Neurology* 9 (Suppl 1), S2-S2

3 Kummar, S. et al. (2006) Drug development in oncology: classical cytotoxics and molecularly targeted agents. *British Journal of Clinical Pharmacology* 62 (1), 15-26

4 Moghimi, S.M. et al. (2012) Factors controlling nanoparticle pharmacokinetics: an integrated analysis and perspective. *Annual Review of Pharmacology and Toxicology* 52 (1), 481-503

5 Snehalatha, M. et al. (2013) Enhanced tumor uptake, biodistribution and pharmacokinetics of etoposide loaded nanoparticles in Dalton's lymphoma tumor bearing mice. *Journal of Pharmacy & Bioallied Sciences* 5 (4), 290-297

6 Joseph, E. et al. (2017) Design and in vivo evaluation of solid lipid nanoparticulate systems of Olanzapine for acute phase schizophrenia treatment: Investigations on antipsychotic potential and adverse effects. *European Journal of Pharmaceutical Sciences* 104, 315-325

7 Choi, K.Y. et al. (2009) Self-assembled hyaluronic acid nanoparticles as a potential drug carrier for cancer therapy: synthesis, characterization, and in vivo biodistribution. *Journal of Materials Chemistry* 19 (24), 4102-4107

8 Turner, P.V. et al. (2011) Administration of Substances to Laboratory Animals: Routes of Administration and Factors to Consider. *Journal of the American Association for Laboratory Animal Science : JAALAS* 50 (5), 600-613

9 Agarwala, S.S. and Kirkwood, J.M. (2000) Temozolomide, a novel alkylating agent with activity in the central nervous system, may improve the treatment of advanced metastatic melanoma. *The Oncologist* 5 (2), 144-151

10 Hirst, T.C. et al. (2013) Systematic review and meta-analysis of temozolomide in animal models of glioma: was clinical efficacy predicted? *British Journal of Cancer* 108 (1), 64-71

11 European Medicine Agency (2011) Committee for Medicinal Products for Human Use (CHMP) assessment report on Temozolomide Sun, Procedure No EMEA/H/C/002198. United Kingdom. Content accessed in June 2018. h*ttp://www.ema.europa.eu/docs/en_GB/document_library/EPAR_Public_assessment_report/human/002198/WC500109707.pdf*.

12 Huang, G. et al. (2008) Solid lipid nanoparticles of temozolomide: Potential reduction of cardial and nephric toxicity. *International Journal of Pharmaceutics* 355 (1), 314-320

13 Manjunath, K. and Venkateswarlu, V. (2005) Pharmacokinetics, tissue distribution and bioavailability of clozapine solid lipid nanoparticles after intravenous and intraduodenal administration. *Journal of Controlled Release* 107 (2), 215-228

14 Neves, A.R. et al. (2016) Brain-targeted delivery of resveratrol using solid lipid nanoparticles functionalized with apolipoprotein E. *Journal of Nanobiotechnology* 14, 27

15 Kaur, I.P. et al. (2008) Potential of solid lipid nanoparticles in brain targeting. *Journal of Controlled Release* 127 (2), 97-109

16 Kreuter, J. (2005) Application of nanoparticles for the delivery of drugs to the brain. *International Congress Series* 1277

17 Wohlfart, S. et al. (2012) Transport of drugs across the blood?brain barrier by nanoparticles. *Journal of Controlled Release* 161 (2), 264-273

18 Khosa, A. et al. (2018) Nanostructured lipid carriers for site-specific drug delivery. *Biomedicine & Pharmacotherapy* 103, 598-613

19 Cataldi, M. et al. (2017) Emerging role of the spleen in the pharmacokinetics of monoclonal antibodies, nanoparticles and exosomes. *International Journal of Molecular Sciences* 18 (6) pii: E1249

20 Adonizio, C.S. et al. (2002) Temozolomide in non-small-cell Lung Cancer: Preliminary Results of a Phase II Trial in Previously Treated Patients. *Clinical Lung Cancer* 3 (4), 254-258

21 Li, S.-D. and Huang, L. (2008) Pharmacokinetics and Biodistribution of Nanoparticles. *Molecular Pharmaceutics* 5 (4), 496-504

7. Conclusions and Future Prospects

7.1. Conclusions

Nanoparticulate drug delivery is emerging as a promising alternative for more specific, selective and effective delivery of therapeutics especially anti-cancer drugs leading to possibility of dose reduction, better targeting efficiency and reduced side effects. Thus the objective of this study was to design and characterize nanoparticulate delivery systems for temozolomide (TMZ), an anti-cancer drug used for the treatment of brain tumors, for prolonged efficacy and enhanced permeation into the brain.

Analytical methods form the backbone of the drug development process including designing and evaluation of drug delivery systems. Therefore, new UV-spectrophotometric and RP-HPLC analytical methods were developed and validated in-house. The methods were simple, specific for TMZ, accurate, precise and robust. The methods were successfully used for preformulation studies, routine analysis for entrapment efficiency, drug loading and in vitro release studies. Further, a rapid, specific, accurate, precise and stable RP-HPLC bioanalytical method was developed and validated in-house for determination of temozolomide in biomatrices such as plasma and various tissues collected during pharmacokinetic and biodistribution studies.

The preformulation studies indicated that TMZ has pH independent solubility from pH 1- 6. A decrease in pH was observed above pH 6 because of degradation of TMZ which increases as pH changes from neutral to alkaline. TMZ has comparable solubility in both water and most of the studied organic solvents such as methanol, acetone etc. Solution state stability indicated that TMZ is stable under acidic conditions and the degradation rate increases as the pH shifts from acidic to basic. Solid state stability revealed that TMZ was stable under refrigerated conditions but was susceptible to moisture mediated degradation. In drug-excipient compatibility studies, TMZ was found to be stable with no interaction with the selected excipients.

Various nanoformulations including polymeric nanoparticle, solid lipid nanoparticles and nanostructured lipid carriers were fabricated. However, polymeric nanoparticles and SLN strategies were not investigated further because of poor drug entrapment and high particle size respectively. Nanostructured lipid carriers (NLC) were fabricated using glyceryl monostearate, Precirol ATO 5 and Compritol 888 ATO as the solid lipids and oleic acid as

the liquid lipid successfully using hot emulsion-ultrasonication technique with satisfactory entrapment efficiency and drug loading. The influence of various parameters such as drug-to-lipid ratio, lipid-to-oil ratio and surfactant concentration on responses such as particle size, entrapment efficiency and drug loading were studied in detail using DoE. The optimized NLC formulations showed prolonged release of the drug for 24h as assessed from in vitro release studies and the release profile was explained by Korsmeyer-Peppas model with n <0.5 indicating Fickian diffusion. The SEM images showed that the particles were anisometric in shape with an irregular surface. The particles were easily redispersible after freeze drying and no significant change was observed in particle size, entrapment efficiency and drug release for formulations stored under refrigerated condition for 6 months. MTT assay indicated that the TMZ loaded nanoparticles show increased cytotoxicity and lower IC_{50} values as compared to the pure drug possibly because of increased cell uptake and internalization.

The pharmacokinetic and biodistribution studies of TMZ solution and NLC formulations in rats confirmed that nanoparticles modified pharmacokinetic parameters and selective distribution can be achieved using the formulations. It was found that as compared to TMZ solution, the NLC formulations showed higher AUC and prolonged residence time in the rat vasculature. More importantly, an enhanced distribution of TMZ into the brain was observed for all the three formulations compared to the TMZ solution. Studies showed low uptake of the nanoparticles in heart and kidneys, decreasing the possibility of cardiotoxicity and nephrotoxicity. An increase in distribution was observed in RES organs spleen and liver which may be due to the uptake of nanoparticles by macrophages. During the course of the study, no adverse events were observed indicating that the nanoformulations were well tolerated by the rats. Further, the formulations can be explored for the treatment of non-small cell lung cancer also.

Collectively, it can be concluded from the results that the designed NLC formulations are promising delivery systems which can enhance the permeation of temozolomide into the brain with reduced adverse effects on the heart and kidneys. Further, the dose can possibly be reduced which will improve the safety profile of the drug.

7.2. Future Prospects

- The formulation can be modified or alternative strategies of nanoparticle formulation such as choice of polymers/lipids, fabrication technique, surfactants etc. can be explore to further increase the entrapment efficiency and drug loading thereby increasing the efficiency of the formulation and reducing the cost.
- Scale up of the formulations may be optimized and performed.
- Dose reduction studies in animal models can be performed.
- The optimized formulations may be further studied in diseased animal models.
- The toxicity and cellular uptake of the formulations can be further investigated by in vitro methods.
- The work can be extended to other routes of administration especially nasal route which can bypass the BBB and the oral route in order to simplify the administration and better safety.
- The work can be extended to other therapeutics intended for delivery to the brain.

Appendixes

List of Publications and Presentations

Publications

1. Archana Khosa, K.V. Krishna, Ranendra N Saha, Sunil Kumar Dubey, Satish Reddi.2018, High throughput and sensitive validated RP-HPLC method for determination of temozolomide in rat plasma and its application to a pharmacokinetic study. *Journal of Liquid Chromatography & Related Technologies*, DOI: 10.1080/10826076.2018.1511803
2. Archana Khosa, Gautam Singhvi, Ranendra N Saha, Gaurav Gupta. 2018, Drug delivery to the CNS, *Panminerva Medica*, DOI: 10.23736/S0031-0808.18.03471-7
3. Archana Khosa, Satish Reddi, Ranendra N Saha. 2018. Nanostructured lipid carriers for site specific drug delivery, *Biomedicine and Pharmacotherapy*, 103, 598-613.
4. Archana Khosa, Shelly Sinha, Satish Reddi, Ranendra N Saha. 2018. Simple rapid and sensitive UV spectrophotometric method for determination of Temozolomide in Polycaprolactone nanoparticles. *Asian Journal of Chemistry*, 30, (4), 868-872.

Book Chapter

1. Archana Khosa, Ranendra N Saha, Gautam Singhvi. Drug Delivery to the Brain in Nanomaterials for drug delivery and therapy, Elsevier Publishing Editor: Alexandru Mihai Grumezescu (In Print).

Paper Presentations

1. A. Khosa, R.N. Saha. Development of a simple and economic UV spectrophotometric estimation of Temozolomide for pre-formulation studies, AAPS-NUS 10th PharmSci @Asia Symposium and Annual Pharmacy Research Awareness Symposium 2015 (April 8-9, 2015) Singapore.
2. A. Khosa, Development of RP-HPLC method for determination of entrapment efficiency and drug loading of Polymeric nanoparticles of temozolomide, International Conference on Challenges in Drug Discovery and Delivery (ICCD3 - 2017), March 2-4, 2017, BITS, Pilani, Pilani Campus.

Biography of Archana Khosa

Ms. Archana Khosa is currently working as an Assistant Professor (II) in the Department of Pharmacy, BITS, Pilani. She has completed her B. Pharm from Dr. K. N. Modi Institute of Pharmaceutical Education and Research, Modinagar and M.Pharm from BITS, Pilani. She has around seven years work experience with several pharmaceutical companies like Ohm Laboratories, New Jersey, USA, Panacea Biotec Ltd, Delhi and Ranbaxy Research Laboratories, Gurgaon in the Formulation Development and Research division. She has also worked as an Assistant Professor in Noida Institute of Engineering and Technology, Greater Noida prior to joining BITS, Pilani. She has a number of patents and publications to her credit and has presented her work in several national and international conferences.

Biography of Chair Prof. Ranendra N. Saha

Dr. Ranendra Narayan Saha is Senior Professor of Pharmacy as well as Director of BITS Pilani, Dubai Campus. He has completed his Bachelor and Master of Pharmacy from Jadavpur University, Kolkata and was awarded Doctor of Philosophy by BITS, Pilani. He has more than 34 years of teaching, research and administrative experience and has guided several doctoral, postgraduate and undergraduate students. He has extensive research experience and specializes in novel drug delivery systems, nanomedicine and pharmacokinetics. He has published books, authored several book chapters and more than 100 research papers in reputed national and international journals of repute. Besides, he has delivered several invited lectures at seminars/conferences organized by various colleges, pharmaceutical industries and universities in India and overseas. He is also a member of advisory board and selection committees of several universities in India and overseas. He has completed several government sponsored projects and has been working closely with the pharmaceutical industry over the years with several patents and commercial products to his credit.

He received *'Pharmacy Professional of the Year 2013'* an award given by Indian Association of Pharmaceutical Scientists and Technologists (IAPST). In 2011, he has been awarded *Shri B. K. Birla and Shrimati Sarala Birla Chair Professorship* at BITS Pilani for his contributions in teaching and research. He is also a recipient of '*The Best Pharmacy Teacher Award'* for the year 2005, awarded by Association of Pharmaceuticals Teachers of India (APTI), in recognition of his contribution in teaching and research in the field of Pharmacy.